

Provision of Information on Chromium Doped Fuel for Use in Light Water Reactors

NNL 15231

ISSUE 1

This document is prepared by National Nuclear Laboratory Limited ("NNL") for ONR pursuant to a contract, dated 08 November 2019, reference ONR/T3450 ("the Contract"). The ownership of this document, and the material contained within it, shall be treated in accordance with the provisions of the Contract

Provision of Information on Chromium Doped Fuel for Use in Light Water Reactors

NNL 15231

ISSUE 1



	Name	Signature	Date
Checked By	[REDACTED]	[REDACTED]	2.3.20
Approved By	[REDACTED]	[REDACTED]	2.3.20
Work Order Number	05776.100		

Keywords

ADDITIVE; CDF; CR2O3; CHROMIA; CHROMIUM; DOPANT; DOPED; FRAMATOME; LWR; UO2; WESTINGHOUSE

Executive Summary

This report details work undertaken as part of the Provision of Information on Chromium Doped Fuel for Use in Light Water Reactors project. The objective is to collate, review and perform an independent evaluation of the publicly available literature covering chromium doped fuel (CDF) – that is, fuel doped with chromium and any other complementary additives. This provides understanding of the performance benefits and potential issues associated with chromium doped fuels, whilst drawing comparisons to undoped fuels to provide context where appropriate. The findings are discussed below.

CDF has been developed to make the fuel cycle more economical, to increase fuel reliability and to increase flexibility to meet energy demand. With a current focus on reducing the consequences of severe accidents in LWRs, a further demand has been placed on the development of accident tolerant (or advanced technology) fuel (ATF), a classification in which CDF is one option.

The addition of a small amount of chromia has been proven to significantly enhance grain growth during the sintering process employed in fuel manufacture. This leads to larger grain sizes than standard UO_2 fuel pellets for shorter sintering times. There is also greater densification of the pellets during sintering than for standard UO_2 , leading to a greater mass of uranium in the pellets and a reduced porosity volume fraction. These factors make the manufacturing process more economical, although careful control of the dopant concentrations and sintering conditions is needed to avoid volatilisation of the chromium and to ensure solubility of the chromia in the fuel matrix.

In reactor, the reduced porosity volume fraction leads to reduced in-pile densification, and hence greater dimensional stability of the fuel pellets. The larger grain size increases the fission product diffusion path to grain boundaries and so reduces the fission gas release from the pellets; this in turn reduces the rod internal pressures and inter-granular fission gas bubble swelling. However, there is a significant increase in intra-granular fission gas bubble swelling. The chromia also enhances the fuel thermal creep rate (despite the larger grain size), without significantly affecting any of the other thermal or mechanical properties, so there is an improvement in the pellet-clad interaction (PCI) behaviour during power transients, making the cladding less susceptible to failure by stress-corrosion cracking. The PCI behaviour is further improved through increased radial cracking of the thinner brittle outer zone of the fuel pellets (noting that the fracture strength is reduced due to the large grain size), and, arguably, by chemical effects (improved corrosive fission product retention, and chromia dissociation and associated generation of free oxygen which can oxidise the cladding inner surface, thereby protecting it from SCC). Finally, post-failure oxidation and washout of CDF is reduced due to the large grain size, thereby reducing the consequences of leaking rods during normal operation and of failed rods after an infrequent fault.

The consequences of limiting infrequent faults – that is, loss of coolant accidents (LOCAs) and reactivity-initiated accidents (RIAs) – can be lessened by reducing the extent of clad ballooning, reducing the cladding oxidation, reducing the volatile fission product release, and/or reducing the extent of fuel fragmentation. Hence, the lower FGR and increased intra-granular fission gas inventory of CDF can potentially reduce the consequences of these faults

OFFICIAL : COMMERCIAL

NNL 15231

ISSUE 1

by reducing the rod internal pressure driving force for clad creepout, reducing volatile fission product release (which is correlated to fission gas release), and reducing the extent of inter-granular fragmentation due to overpressurisation of inter-granular fission gas bubbles. However, there are currently limited experimental data – and no data from integral rod testing – to support this.

There are two main vendors of CDF: Westinghouse and Framatome. The Westinghouse product uses a combination of chromia and alumina as dopants (ADOPT fuel), while the Framatome product uses only chromia. Both Westinghouse and Framatome have significant operating experience associated with lead fuel rods and lead fuel assemblies of their CDF products in commercial LWRs; in addition, reload quantities of Westinghouse ADOPT fuel have been irradiated. Ramp tests have also been performed to determine the PCI behaviour (although these appear to be limited in the case of Westinghouse ADOPT fuel), and various experimental irradiations have been carried out to investigate the phenomenology. Further irradiations are planned in the near future.

Modelling of CDF using fuel performance codes has been relatively limited, both in terms of codes used and their application. The necessary modifications to the material properties and models for undoped UO₂ have also been relatively minor. Of the five codes for which information is available – BISON, COPERNIC, RODEX, STAV and ALCYONE – only RODEX is known to have been validated for modelling of chromia doped fuel or to have been used for licensing of such fuel (for BWR applications).

No information was available on the storage or disposal of spent CDF. This is probably because storage and disposal are/will be as per existing routes (wet storage in ponds, potentially followed by dry storage in casks, vaults or silos, followed by disposal in a geological repository) with no impact foreseen for CDF. It is also consistent with the main mechanisms for fuel degradation in wet storage – cladding corrosion and hydriding – being independent of the fuel pellet type. In addition, there is a sparsity of information on the behaviour of CDF when exposed to water in post-irradiation storage and disposal conditions. The only information available is on fuel pellet leaching and dissolution in groundwater in the context of disposal of spent CDF, and is only from two sources: the Euratom FIRST-Nuclides and DisCo projects. Preliminary results from the DisCo project suggest that the larger grain size of CDF reduces the instant release fractions (IRFs) of volatile fission products after disposal canister penetration by groundwater.

Further qualification and testing in the form of in-pile ramp tests on Westinghouse CDF may be required. Similarly, additional PIE on ramp-tested fuel may be required if the potential chemical benefits of CDF with respect to PCI resistance are to be properly understood and/or taken credit for (over and above what is already implicitly taken credit for on the basis of ramp test results).

The main impact of CDF on Limits and Conditions of Operation (LCO) is likely to be on PCI thresholds. Reduced fission gas release during normal operation may also allow increased burnup limits (assuming it can be demonstrated that rod internal pressure and clad hoop strain during normal operation remain below existing limits). The main remaining in-reactor fuel licensing issues are likely to be as follows:

OFFICIAL : COMMERCIAL

OFFICIAL : COMMERCIAL

NNL 15231

ISSUE 1

- The reduced densification and increased intra-granular gas bubble swelling of CDF may (notwithstanding the increased fuel creep)
 - reduce margin to clad hoop strain and rod growth limits during normal operation
 - reduce margin to clad hoop strain increment limits during frequent faults
 - increase the number of rod failures during a RIA
- A lack of sufficient data (in particular for Westinghouse CDF) on ramp test behaviour to justify proposed PCI thresholds in a statistically meaningful manner.
- The lack of data on performance of the fuel during a RIA, and the limited data on performance of the fuel during a LOCA.
- The use of data on fuel from the early phases of product development which is not prototypic of the commercial fuel product; in particular, this would apply to the use of material property data and irradiation data for calibration and/or validation of the fuel performance code used in the licensing.
- Where applicable, the lack of data on the material properties and/or performance of CDF including the chosen burnable absorber material.

Further impacts on in-reactor fuel licensing and on reactor licensing are likely to be positive rather than negative.

OFFICIAL : COMMERCIAL

OFFICIAL : COMMERCIAL

NNL 15231

ISSUE 1

Verification Statement

This document has been verified and approved in accordance with NNL's procedures for the reporting of work.

History Sheet

Issue Number	Date	Comments
Draft 1	28/1/20	Verified draft sent to external reviewer for comment.
Draft 2	11/2/20	External reviewer's comments addressed and changes verified.
Draft 3	14/02/20	Internal approver's comments addressed and changes verified. Sent to customer for comment.
Issue 1	02/03/20	Customer satisfied with document. Final document issued.

OFFICIAL : COMMERCIAL

Table of Contents

1. Introduction	12
2. Background	13
3. Fuel Manufacture, Microstructure and Properties	15
3.1. Fuel Manufacture	15
3.1.1. Westinghouse	15
3.1.2. Framatome (formerly AREVA NP)	17
3.1.3. Issues associated with the manufacture of CDF.....	20
3.2. Microstructure and Properties.....	26
3.2.1. Grain size.....	26
3.2.2. Density	27
3.2.3. Porosity	28
3.2.4. Thermal properties.....	29
3.2.5. Mechanical properties	31
4. Phenomenology	36
4.1. Halden Reactor Project Experiments.....	36
4.1.1. IFA-677	36
4.1.2. IFA-716	37
4.1.3. IFA-720.3	38
4.2. Behavioural Assessment	38
4.2.1. In-pile densification and dimensional stability	38
4.2.2. Swelling.....	39
4.2.3. Pellet-cladding interaction (PCI).....	42
4.2.4. Fuel pellet cracking	45
4.2.5. Oxidation and washout characteristics	48
4.2.6. Fission gas release (FGR)	50
4.2.7. Behaviour during accidents	57
5. Operating Experience and Qualification Data.....	59
5.1. Westinghouse.....	59
5.1.1. Commercial reactor irradiations	59

5.1.2.	Ramp tests.....	61
5.2.	Framatome	62
5.2.1.	Commercial reactor irradiations	62
5.2.2.	Ramp tests.....	64
6.	Prediction of Behaviour and Validation	67
7.	Spent Fuel Storage and Disposal	73
7.1.	Spent fuel storage	73
7.2.	Spent fuel disposal.....	73
8.	Future Qualification, Research, Development and Testing Needed	76
9.	Impact on Limits and Conditions of Operation	79
10.	Licensing and Regulatory Issues.....	80
11.	Conclusions	82
12.	References	85

List of Tables

Page

Table 1:	The fuel pellets used in the Halden IFA-677 experiment [29].	37
Table 2:	The fuel pellets used in the IFA-716 experiment [30].	38
Table 3:	Estimated end-of-life FGR for the IFA-677 rods [29].	52
Table 4:	Claims for CDF performance benefits made by Framatome and Westinghouse, together with suitable metrics for determining whether or not claimed benefits are achieved.	76
Table 5:	Available data for Framatome CDF demonstrating that suitable metrics from Table 4 have been met.....	77
Table 6:	Available data for Westinghouse CDF demonstrating that suitable metrics from Table 4 have been met.....	77

List of Figures

Figure 1: ADOPT grain size against Al ₂ O ₃ content [7].	16
Figure 2: Plots showing the stability of the ADOPT pellet as-manufactured density (a) and grain size (b) [1].	17
Figure 3: The effect of dopant concentration on grain size for various additives [12].	18
Figure 4: Deformation rate against pellet grain size for various additives [12].	19
Figure 5: Data illustrating stability of Framatome CDF as-manufactured density and grain size [9].	20
Figure 6: Full diameter EPMA line scans of UO ₂ pellets doped with 500, 1000 and 1600 ppm Cr ₂ O ₃ (IFA0,2,3 respectively) [18].	22
Figure 7: EPMA local area mapping of IFA0 (top), IFA2 (middle) and IFA3 (bottom). The images represent the: secondary electron image (left), UMa intensity map (middle) and CrKa intensity map (right) [18].	23
Figure 8: Comparisons with results from experimentation, literature and a thermal solubility model for variations with the oxygen partial pressure of the Cr ₂ O ₃ solubility in UO ₂ : (a) within the stability areas of Cr ₂ O _{3(s)} , CrO _(l) and Cr _(s) for 1700°C and above; (b) within the stability areas of Cr ₂ O _{3(s)} , CrO _(l) and Cr _(s) for 1500-1760°C [20].	25
Figure 9: Comparisons with results from experimentation, literature and a thermal solubility model for variations in the solubility of Cr ₂ O ₃ in UO ₂ as a function of the temperature [20].	26
Figure 10: An image showing the enlarged grain size of the Framatome Cr ₂ O ₃ -doped UO ₂ fuel pellets when compared to standard UO ₂ [13].	27
Figure 11: Pore shape of standard UO ₂ (left) and ADOPT (right) pellets [1].	28
Figure 12: Strain vs. time results from out-of-pile creep tests on Framatome undoped UO ₂ and doped fuel with various dopant concentrations and grain sizes (at 1470°C and with an applied stress of 45 MPa) [24].	32
Figure 13: Strain vs. time results from out-of-pile creep tests on Framatome chromium doped UO ₂ at various stresses (0.2 wt% Cr ₂ O ₃ at 1470°C) [24].	33
Figure 14: Strain vs. time results from out-of-pile creep tests on ADOPT fuel [25].	33
Figure 15: (Irradiation-induced) creep rate of chromia doped (ADOPT) and undoped UO ₂ fuel as measured in the IFA-701 in-pile creep experiment [26].	34
Figure 16: Fuel volume change versus burnup behaviour calculated from fuel stack elongation measurements in IFA-677 (ignore results for rods 1 and 4) [35].	39

Figure 17: Fuel density versus burnup data for commercial irradiations of Framatome doped and undoped fuel [11] (poor quality of image is as in the cited reference).	41
Figure 18: Comparison of fission gas bubbles in Framatome chromia doped and undoped UO ₂ fuel after irradiation [13].....	42
Figure 19: The hourglass shape of a fuel pellet (idealised and exaggerated) [37].	43
Figure 20: Pellet dish filling after power ramps to 40 kW/m: Framatome undoped fuel on left and Framatome CDF on right [24].....	44
Figure 21: Measurement of Cr concentration radial distribution before and after the Framatome PR1 ramp test [42].	45
Figure 22: Pellet cracking after irradiation in the IFA-677 experiment for undoped fuel (left), fuel with 500 ppm chromia (middle), and fuel with 900 ppm chromia (right) [2].....	46
Figure 23: Sections of Framatome chromia doped fuel (left) and standard UO ₂ fuel (right) after ramping to 40 kW/m [24].	47
Figure 24: Sections of Framatome chromia doped fuel ramped to 40 kW/m (left) and 47 kW/m (right) [24].....	47
Figure 25: Comparison of the weight gain (measure of oxidation) vs. time for chromia doped and undoped UO ₂ fuel pellets with various densities and grain sizes tested at 380°C in an Ar-0.01% O ₂ atmosphere [14].	48
Figure 26: Pellet degradation associated with the weight gain shown in Figure 25 [14].	49
Figure 27: FGR vs. burnup for ADOPT and standard UO ₂ pellets after irradiation in a commercial LWR [2].	51
Figure 28: FGR and peak fuel temperature versus burnup behaviour in IFA-677, as inferred from pressure transducer and fuel thermocouple measurements [29].....	52
Figure 29: FGR and peak fuel temperature versus burnup behaviour in IFA-720.3, as inferred from pressure transducer and fuel thermocouple measurements [33].....	53
Figure 30: FGR vs. burnup for doped and undoped Framatome fuel after irradiation in commercial PWRs [36].	54
Figure 31: FGR vs. time behaviour in IFA-716 experiment after December 2013 power uprating, as derived from rod internal pressure measurements (the bars represent estimated uncertainties) [31].	55
Figure 32: Fission gas release vs. ramp terminal level for Framatome CDF [12].	56
Figure 33: ⁸⁵ Kr release vs. grain size for post-irradiation annealing of Framatome low burnup fuel with various dopants at 1700°C for 5 hours [48].	57
Figure 34: The evolution of Westinghouse BWR assembly designs [53].	60

Figure 35: Rod length and diameter vs. rod average burnup for commercially irradiated rods containing ADOPT and undoped UO ₂ fuel pellets [1].	61
Figure 36: Framatome GAIA fuel assembly design [59].	63
Figure 37: Rod length data from commercial irradiations of Framatome CDF [36] [57].	64
Figure 38: Rod diameter data from commercial irradiations of Framatome GAIA fuel [36].	64
Figure 39: Ramp test results for Framatome chromia doped fuel and standard UO ₂ fuel: BWR data (the lines represent BWR failure thresholds, and PWR data are included for comparison purposes) [12].	65
Figure 40: Ramp test results for Framatome chromia doped fuel and standard UO ₂ fuel: PWR data [9].	66
Figure 41: BISON prediction and measurement of FGR in IFA-677 rod 1 (ADOPT with 900 ppm chromia) [61].	68
Figure 42: BISON prediction and measurement of FGR in IFA-716 rod 1 (Framatome CDF with 1600 ppm chromia) [61].	69
Figure 43: BISON prediction and measurement of FGR vs ramp terminal level for Framatome ramp tests [60].	69
Figure 44: BISON predictions of the FGR and plenum pressure for chromia doped and standard UO ₂ rods during a LOCA simulation (pre-fault predictions are on the left, and LOCA predictions are on the right) [60].	70
Figure 45: RODEX prediction and measurement of FGR in IFA-677 rod 1 (ADOPT with 900 ppm chromia) [63].	70
Figure 46: RODEX prediction and measurement of FGR in IFA-716 rod 1 (Framatome CDF with 1600 ppm chromia) [63].	71
Figure 47: STAV prediction and measurement of FGR in IFA-677 rod 1 (ADOPT with 900 ppm chromia) [2].	71
Figure 48: ALCYONE prediction and measurement of Cr concentration radial distribution before and after the hold period of the Framatome PR1 ramp test [42].	72
Figure 49: Measured concentrations of fission product and actinide isotopes in simulated groundwater obtained as part of DisCo leaching/dissolution experiments on 59 MWd/kgU BWR ADOPT fuel and 57 MWd/kgU BWR undoped fuel [69].	75

1. Introduction

This report details work undertaken as part of the Provision of Information on Chromium Doped Fuel for Use in Light Water Reactors project. The objective is to collate, review and perform an independent evaluation of the publicly available literature covering chromium doped fuel (CDF) – that is, fuel doped with chromium and any other complementary additives. This provides understanding of the performance benefits and potential issues associated with chromium doped fuels whilst drawing comparisons to undoped fuels to provide context where appropriate.

The literature collation and review aspect of this report has been carried out by using the Science Direct and Google Scholar search engines and the following NNL archives: “The Fuel Performance Reference Library”, a collection of references collated previously for use in the NNL Reactor Physics Team; papers, reports and presentations from fuel performance related conferences such as TopFuel (where not already included in the Fuel Performance Reference Library); and OECD Halden Reactor Project reports and Enlarged Halden Programme Group (EHPG) meeting proceedings. The collation was achieved by first using key search words, for example “chromium” and “doped”, to find relevant literature. After reading this literature, the search was then focused on the specific areas of interest of the report, for example “ramp test” and “Westinghouse doped fuel”. After finding further references of interest from this more specific search, more resources were identified through the references and the authors. The full set of literature found for this report (which is not all referenced here) is documented in a Microsoft Excel spreadsheet.

The results of the review are documented in Sections 2 to 7, and cover the background to the use of CDF (Section 2), fuel manufacture, microstructure and properties (Section 3), phenomenology (Section 4), operating experience and qualification data (Section 5), prediction of behaviour and validation (Section 6) and spent fuel storage and disposal (Section 7). The future qualification, research, development and testing needed, impact on limits and conditions of operation, and licensing and regulatory issues are then determined in Sections 8 to 10. Finally, conclusions are drawn summarising the main points covered within the report.

2. Background

Fuel manufacturers in the UK and globally are attempting to modify the uranium dioxide (UO_2) fuel they produce to improve its performance. The reasoning behind this includes: enhanced accident tolerance by reducing the consequences of severe accidents in light water reactors (LWRs), increased flexibility to meet demand, reduced fuel cycle cost, and improved reliability of fuel during operation [1]. Such requirements can be met by optimising the properties and behaviour of the fuel under irradiation.

The main aspects of the fuel performance which can be modified to achieve the above requirements are: fuel densification, fission gas (and hence also volatile fission product) retention, pellet-cladding interaction (PCI) performance, post-failure fuel performance and stored energy (via changes to thermal conductivity) [2]. Significant stored energy improvements can only be made by developing two-phase materials (see below). To make improvements in the other areas, additives are used to 'dope' the fuel pellets. These additives are added in such small quantities ($< \sim 1$ wt%) that they can facilitate the enhancement of properties without fundamentally changing the fuel type.

Additives have been used since the 1960s to improve the manufacture and performance of nuclear fuels [3]. The additives studied most extensively are alumina (Al_2O_3), chromia (Cr_2O_3), magnesia (MgO), titania (TiO_2), niobia (Nb_2O_5) and silica (SiO_2). Many of these additives have been used to manufacture fuel by UK and overseas fuel vendors and have been subject to irradiation trials. Burnable neutron absorbers, including gadolinia (Gd_2O_3), erbia (Er_2O_3) and zirconium diboride (ZrB_2) [3], are also added to UO_2 fuel, but these are not additives in the sense used here. Furthermore, other materials, such as beryllium oxide (BeO) and molybdenum (Mo), have been used to produce advanced fuel types (to increase the thermal conductivity of fuel pellets in the case of BeO and Mo), but these are added at such levels (> 1 wt%) that they do not constitute additives as considered here: the fuel microstructure is fundamentally modified such that there is a two-phase material.

Through extensive testing and irradiation programmes, chromia has become the chosen additive by several fuel vendors. This is due to the beneficial behaviour of chromia doped UO_2 fuel that can be achieved at relatively low dopant concentrations, without greatly affecting the neutron absorption. This beneficial behaviour is caused by:

- (a) an increase in grain size and consequent increase in the distance that fission gas and volatile fission product atoms must diffuse to reach a grain boundary and be released; this in turn gives reduced fission gas release
- (b) an increase in creep rate and consequent reduction in fuel pellet imposed clad stresses during transients; this in turn gives a reduced PCI failure propensity
- (c) a reduction in fuel porosity volume fraction, with a consequent increase in fissile material (uranium) density; this in turn reduces fuel cycle costs

Some or all of these benefits can also be achieved with other additives, for example niobia, but in many cases the benefits of the increase in grain size are offset by an increase in the intra-granular fission gas diffusion coefficient. This report therefore focuses on uranium

OFFICIAL : COMMERCIAL

NNL 15231

ISSUE 1

dioxide (UO₂) doped with chromia, although fuel which is doped with both Cr₂O₃ and other additives is also considered.

As an aside, it is also worth noting the use of chromia as an additive in MOX fuels for irradiation in LWRs is also being investigated. This CHROMOX concept is being considered by the fuel vendor Framatome to enable better distribution of plutonium in the fuel matrix, enhance grain size and limit fission gas release, thereby reducing safety concerns in both normal operation and accident scenarios [4]. Such chromia doped MOX fuel will not be discussed further in this report.

OFFICIAL : COMMERCIAL

3. Fuel Manufacture, Microstructure and Properties

3.1. Fuel Manufacture

There are two main chromium doped fuel (CDF) vendors that will be considered in this report: Westinghouse and Framatome (formerly AREVA NP). There are other vendors who have been involved with the manufacture, experimentation, and irradiation of CDF, but the corresponding fuel products do not have a technology readiness level (TRL) high enough to be considered here (that is, the TRL is less than 5, the level at which test rods have been irradiated and performed successfully in a test reactor [5]).

From the literature review, there are limited references which describe the manufacturing process of the doped fuels; this is assumed to be due to the proprietary nature of the process. The ones that have been found are assumed to describe a process which is common to all vendors.

All the literature reviewed agrees that the sintering time required for doped pellets is reduced. This will result in increased production rate, saving time, money and resources – and making the fuel manufacturing more economical for the vendors.

3.1.1. Westinghouse

Westinghouse have been studying the use of doped UO_2 fuel for several decades. In the 1980s they investigated the use of Nb_2O_5 as an additive; this successfully resulted in fuel pellets with a large grain size and good PCI resistance, however, this addition also resulted in high fuel swelling and too much neutron absorption [6]. In 1998, Westinghouse began development of a new type of doped fuel pellet. They experimented with many of the additives discussed in Section 2; this resulted in the selection of chromia as their preferred choice.

Cr_2O_3 is a neutron absorber, so to reduce this effect, alumina (Al_2O_3) was also added to the fuel; magnesia (MgO) was used as an alternative to alumina in the earlier stages of development [6]¹. The alumina also enhances the grain growth induced by the chromium oxide. This synergy between the two dopants allows for a smaller chromia content (less neutron absorption), while still having the beneficial grain growth effects (Figure 1) [7]. The chromia content of Westinghouse fuel is limited to 1000 ppm or less [8], which can be compared with the 1600 ppm value for Framatome's CDF [9] (see next section). Westinghouse named their UO_2 fuel doped with chromium and aluminium oxides ADOPT (Advanced Doped Pellet Technology) fuel.

¹ As a comparison, the thermal (0.0253 eV) neutron absorption cross-sections of naturally-occurring Cr, Mg and Al are 3.1 barns, 0.06 barns and 0.23 barns, respectively (based on the JEFF-3.2 nuclear data library: see <http://www.oecd-nea.org/janisweb/tree/N/JEFF-3.2/SIG>).

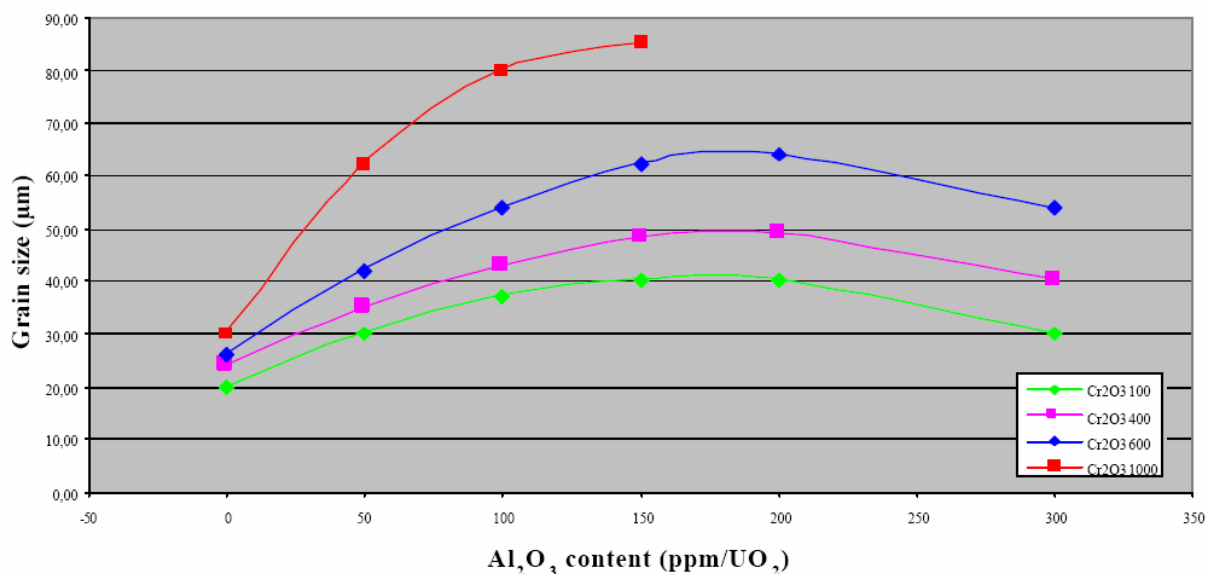


Figure 1: ADOPT grain size against Al₂O₃ content [7].

The manufacture of Westinghouse ADOPT pellets is described by Arborelius *et al.* [1] and Lindbäck [6]: AUC converted UO₂ powder is mixed with small quantities of Cr₂O₃ and Al₂O₃ for approximately 1 hour until they form full homogeneity. The mixed powder is then pressed to green pellets with a force of ~50 kN. The green pellets are sintered in a H₂/CO₂ atmosphere at a maximum temperature of 1800°C for 14 hours to form the final fuel product.

The ADOPT manufacture process has been monitored during several campaigns which covered several tons of production. By comparing how key parameters including density and grain size varied during several lots of production, it has been concluded that the manufacturing process is stable (Figure 2) [1].

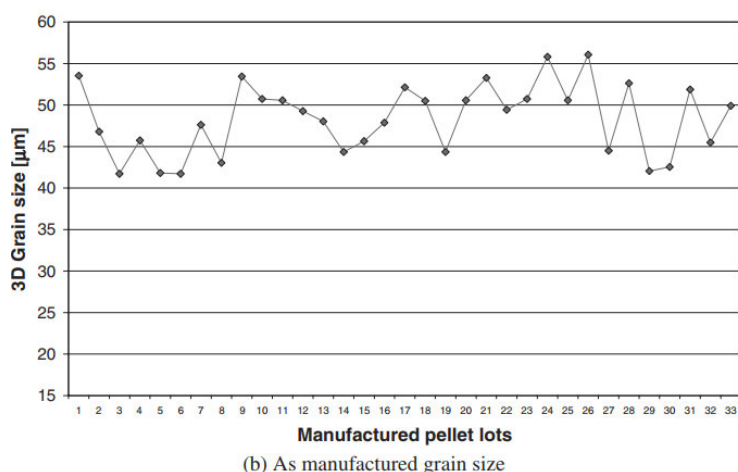
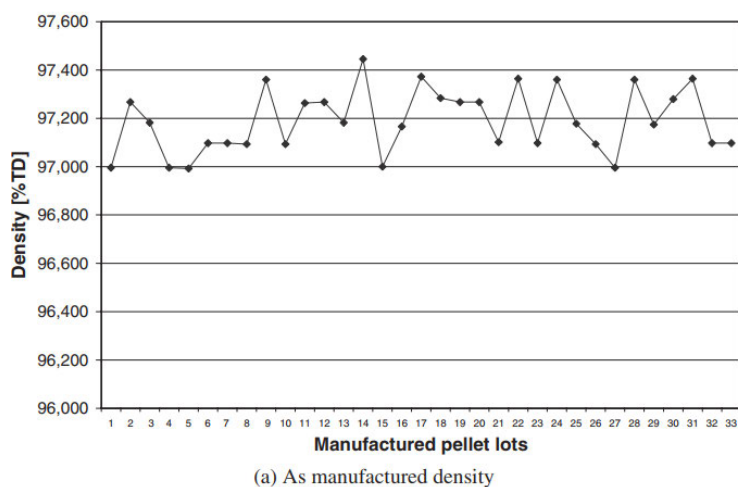


Figure 2: Plots showing the stability of the ADOPT pellet as-manufactured density (a) and grain size (b) [1].

It is not known whether ADOPT pellets with burnable absorber added have been manufactured or not, but it is highly likely that this has been the case given that full reloads of ADOPT fuel have been irradiated (see Section 5.1.1).

All ADOPT fuel has been manufactured at Westinghouse's Västeraås fuel fabrication facility in Sweden [1] [10].

3.1.2. Framatome (formerly AREVA NP)

In the early 1990s, Framatome began a programme of fuel pellet development designed to improve the fuel economics and performance without a reduction in safety margins [11]. One possibility considered by Framatome was to modify the manufacturing process to enlarge the grain size of the UO₂; this could be achieved through increased sintering time and duration, or through oxidative sintering [12]. These options, however, are not economical for industrial scale production.

OFFICIAL : COMMERCIAL

NNL 15231

ISSUE 1

The next step was to consider utilising an oxide dopant in the manufacturing process. Several oxides were investigated by Framatome, with Cr_2O_3 , TiO_2 and Nb_2O_5 giving the largest increases in grain size (Figure 3). However, TiO_2 was found to be too highly neutron absorbing (twice as much as Cr_2O_3) and Nb_2O_5 had a negative effect on diffusion and the release of fission gases [12]. In addition, further mechanical tests revealed that the TiO_2 and Nb_2O_5 additives gave lower plasticity than the Cr_2O_3 (Figure 4). The enhanced grain size and plasticity related to the chromia additive therefore made it the optimum choice for Framatome.

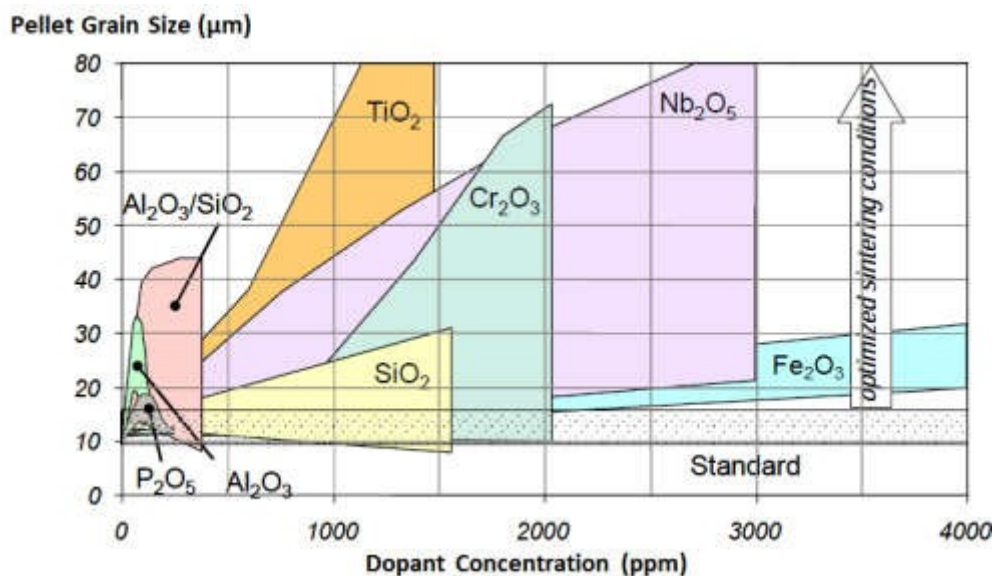


Figure 3: The effect of dopant concentration on grain size for various additives [12].

OFFICIAL : COMMERCIAL

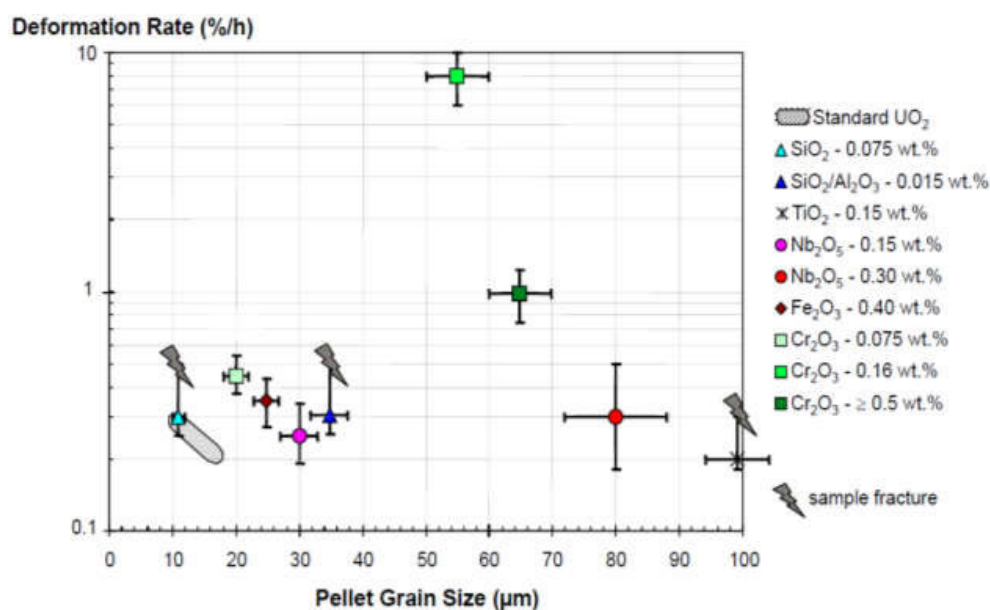


Figure 4: Deformation rate against pellet grain size for various additives [12].

Framatome then performed further studies to determine the fundamental mechanisms which governed the UO₂ doping with chromia; this included the sintering conditions necessary to favour chromia dissolution in the UO₂ matrix and the solubility limit of the chromia in UO₂ (discussed in more depth in Section 3.1.3) [13]. Through this, Framatome were able to specify an optimum value of 0.16 wt% Cr₂O₃ (1600 ppm); this allowed the chromia to change the desired aspects of the microstructure and plasticity without changing the thermal properties of the fuel pellets [12].

There was no specific reference found to describe the Framatome CDF manufacture process: as mentioned earlier, it is assumed that this process is similar to the one used by Westinghouse. However, Framatome have (a) published data demonstrating the stability of their fuel product (Figure 5), and (b) demonstrated improved resistance to pellet chipping during pellet handling and rod loading [12]. With respect to (b), impact testing showed a 40% reduction in weight loss relative to undoped pellets with the same end-face design. Framatome infer that this is due to the larger grain size being able to absorb the impact energy more efficiently.

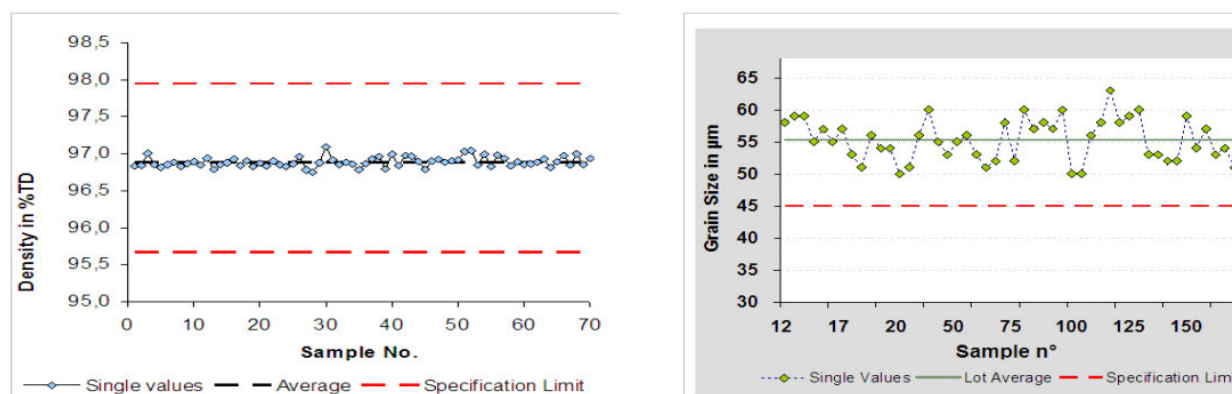


Figure 5: Data illustrating stability of Framatome CDF as-manufactured density and grain size [9].

Framatome CDF can be manufactured with or without gadolinia included as a burnable absorber. The chromia content of the gadolinia-doped pellets appears to be the same as that of the 'standard' CDF – that is, 0.16 wt% [14].

Framatome CDF was originally manufactured in the FBFC facility in Belgium [15]. More recently, fuel was manufactured at the Horn Rapids Road facility in the USA as part of the USDOE enhanced accident tolerant fuel (EATF) programme [16]. Fabrication in other Framatome facilities is also possible.

3.1.3. Issues associated with the manufacture of CDF

3.1.3.1. Volatilisation

An issue that can occur in the manufacture of chromium doped fuels is the volatilisation of chromium from CDF during the sintering process. This volatilisation results in chromium escaping the pellets and possibly damaging the furnace. Since chromium (at least in its hexavalent form) is both toxic and carcinogenic, there is also the potential for adverse health effects to operators [16]. In terms of the impact on the fuel pellets, the loss of chromium from the pellets will give an unwanted non-uniform distribution of chromium and will adversely affect the pellet properties and microstructure.

Through thermogravimetric experiments, dilatometry and differential thermal analysis, Peres *et al.* determined that the release of Cr due to volatilisation occurs due to: (a) the dissociation of Cr_2O_3 in second-phase particles (not dissolved in UO_2) and the subsequent release of Cr from open porosity; (b) the volatilisation of chromium dissolved in UO_2 and the subsequent release from open porosity; and (c) the volatilisation of Cr dissolved in UO_2 and the subsequent release via diffusion through the fuel matrix and along grain boundaries [17]. The relative importance of each of these mechanisms is in turn dependent on the temperature, heating rate and atmospheric conditions of the sintering process.

By comparing with the results from volatilisation of Cr_2O_3 powder, which began at temperatures which increased from 1430°C at the lowest oxygen potential to 1660°C at the highest oxygen potential [17], the volatilisation of the chromium doped UO_2 pellets could be

further understood. For the CDF samples with a high concentration of dopant (0.9 mol%), the volatilisation was found to be similar to that of the Cr_2O_3 powder, since the concentration is so high that a significant fraction of the chromia is precipitated (that is, not dissolved) in the UO_2 crystal structure [17].

It is therefore important for fuel vendors to control the sintering conditions carefully to ensure the lowest possible levels of chromium volatilisation. This will involve a temperature high enough to complete the sintering process but not so high that it causes excess chromium volatilisation, and an oxygen potential high enough to minimise the chromium volatilisation but low enough to meet stoichiometry and grain size requirements for the sintered material [17].

The Cardinaels *et al.* data discussed in Section 3.1.3.2 show that – even for controlled volatilisation in Framatome’s industrial process – there remains a near-surface effect whereby there is preferential volatilisation in the outer $\sim 200 \mu\text{m}$ of the finished pellets (after grinding has removed the outer $135 \mu\text{m}$ of material) [18].

3.1.3.2. Solubility

Another known issue for chromium doped fuels is the solubility of chromium oxide in UO_2 . If the solubility limit of chromium oxide is exceeded, then the chromia will no longer be fully dissolved in the matrix, the effects of the addition will be saturated, and there may be unwanted effects due to the presence of second-phase particles.

The through-pellet distribution of chromia in Framatome CDF pellets was investigated by Cardinaels *et al.* using electron probe microanalysis (EPMA) to perform full diameter line scans of UO_2 pellets doped with varying chromia concentrations [18]. The pellet designations were:

- IFA0 – Framatome UO_2 with 500 ppm Cr_2O_3
- IFA2 – Framatome UO_2 with 1000 ppm Cr_2O_3
- IFA3 – Framatome UO_2 with 1600 ppm Cr_2O_3

The IFA2 and IFA3 pellets (but not the IFA0 pellets) were sampled from those manufactured for irradiation in the OECD Halden Reactor Project IFA-716 experiment.

Figure 6 shows the results from the full diameter scans of these pellets; the sharp peaks in chromia content are associated with chromia precipitates. The peaks are highest for IFA3 due to the amount of dopant added exceeding the solubility limit of chromia in UO_2 . Despite the dopant concentrations of IFA0 and IFA2 being lower than the solubility limit, precipitates still form; this is due to the slow kinetics of solubilisation of chromia in the UO_2 matrix [18] [19].

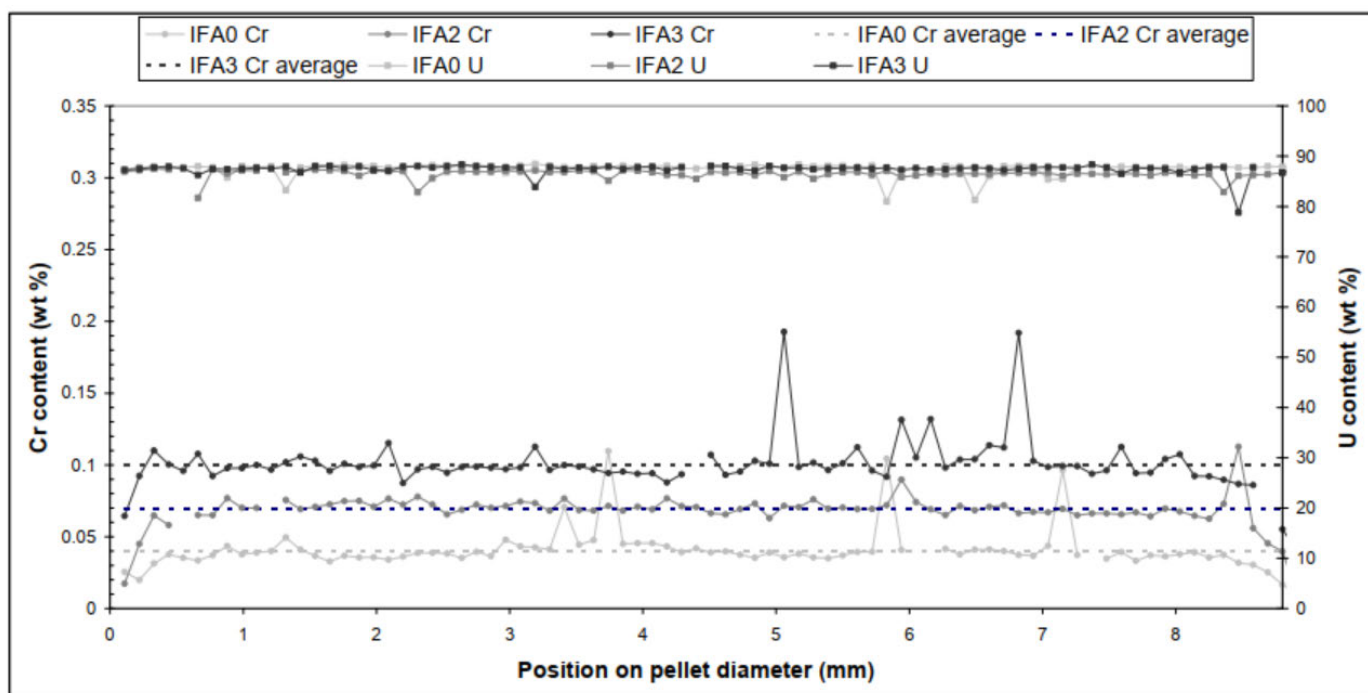


Figure 6: Full diameter EPMA line scans of UO_2 pellets doped with 500, 1000 and 1600 ppm Cr_2O_3 (IFA0,2,3 respectively) [18].

Further detail on the extent of precipitates was obtained by mapping three zones of each of the different fuel pellets. From Figure 7 it can be seen that the higher the chromia content, the greater the number and greater the size of the precipitates that form; this is due to the non-solubilisation of the chromia during the sintering process [18].

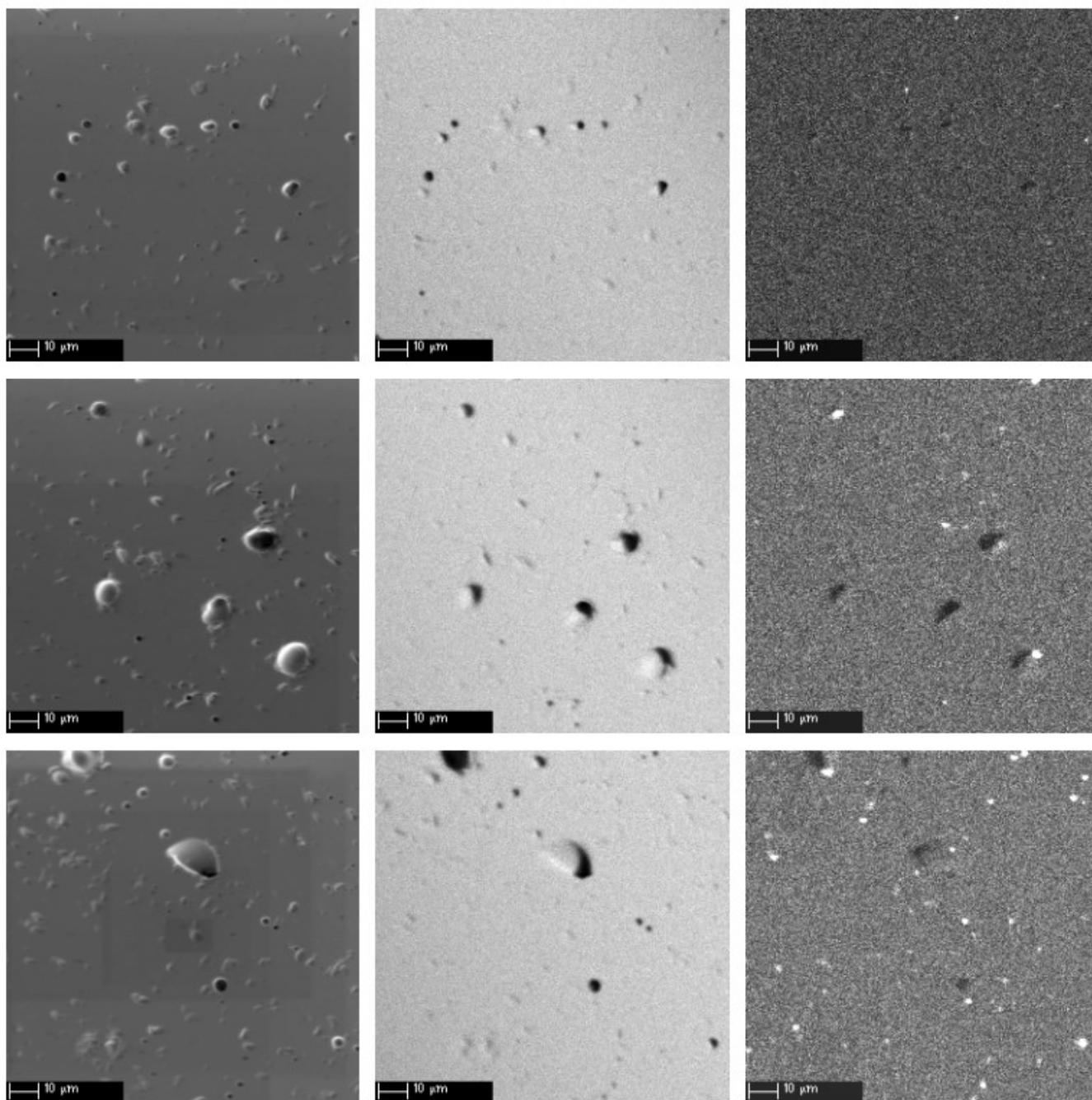


Figure 7: EPMA local area mapping of IFA0 (top), IFA2 (middle) and IFA3 (bottom). The images represent the: secondary electron image (left), UMa intensity map (middle) and CrKa intensity map (right) [18].

The solubility limit is dependent on the sintering conditions used during fuel manufacture, namely the temperature and oxygen potential, with the latter itself dependent on the oxygen partial pressure.

Riglet-Martial *et al.* performed experiments to determine the solubility limit of Cr_2O_3 in different conditions using electron probe microanalysis (EPMA) and scanning electron microscopy (SEM). In doing so, they also confirmed the strong influence of the oxygen potential on the grain size of the fuel during sintering (as suggested previously by Bourgeois) [20]. At low oxygen potentials, the stable state of chromium was as solid (s) chromium metal, and no increases in grain size were observed, whereas at higher oxygen potentials, the stable state of chromium was as liquid (l) CrO or solid (s) Cr_2O_3 , and significant increases in grain size were observed [20].

Riglet-Martial *et al.* combined their experimental results with those available in the literature to further understand the process. They found that the solubility of Cr_2O_3 in UO_2 increases with both increasing oxygen partial pressure (Figure 8) and increasing temperature (Figure 9). This behaviour is consistent with the solubility increasing with increasing oxidation state of the chromium in the stable chromium phase; that is, the solubility where the stable phase is solid Cr metal (Cr^0 oxidation state) is less than the solubility where the stable phase is liquid CrO (Cr^{2+} oxidation state) which in turn is less than the solubility where the stable phase is solid Cr_2O_3 (Cr^{3+} oxidation state) [20].

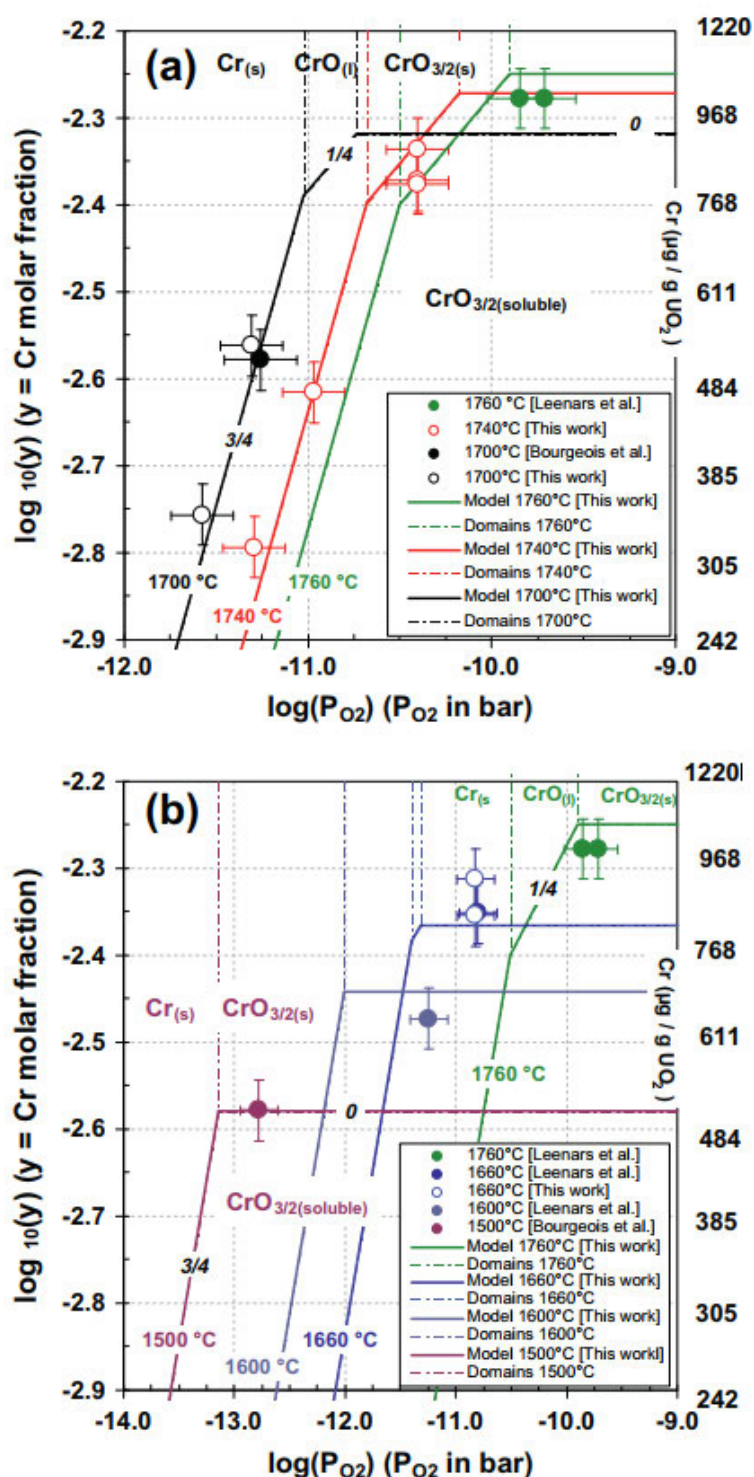


Figure 8: Comparisons with results from experimentation, literature and a thermal solubility model for variations with the oxygen partial pressure of the Cr_2O_3 solubility in UO_2 : (a) within the stability areas of $Cr_2O_3(s)$, $CrO(l)$ and $Cr(s)$ for 1700°C and above; (b) within the stability areas of $Cr_2O_3(s)$, $CrO(l)$ and $Cr(s)$ for 1500-1760°C [20].

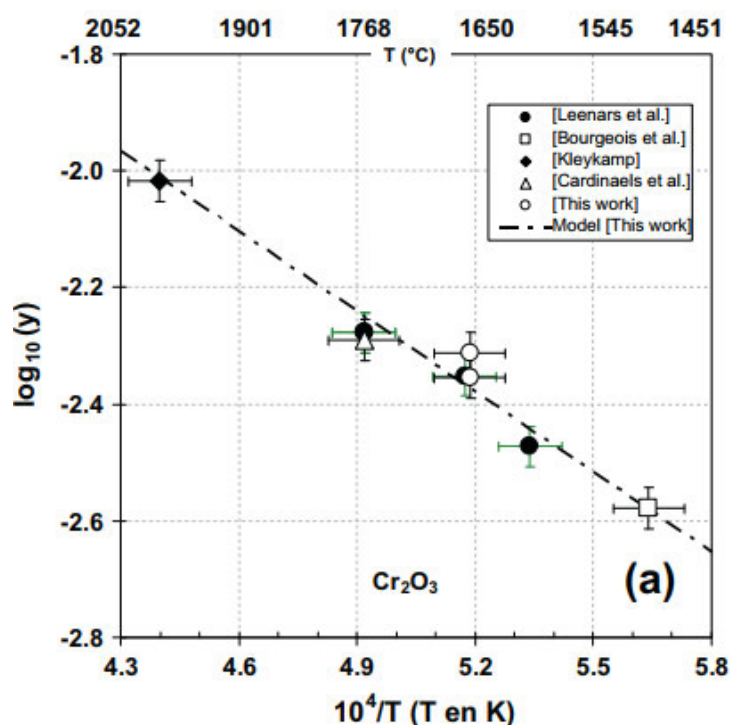


Figure 9: Comparisons with results from experimentation, literature and a thermal solubility model for variations in the solubility of Cr_2O_3 in UO_2 as a function of the temperature [20].

Cr_2O_3 contents above the solubility limit may also give rise to a decrease of fuel density due to solarisation (bloating associated with formation of gas-filled porosity), at least in gadolinia-doped pellets [14].

3.2. Microstructure and Properties

3.2.1. Grain size

All the literature reviewed agree that the addition of chromium dopants to UO_2 fuel pellets enlarges the grain size. This is viewed by many sources as one of the most important effects of the chromia addition to the fuel. The main benefit of an enlarged grain size is that it extends the diffusion length the fission gas and volatile fission product atoms must travel to be released through the grain boundaries of the pellets, thereby reducing the volume of fission gases and volatile fission products released [21]. Discussed further in Section 4.2.6, a reduction in fission gas release (FGR) reduces the internal pressure of the fuel rods in normal operation, thereby increasing margins to design limits intended to prevent clad creep rupture. The consequent reduction in inter-granular fission gas bubble swelling also reduces the likelihood of PCI failures and enhances the accident tolerance of the fuels via reduced burst fission gas release and reduced fragmentation during high temperature faults.

The extent of the grain size enlargement is dependent on the concentration of the chromium oxide in the fuel and the sintering conditions (in particular, the sintering temperature). For

the Westinghouse ADOPT pellets, the increase in grain size as a function of chromium oxide (and aluminium oxide) concentration was shown in Figure 1. The addition of alumina was found to contribute to the grain growth enhancement for contents up to 200 ppm [1]. For ADOPT pellets with 500 ppm chromia and 200 ppm alumina, the grain size was measured to be 50 μm : a 5x increase in grain size over undoped pellets [1]. Similarly, the Framatome Cr_2O_3 -doped UO_2 fuel (0.16 wt% Cr_2O_3) also showed an increase in grain size from 8 μm for the standard UO_2 to around 60 μm for the chromium doped UO_2 (Figure 10) [13].

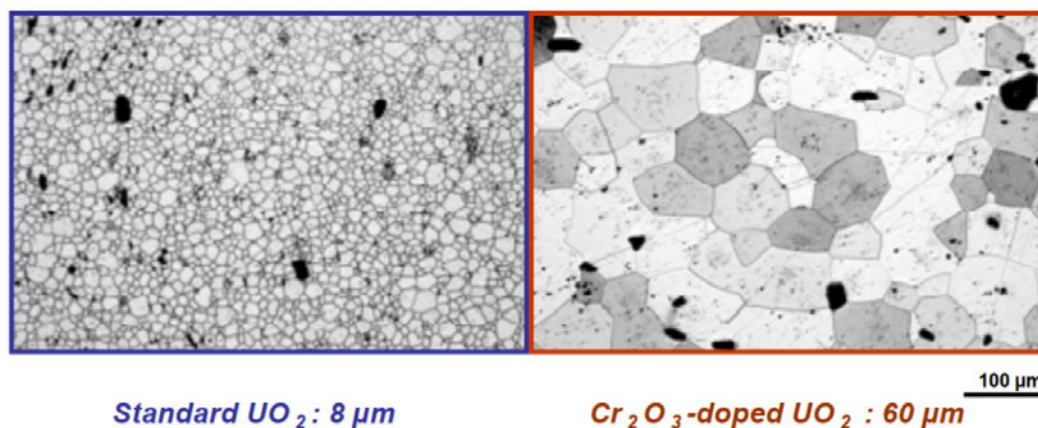


Figure 10: An image showing the enlarged grain size of the Framatome Cr_2O_3 -doped UO_2 fuel pellets when compared to standard UO_2 [13].

The average grain size of Framatome's gadolinia-doped CDF appears to be similar to that of 'standard' CDF, at "larger than 40 μm " [14].

3.2.2. Density

Based on the low chromia levels, the chromium being in solid solution, and the negligible difference in lattice parameter between doped and undoped fuel, the theoretical density of CDF (the density of the fuel matrix, or the hypothetical density of fuel with zero porosity) is expected to be very similar to that of undoped UO_2 [22]. Hence, differences in density are dominated by differences in densification behaviour of the green pellets during the sintering process which forms part of the pellet manufacture. As discussed in Section 3.1, the addition of a chromium dopant to the UO_2 fuel during manufacture reduces the necessary sintering time. This is caused by the effect of the additive on the densification of the pellets during the sintering process.

As the additive is added in such quantities that it is at or below the solubility limit of chromia in UO_2 , no large chromia second-phase particles are observed in the fuel matrix [13]. This means that densification is dominated by bulk diffusion of vacancies in the matrix, which is enhanced in CDF consistent with the enhanced grain growth. Thus, there is greater densification of the fuel pellets during manufacture.

All of the literature reviewed agrees that the density of the fuel pellets increases with the addition of Cr_2O_3 . For ADOPT pellets, Arborelius *et al.* reported an increase in pellet density from 96.7% of theoretical for UO_2 pellets to 97.3% of theoretical for the doped pellets when starting from a similar green pellet density [1]. The level of Al_2O_3 addition has little influence on the densification of the pellet. For Framatome pellets, Delafoy *et al.* report a density of greater than 96% the theoretical density [13].

The density of Framatome's gadolinia-doped CDF may be somewhat lower than that of the 'standard' CDF [14].

The increased density of the fuel has the main benefit of an increase in the fissile material (^{235}U) density, making the fuel cycle more economical [13]. The reduced porosity volume fraction also increases the fuel thermal conductivity, giving reduced fuel temperatures and hence reduced fission gas release and increased margin to fuel melting.

3.2.3. Porosity

For Westinghouse ADOPT pellets, the additional densification of the fuel pellets during sintering leads to a decrease in the porosity volume fraction while the size distribution of the porosity remains constant [1]. The shape of the pores can also change as a result of the additives: Arborelius *et al.* reported that the pores of the standard UO_2 are more irregular whereas the pores of the doped pellets have a rounder cross-section (Figure 11). The reduced porosity and increased regularity of the pores enhances the dimensional stability of the pellets under irradiation.

Framatome's chromia doped fuel also has reduced porosity and therefore increased dimensional stability under irradiation [13]. No information on pore shapes in Framatome CDF is available.

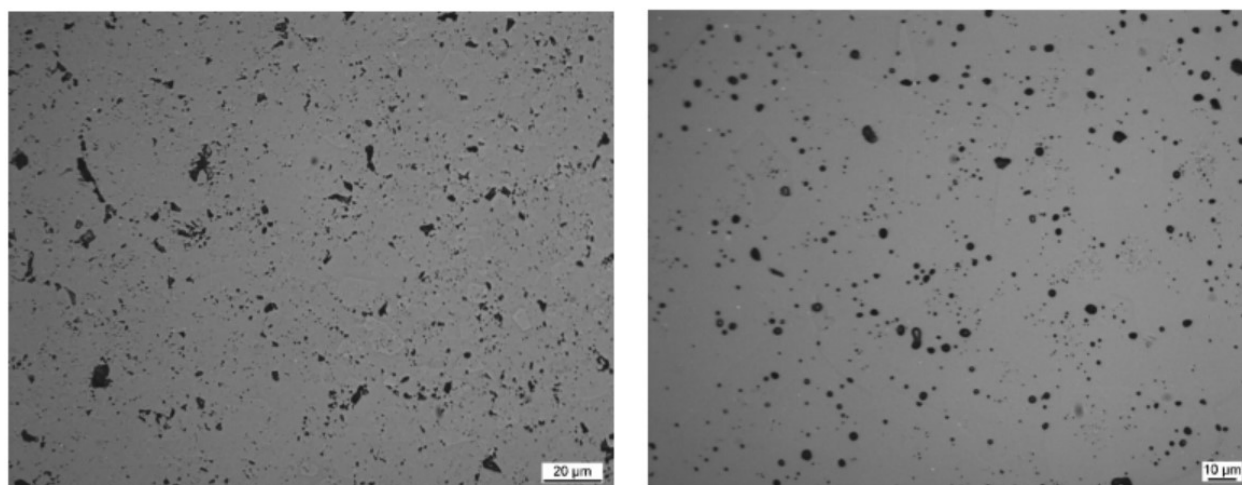


Figure 11: Pore shape of standard UO_2 (left) and ADOPT (right) pellets [1].

3.2.4. Thermal properties

There is generally very little experimental evidence of the effect of dopants on the thermal properties of fuel pellets. It is assumed that when added in small enough concentrations, the chromium oxide dopants do not greatly affect the thermal properties of the fuel [12].

Arborelius *et al.* describe some experiments performed to test this assumption for Westinghouse ADOPT pellets. Similarly, a report from Framatome describes the experiments performed on their fuel, both in-house (thermal diffusivity) and at the Materials Research Unit of JRC-ITU, but much of this report has been redacted (due to the proprietary nature of the results). All of these experiments were performed on unirradiated fuel.

3.2.4.1. Thermal expansion

Using a differential dilatometer, the thermal expansion coefficient for ADOPT fuel was determined in the temperature range of 20-1500°C [1]. The results showed that the difference between the ADOPT and standard UO₂ pellets is small and within the uncertainty of the measurements.

Framatome do not appear to have performed measurements of the thermal expansion of their CDF; instead, they argue (as part of US licensing) that: (a) the chromium is in solid solution in the UO₂ fuel matrix at a concentration typical of impurity levels; (b) plutonium and gadolinium in solid solution in the UO₂ fuel matrix (in the context of mixed oxide fuel and gadolinia-doped fuel) at much larger concentrations has only a minor impact on thermal expansion coefficient; (c) there is no significant effect of fission products in solid solution on thermal expansion coefficient (in the context of irradiated UO₂ fuel); and hence (d) that the impact of the addition of chromia on the thermal expansion coefficient of UO₂ is negligible [22]. It is judged that this is a reasonable argument.

3.2.4.2. Specific heat capacity

The specific heat capacity for Westinghouse ADOPT fuel was measured using a differential scanning calorimeter [1]. The results show that there is a negligible difference between the specific heat capacity of the ADOPT and standard UO₂ pellets.

Differential scanning calorimetry was also used to measure the specific heat capacity of Framatome chromia doped fuel (with and without gadolinia included as a burnable absorber). The results also showed a negligible difference between the specific heat capacity of the doped pellets and the standard UO₂ pellets [22].

3.2.4.3. Thermal diffusivity

For Westinghouse ADOPT fuel, the thermal diffusivity of the fuel pellets was measured using a laser flash technique. This involved samples of doped and undoped pellets being sliced into discs. One side of the discs was heated with a laser flash and the temperature on the other side of the disc as a function of time was measured [1]. After taking measurements between 20°C and 1400°C in steps of 100°C, there was no significant difference measured between the ADOPT and standard UO₂ pellets (presumably after correcting for the effects of differences in porosity volume fraction).

The same laser flash technique was used to determine the thermal diffusivity of Framatome CDF (with and without gadolinia included as a burnable absorber [14]). The measurements were performed at several temperature levels with long hold times at each temperature step to ensure stable measuring conditions [22]. The maximum temperature used was 1650°C (the limit of the furnaces) [22]. The results are not available: they were redacted from the Framatome report. However, Framatome note that: (a) "The thermal resistivity increases (and thermal conductivity decreases) as the chromia content increases" (in the context of development of a CDF thermal conductivity model for the RODEX fuel performance code) [22]; and (b) "Cr₂O₃ doping has no significant influence on the thermal conductivity of the (U-Gd)O₂ fuel within the margin of measurement uncertainty" [14]. Hence, it can be tentatively concluded that: (1) the thermal diffusivity of Framatome CDF without gadolinia included is somewhat lower than that of chromia-free fuel, with the reduction increasing with increasing chromia content (due to chromia – like impurities and fission products – increasing phonon scattering); and (2) the thermal diffusivity of Framatome CDF with gadolinia included is essentially unchanged from that of chromia-free fuel (presumably because the phonon scattering effect of the chromia is dominated by that of the gadolinia).

3.2.4.4. Thermal conductivity

The thermal conductivity of the fuel matrix is dependent on its thermal diffusivity, heat capacity and density (Equation 1). In the case of unirradiated ADOPT fuel and unirradiated Framatome CDF with gadolinia, none of these are significantly changed by the addition of chromia (see above). It can therefore be concluded that the thermal conductivity of the unirradiated fuel matrix is also unchanged. However, the thermal conductivity of the unirradiated doped fuel pellets will still be increased somewhat over that of undoped pellets due to the reduced porosity volume fraction (see Section 3.2.2). In the case of unirradiated Framatome CDF without gadolinia, the thermal diffusivity is reduced somewhat, while the heat capacity and density are unchanged, and so the thermal conductivity of the unirradiated fuel matrix is also reduced somewhat. The net effect of this and the reduced porosity volume fraction on the thermal conductivity of the unirradiated doped pellets is unclear.

$$\lambda = \alpha \cdot \rho \cdot C_p$$

Equation 1: Thermal conductivity equation. λ = thermal conductivity, α = thermal diffusivity, C_p = isobaric specific heat capacity [6].

In-pile thermal conductivity – and in particular degradation of thermal conductivity with burnup – has not been measured directly, but can be inferred from in-pile measurements of fuel centreline temperature in test reactor irradiations carried out with a fuel thermocouple. Of such irradiations, both the Halden Reactor Project experiments described in Section 4.1 and the REMORA irradiation of Framatome CDF (performed in the Osiris test reactor using a single segment pre-irradiated in a commercial PWR to ~ 62 MWd/kgU) [23] suggest that the in-pile thermal conductivity of CDF – including the thermal conductivity degradation with burnup – is unchanged from that of undoped UO₂.

3.2.4.5. Melting temperature

The melting temperature of the ADOPT and standard UO₂ pellets was determined using a laser-pulse melting method and a high-speed mono- and poly-chromatic pyrometer [1]. The results showed no significant difference between the ADOPT and standard UO₂ pellets.

For the Framatome chromia doped fuel, the melting temperature of samples both with and without gadolinia added as a burnable absorber was determined using laser heating and fast multi-channel pyrometry [22]. The results are not available: they were redacted from the Framatome report. However, there is the suggestion that the melting point was lowered slightly by the addition of chromia (since Framatome note that the addition of impurities or dopants decreases melting temperature).

3.2.5. Mechanical properties

3.2.5.1. Creep rate

The creep rate is an important property of nuclear fuel: the higher the creep rate, the softer the fuel pellets, resulting in reduced stresses on the cladding during power transients, and hence a reduced propensity for PCI failure (see Section 4.2.3 for more information on the pellet-cladding interaction behaviour). For undoped UO₂ fuel, out-of-pile creep occurs by two thermal mechanisms: diffusional creep, which dominates at low stresses, and dislocation climb and annihilation creep, which dominates at high stresses (there is also arguably a third diffusion mechanism which applies at very high stresses, possibly due to dislocation core diffusion, but this can in general be ignored). The net result is a two-term (secondary) creep rate equation as follows:

$$\dot{\epsilon} = \frac{C_1 \sigma}{g^2} \exp\left(-\frac{Q_1}{kT}\right) + C_2 \sigma^{4.5} \exp\left(-\frac{Q_2}{kT}\right)$$

Equation 2: (Secondary) out-of-pile creep rate equation for undoped UO₂. C₁ and C₂ are constants, σ = stress, g = grain size, Q₁ and Q₂ are activation energies, k = Boltzmann's constant, T = absolute temperature.

where the first term on the right-hand side represents low-stress thermal creep, and the second term on the right-hand side represents high-stress thermal creep.

Thus, in undoped UO₂, the out-of-pile creep rate at low stresses is inversely proportional to the square of the grain size, and the out-of-pile creep rate at high stresses is independent of the grain size.

Experiments have been performed by both Framatome and Westinghouse to determine the extent of the effect of chromium doping (and aluminium doping in the case of Westinghouse) on the out-of-pile creep of UO₂ fuel pellets. These experiments involved applying a compressive load to the fuel at high temperatures (1200-1600°C for the Framatome experiments, and 1000-1700°C for the Westinghouse experiments) for several hours and measuring the deformation as a function of time [2] [6] [14] [24] [25].

The experiments performed by Framatome on their CDF (which included tests on CDF with gadolinia included as a burnable absorber [14]) found that the behaviour described above for

undoped UO_2 fuel is not observed: instead, the thermal creep rate increases with increasing chromia content, and therefore with increasing grain size, at all stress levels investigated (20-90 MPa): see Figure 12 and Figure 13. This is attributed to a lack of diffusional creep and a dislocation climb and annihilation mechanism which is more effective in doped fuel (due to an increase in the density of mobile dislocations [14]). The (secondary) creep rate was increased by a factor of up to 10 when compared to undoped UO_2 [24]. The effect of the chromia addition saturates at high additive concentrations even if the grain size is enlarged, since the solubility limit of the Cr_2O_3 in UO_2 is then exceeded [24].

The experiments performed by Westinghouse on ADOPT fuel showed a much more modest effect of the chromia (and alumina) on (secondary) creep rate: see Figure 14. (At a temperature of 1500°C and an applied stress of 45 MPa, the increase in creep strain rate was only from 0.4% per hour to 0.5% per hour [2].) This is perhaps not surprising, given that their chromia levels were in the range 300-650 ppm (together with alumina levels of 70-150 ppm), compared with the 750-2250 ppm levels investigated by Framatome. The Westinghouse experiments also showed that there is no increase in creep rate at 1000°C (at least at the stress of 25 MPa investigated) [6], and that the increase in creep rate becomes more significant as temperature increases [25]. Any mechanistic differences in creep for doped UO_2 (that is, any deviations from the behaviour described by Equation 2) do not appear to have been explored by Westinghouse; it is unclear whether the mechanistic differences deduced by Framatome for their CDF are also relevant to ADOPT fuel.

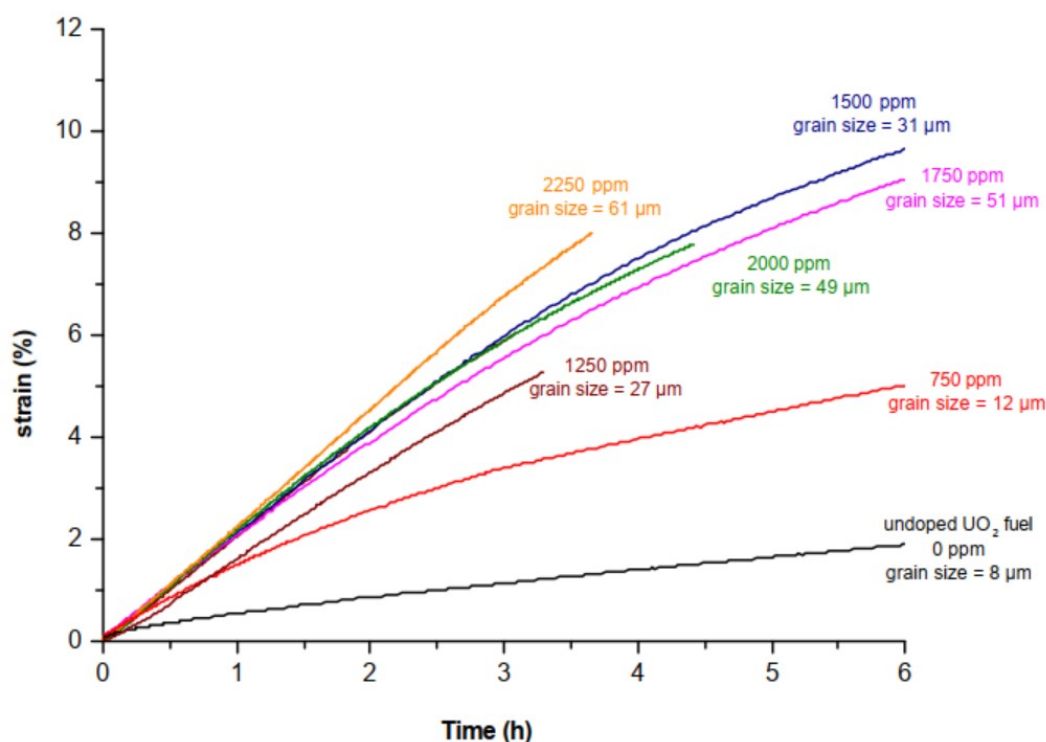


Figure 12: Strain vs. time results from out-of-pile creep tests on Framatome undoped UO_2 and doped fuel with various dopant concentrations and grain sizes (at 1470°C and with an applied stress of 45 MPa) [24].

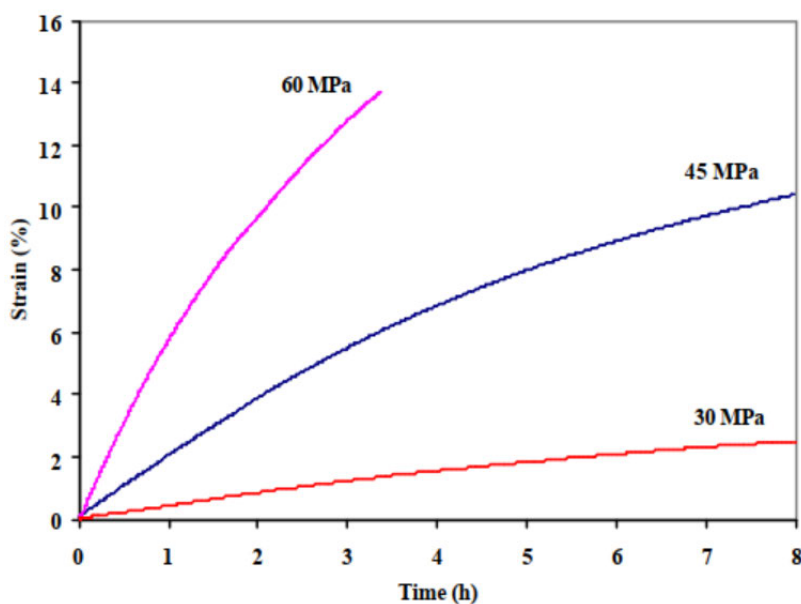


Figure 13: Strain vs. time results from out-of-pile creep tests on Framatome chromium doped UO₂ at various stresses (0.2 wt% Cr₂O₃ at 1470°C) [24].

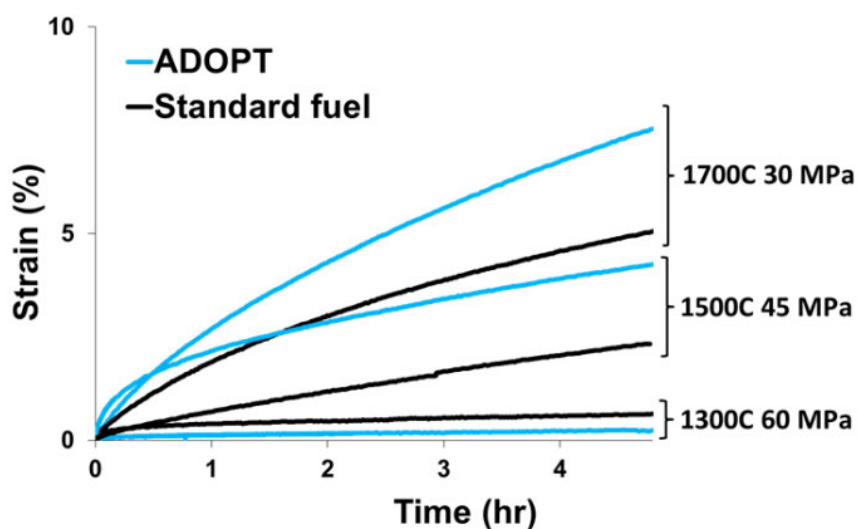


Figure 14: Strain vs. time results from out-of-pile creep tests on ADOPT fuel [25].

In undoped UO₂ fuel, irradiation-induced creep occurs in-pile in addition to thermal creep, and the diffusional (low-stress) creep rate is enhanced. With reference to Equation 2, the net result in-pile is therefore a three-term (secondary) creep rate equation as follows:

$$\dot{\epsilon} = \frac{C_1(1 + C_3\dot{F})\sigma}{g^2} \exp\left(-\frac{Q_1}{kT}\right) + C_2\sigma^{4.5} \exp\left(-\frac{Q_2}{kT}\right) + C_4\dot{F}\sigma$$

Equation 3: (Secondary) in-pile creep rate equation for undoped UO₂. C₁ to C₄ are constants, σ = stress, g = grain size, Q_1 and Q_2 are activation energies, k = Boltzmann's constant, T = absolute temperature, \dot{F} = fission rate per unit volume.

where, from left to right, the three terms on the right-hand side represent low-stress thermal creep, high-stress thermal creep, and irradiation-induced creep. Measurements obtained from the OECD Halden Reactor Project in-pile fuel creep experiment IFA-701 show that – at least for the ADOPT fuel that was tested – irradiation-induced creep also occurs for CDF, and that the irradiation-induced creep rate is unchanged from that of undoped fuel (Figure 15). Assuming the absence of diffusional creep in-pile (since it was shown to be absent out of pile for Framatome CDF), and noting the absence of irradiation enhancement of dislocation climb and annihilation creep for undoped fuel, it can therefore be tentatively concluded that the in-pile creep of CDF is as out of pile, but with an additional irradiation-induced creep component identical to that for undoped fuel.

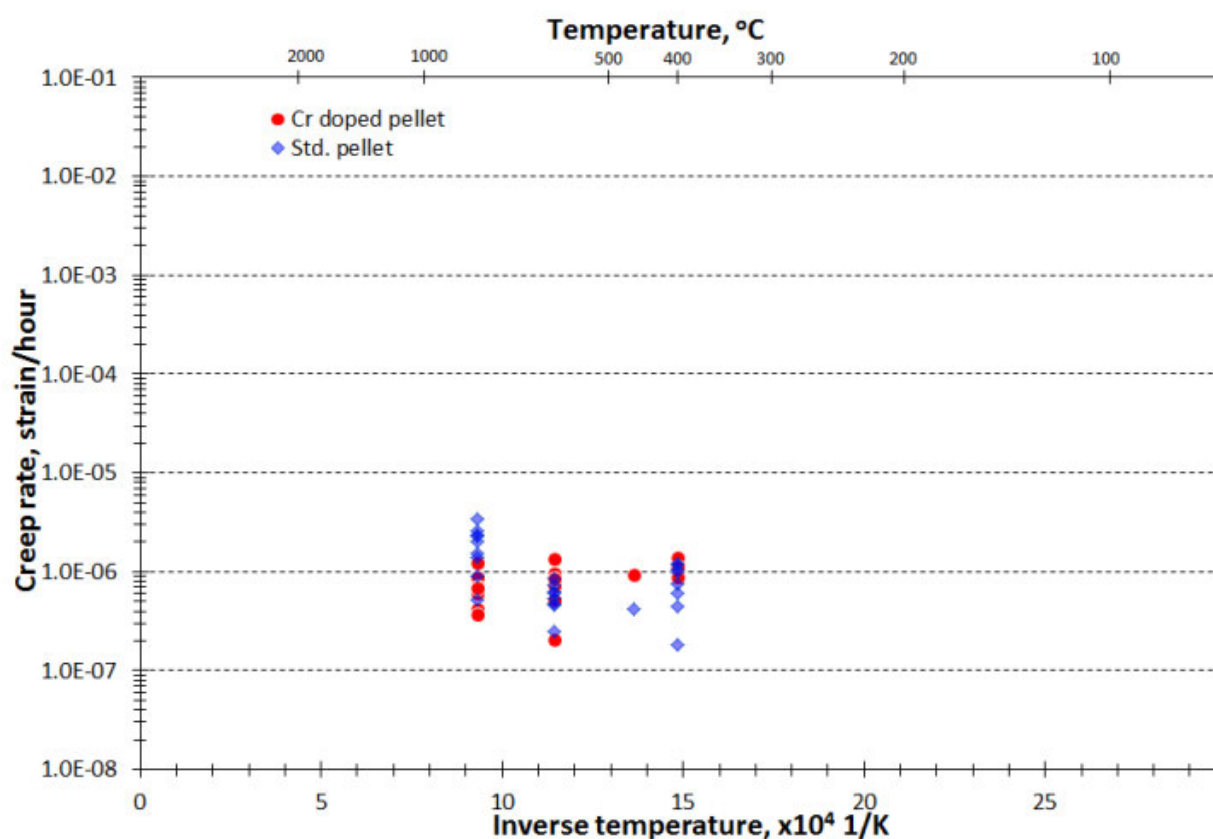


Figure 15: (Irradiation-induced) creep rate of chromia doped (ADOPT) and undoped UO₂ fuel as measured in the IFA-701 in-pile creep experiment [26].

3.2.5.2. Elastic moduli

It appears that no measurements of fuel elastic moduli have been performed on CDF. However, as part of US licensing of CDF, Framatome convincingly argue that [22]:

- (a) The possible variation of elastic properties is not fundamentally affecting the fuel behaviour under normal operating conditions or anticipated operational occurrence (AOO) and accident conditions.
- (b) According to the data published in the literature, the Young's modulus of standard UO_2 can vary with characteristics such as grain size, stoichiometry or fuel porosity, however, the effect of these parameters is very limited compared to that of temperature.
- (c) The intrinsic impact of additives, including gadolinium or plutonium, up to high amounts (10-20 wt%) remains low with respect to Young's modulus and negligible for Poisson's ratio.
- (d) Considering that the chromia addition in UO_2 is low, no effect is anticipated on the UO_2 fuel Young's modulus and Poisson's ratio.

3.2.5.3. Fracture strength

There is only evidence of CDF fracture strength measurements having been performed by Framatome. The details of the testing are unavailable, but Framatome conclude that the fracture strength is consistent with that of undoped UO_2 with the same (large) grain size – that is, they conclude that the fracture strength is in line with the microstructural differences, and not due to any intrinsic effect of chromia itself [22]. Since the fracture strength of undoped UO_2 decreases with increasing grain size [22], this suggests that the fracture strength of CDF is lower than that of standard undoped UO_2 (but only due to the larger grain size). This behaviour is also proposed by Westinghouse [25].

4. Phenomenology

In this section, the phenomenology of chromium doped UO₂ fuel pellets will be discussed. This will include descriptions of the results from experimental irradiations in test reactors. There is a particular focus on the experiments performed within the OECD Halden Reactor Project, since these constitute independent irradiation testing of fuel-vendor-provided material.

4.1. Halden Reactor Project Experiments

Situated in Halden, Norway, the Halden boiling water reactor (HBWR) operated from 1958 to June 2018 and was used to perform hundreds of successful test irradiations of fuels and other nuclear materials under the framework of the OECD Halden Reactor Project (which is still ongoing despite the shutdown of the HBWR) [27]. The project is managed by the Norwegian Institute for Energy Technology (IFE) and is funded by various international organisations and research groups.

Three integral rod Halden experiments involving CDF have been performed in the Halden Reactor Project: IFA-677, IFA-716 and IFA-720.3. For each experiment, the experimental setup is explained below (Sections 4.1.1 to 4.1.3), and the relevant phenomenology displayed by the fuel pellets is included in the phenomenology discussion in Section 4.2. CDF was also included in the separate effects experiment IFA-701; results from this dedicated fuel creep test were discussed in Section 3.2.5.1.

4.1.1. IFA-677

The IFA-677 experiment was designed to investigate the effects of a change in fuel assembly loading strategy. Historically, an “out-in-in” strategy was preferred for assembly loading patterns; this involves loading the fresh fuel assemblies into positions towards the periphery of the core to minimise their initial operating power [28]. More recently, there has been a trend towards an “in-out-out” strategy whereby the fresh fuel assemblies are loaded closer to the centre of the core and then gradually moved outwards during subsequent reloads [28]. The benefits of the “in-out-out” approach are increased neutron economy and the minimisation of the fast neutron dose to the pressure vessel. However, this approach leads to high powers in the first cycle of irradiation [28]. The effects of this high initial rating on the thermal performance of the fuel were the subject of the Halden IFA-677 experiment.

The experiment used a single cluster of 6 rods with fuels from Westinghouse, Framatome and Global Nuclear Fuels (GNF) with various grain sizes, densities and additives (Table 1) [29], and operated under normal Halden BWR coolant conditions. All rods were equipped with upper and lower fuel thermocouples to measure fuel centreline temperature, a fuel extensometer to measure fuel stack elongation, and a pressure transducer to measure rod internal pressure. Rod 2 was also equipped with a clad extensometer to measure cladding elongation. Rods containing CDF were limited to two of the rods (1 and 5) supplied by Westinghouse (ADOPT fuel). The irradiation began in January 2005 and was completed in

September 2007 at a rig average burnup of 26 MWd/kgU. Powers were kept high throughout the irradiation, initially at ~ 45 kW/m and later at ~ 35 kW/m [29].

Table 1: The fuel pellets used in the Halden IFA-677 experiment [29].

Rod	Manufacturer	Cr ₂ O ₃ Content (ppm)	Al ₂ O ₃ Content (ppm)	Grain Size (μ m)	Density (g/cm ³)
1	Westinghouse	900	200	56	10.69
2	Framatome	-	-	16	10.451
3	GNF	-	-	15	10.58
4	GNF	-	-	15	10.58
5	Westinghouse	500	200	45	10.70
6	Westinghouse	-	-	11.7	10.63

4.1.2. IFA-716

The IFA-716 experiment was designed to investigate the thermal performance and fission gas release of fuel with different grain size and dopants [30]. As fission gas release is dependent on the balance between the diffusion distance to grain boundaries (determined by the grain size) and the fission gas diffusion coefficient (dependent on the dopant concentration), IFA-716 focuses heavily on the effects these factors have on fission gas release [30].

This experiment was set up in a similar way to IFA-677, with a single cluster of 6 rods made up of both standard UO₂ fuel (with a range of grain sizes) and Cr₂O₃ doped fuel (Table 2); beryllium oxide (BeO) doped fuel was also included to investigate the effects of an increased fuel thermal conductivity. All rods were equipped with a fuel thermocouple to measure fuel centreline temperature, a fuel extensometer to measure fuel stack elongation, and a pressure transducer to measure rod internal pressure. The fuel vendors for this experiment were Framatome (undoped and Cr₂O₃ doped fuel) and Ulba (undoped and BeO doped fuel).

The irradiation began in January 2010 and was completed in May 2015 at a rig average burnup of ~ 36 MWd/kgU [31] [32].

Table 2: The fuel pellets used in the IFA-716 experiment [30].

Rod	Manufacturer	Cr ₂ O ₃ Content (ppm)	BeO Content (wt%)	Grain Size (µm)	Density (g/cm ³)
1	Framatome	1600	-	70	10.50
2	Framatome	-	-	11	10.55
3	Ulba	-	3	9	9.75
4	Ulba	-	-	45	10.68
5	Framatome	-	-	55	10.48
6	Framatome	1000	-	59	10.53

4.1.3. IFA-720.3

The IFA-720.3 experiment was designed to investigate the effect of chromia doping on the fission gas release behaviour at high burnup. The experiment included two test rods which were segments cut from BWR commercial fuel rods base irradiated in the Oskarshamn 3 reactor in Sweden; one rod contained ADOPT pellets and the other contained undoped UO₂ pellets [33].

Both parent rods were manufactured by Westinghouse and were pre-irradiated up to ~ 66 MWd/kgU in the same fuel assembly, so have similar base irradiation power histories [33].

The IFA-720.3 irradiation was a short irradiation of ~ 80 days and consisted of a step-wise power ramp to full power followed by a hold at the maximum power. The test rods were both equipped with a fuel thermocouple to measure fuel centreline temperature and a pressure transducer to measure rod internal pressure.

4.2. Behavioural Assessment

4.2.1. In-pile densification and dimensional stability

Under irradiation, gas atoms and vacancies in the as-manufactured pores of fuel pellets can diffuse into the surrounding fuel matrix, or be ejected into the matrix by the disruptive action of fission fragments; once in the matrix, the vacancies diffuse to grain boundaries, where they are absorbed [34]. The result is an in-pile densification of the fuel. (This densification is in addition to that which occurs during sintering as part of fuel manufacture.) In the IFA-677 experiment the densification during irradiation was determined through calculations of the

fuel volume changes based on the fuel stack elongation measurements (assuming isotropic densification behaviour). The extensometers for rods 1 and 4 did not give reliable data, so only the data for rods 2, 3, 5 (doped) and 6 should be considered (Figure 16).

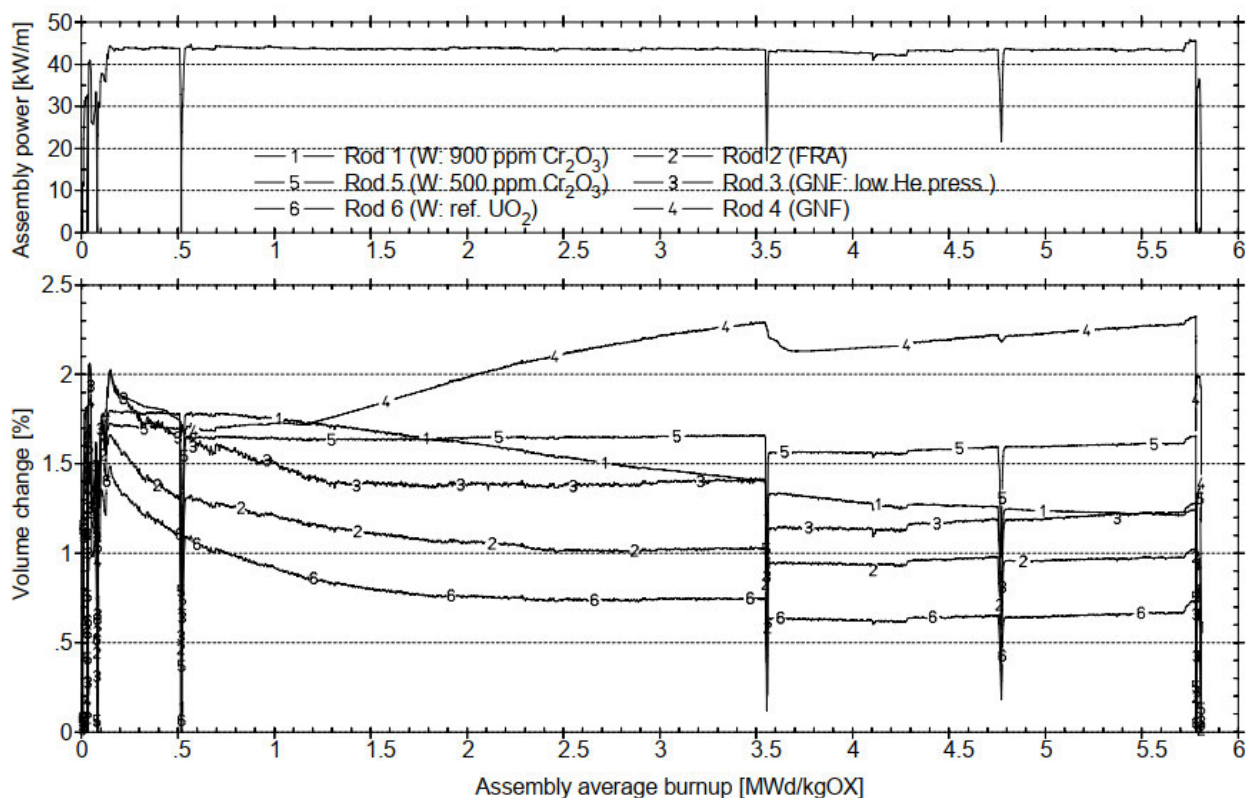


Figure 16: Fuel volume change versus burnup behaviour calculated from fuel stack elongation measurements in IFA-677 (ignore results for rods 1 and 4) [35].

During the irradiation, there was a densification volume change measured for the standard UO_2 pellets (which all had grain sizes of 12 to 16 μm) in the range of 0.50-0.70%. There was, however, almost no densification observed for the ADOPT pellets [29]. The same results were obtained for Framatome CDF in the IFA-716 experiment via the same method [30].

This minimal in-pile densification during irradiation (that is, greater dimensional stability) of the chromia doped fuel compared to the standard UO_2 fuel [21] is consistent with expectation based on the larger fuel grain size and reduced initial porosity volume fraction [28]; the presence of the chromia does not in itself affect the in-pile densification behaviour. It is also consistent with re-sintering tests performed as part of fuel manufacture quality assurance for both Westinghouse and Framatome CDF [1] [13], since densification observed during such tests – which is known to be correlated to in-pile densification – is very small.

4.2.2. Swelling

Fuel pellets swell during irradiation as a result of several mechanisms [28] [34]:

OFFICIAL : COMMERCIAL

- (a) Accumulation of solid fission products in the fuel matrix
- (b) Accumulation of fission gas atoms in the fuel matrix
- (c) Precipitation of intragranular fission gas bubbles (situated within the grains), and subsequent diffusion of fission gas atoms and vacancies to these bubbles
- (d) Precipitation of intergranular fission gas bubbles (situated on grain boundaries), and subsequent diffusion of fission gas atoms and vacancies to these bubbles

(a) and (b) are collectively known as “inexorable swelling” as they cause a change in volume which is dependent only on burnup, and are associated with normal operation behaviour. (c) and (d) are collectively known as “gaseous swelling”, only occur at temperatures high enough to permit atomic migration [28], and are associated with both normal operation and transients.

Inexorable swelling of CDF has been measured as part of both the Halden experiments described above and commercial irradiation PIE. In the case of the former, rates of fuel volume change due to swelling were calculated from on-line measurements of fuel stack elongation. In the case of the latter, cumulative fuel volume increases due to swelling were inferred from fuel density measurements via an immersion technique.

The inexorable swelling rates calculated from IFA-677 fuel stack elongation measurements were in the range of 0.2-0.6 vol% per 10 MWd/kgUO₂ for all rods, with no identifiable dependence on fuel type [29]. Higher swelling rates of 0.7-0.9 vol% per 10 MWd/kgUO₂ were observed in IFA-716, but, again, there was no identifiable dependence on fuel type [31]. Given that 0.2-0.9 vol% per 10 MWd/kgUO₂ reflects the typical range of swelling rates observed in Halden experiments with undoped UO₂ fuel, it can be concluded that the Halden data do not indicate any differences in inexorable swelling behaviour (relative to undoped UO₂) of either Westinghouse or Framatome CDF. As illustrated in Figure 17, such invariance in inexorable swelling behaviour (up to at least ~ 80 MWd/kgU) is also evident from measurements of fuel density from PIE of commercially-irradiated Framatome CDF (presumably for irradiation at conditions where fuel swelling was dominated by inexorable swelling rather than gaseous swelling) [11].

OFFICIAL : COMMERCIAL

NNL 15231

ISSUE 1

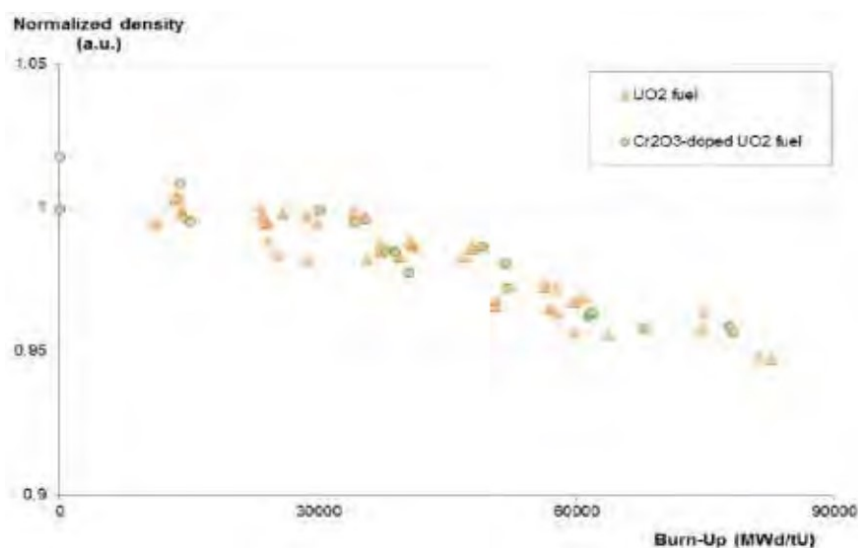


Figure 17: Fuel density versus burnup data for commercial irradiations of Framatome doped and undoped fuel [11] (poor quality of image is as in the cited reference).

Measurements of gaseous swelling via destructive PIE (ceramography images) of irradiated Framatome CDF have been obtained, but are proprietary [22]. Gaseous swelling induced fuel volume changes can also be inferred from clad diameter measurements performed after both normal operation and ramp tests; such 'inferred data' are available for Framatome CDF, but, with the exception of normal operation data for GAIA rods [36], are, again, proprietary [22]. Although the full data are not available, Framatome note that there is larger intra-granular bubble swelling and smaller inter-granular bubble swelling in irradiated CDF due to larger grain size (so that there is a higher probability of fission gas atoms being trapped by intra-granular bubbles as they diffuse to grain boundaries, while less gas atoms reach these boundaries) and increased creep rate (so that intra-granular bubble growth is less retarded by stresses induced in the surrounding fuel matrix) [22]. This is supported by Figure 18, which shows more and larger intra-granular bubbles, and fewer and smaller inter-granular bubbles (the large black objects are as-manufactured pores) in irradiated Framatome CDF.

OFFICIAL : COMMERCIAL

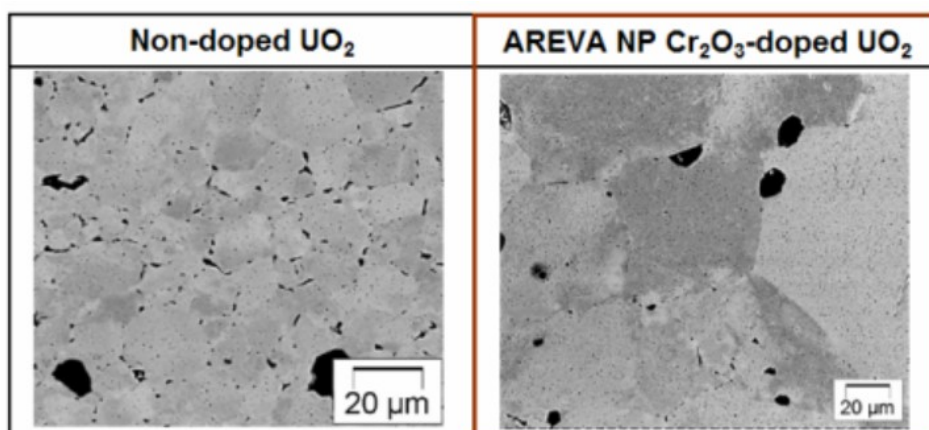


Figure 18: Comparison of fission gas bubbles in Framatome chromia doped and undoped UO_2 fuel after irradiation [13].

Larger intra-granular bubble swelling and smaller inter-granular bubble swelling has also been reported for ADOPT fuel that has been subject to a ramp test [1] [2].

4.2.3. Pellet-cladding interaction (PCI)

During irradiation, the fuel pellets experience cracking and form fragments; this, along with the large radial temperature gradient across the pellets gives them an hourglass shape (Figure 19) [37]. There is initially a gap between the pellets and cladding, however, during irradiation, fuel swelling causes this gap to decrease. Cladding creep due to the compressive stress exerted by the high pressure coolant further decreases the gap size [37]. Eventually the pellets and cladding contact and the gap is closed. Due to the cracked and hourglass pellets, clad stress is concentrated at the pellet ends (axially) and over the radial fuel cracks (circumferentially).

If there is an increase in power in the reactor, the pellet diameter can increase further due to: thermal expansion, gaseous swelling and the opening of cracks. If the pellet-cladding gap is already closed, this further pellet expansion can cause stresses in the cladding that are high enough to lead to clad failure via yielding or creep rupture [37]. However, in practice, the cladding will fail at lower stresses due to stress-corrosion cracking (SCC), which depends on both the clad stress, but also the chemical effects of corrosive fission products; this is pellet-cladding interaction (PCI) failure and imposes a significant restriction on the flexibility of operation of the reactor. It is therefore clear that to minimise the probability of rod failure and enhance accident tolerance, the PCI behaviour must be improved.

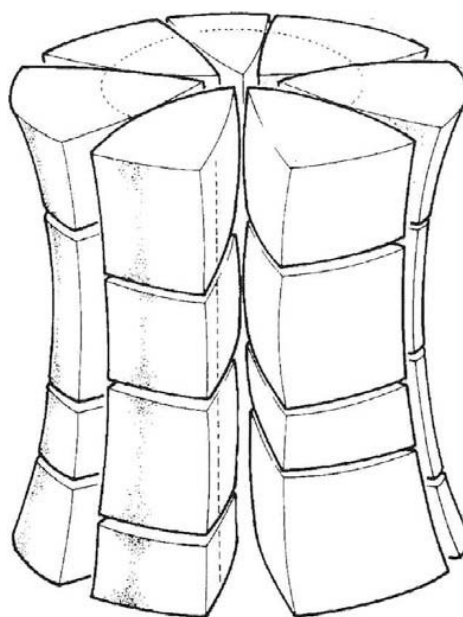


Figure 19: The hourglass shape of a fuel pellet (idealised and exaggerated) [37].

An improvement in PCI performance is often linked to an increase in pellet plasticity via the consequential reductions in cladding stress during hard pellet-clad contact. The addition of chromia to UO_2 fuel pellets therefore (via the increased creep rate: see Section 3.2.5.1) improves the PCI behaviour and enhances accident tolerance through the mitigation of fuel cladding failure [24] [38] [39]. Increased fuel creep in the central regions of the fuel pellets is evidenced by increased dish filling (Figure 20); the resulting axial extrusion of fuel reduces the pellet outer diameter to some extent.

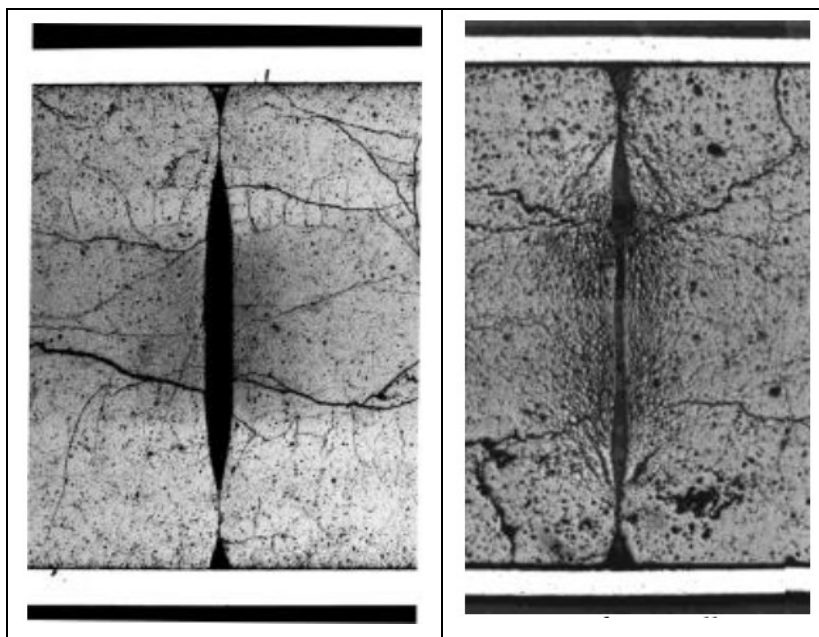


Figure 20: Pellet dish filling after power ramps to 40 kW/m: Framatome undoped fuel on left and Framatome CDF on right [24].

There is also evidence for an improvement in PCI performance with CDF due to chemical effects – namely, improved corrosive fission product retention, and chromia dissociation and associated generation of free oxygen which can oxidise the cladding inner surface, thereby protecting it from SCC [12] [38] [39] [40] [41] [42] – but this is tentative only. Finally, increased cracking at the pellet periphery during power ramps (see Section 4.2.4.2) reduces the maximum stresses (over radial fuel cracks) in the cladding by reducing the crack mouth openings [24], further improving PCI performance.

Chromia dissociation has been observed after Framatome ramp tests. The pellet Cr concentration radial distribution before and after the PR1 ramp test, as measured by electron probe microanalysis (EPMA), are shown in Figure 21. This test was in the Osiris test reactor to a peak power of 47 kW/m, which was held for 12 hours. The fuel tested was CDF with 0.16 wt% chromia pre-irradiated to 38 MWd/kgU in an EDF commercial PWR.

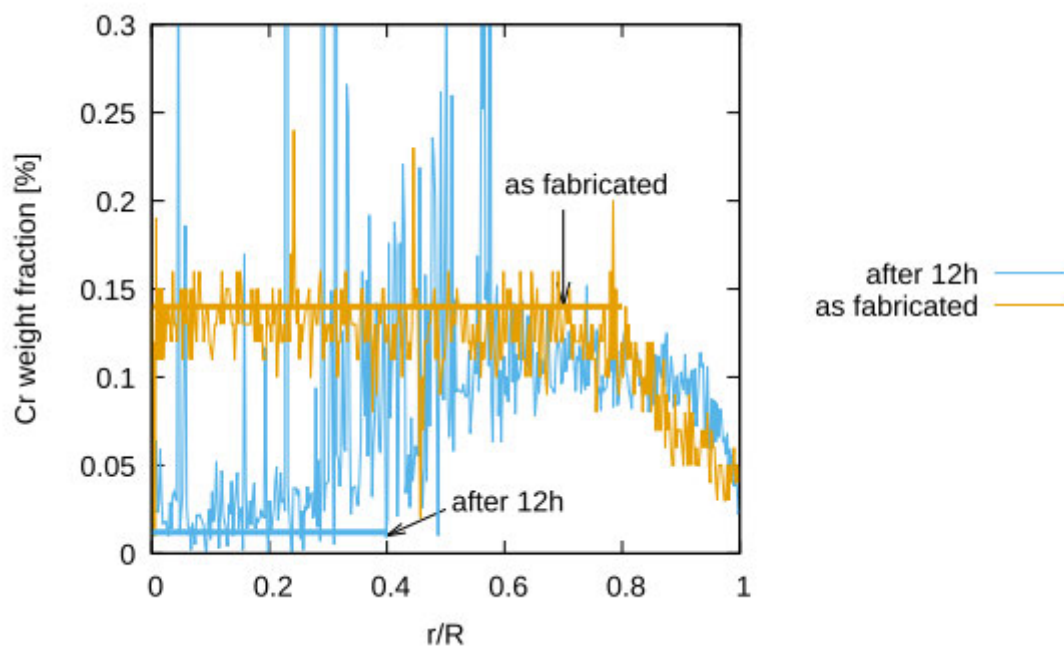


Figure 21: Measurement of Cr concentration radial distribution before and after the Framatome PR1 ramp test [42].

There may be a reduction in PCI performance due to the increased intra-granular fission gas bubble swelling (see Section 4.2.2), and therefore increased stress on the cladding, but this is outweighed by the combination of the reduced inter-granular fission gas bubble swelling (again, see Section 4.2.2) and the positive effects described above.

Ramp tests are routinely performed as part of fuel qualification to evaluate the PCI behaviour and to determine the increases in power which lead to fuel failure. Data on the PCI behaviour of CDF are therefore primarily those obtained from qualification of fuel designs employing CDF; such data are discussed further in Section 5.

4.2.4. Fuel pellet cracking

4.2.4.1. Normal operation

Framatome suggest comparable cracking behaviour in chromia doped and undoped UO_2 during normal operation [22], but ceramography images are unavailable to confirm this. Westinghouse note a larger number of small cracks in the pellet periphery for ADOPT fuel, but the effect, if it exists, appears marginal, even in the high rating conditions of the IFA-677 experiment (Figure 22).

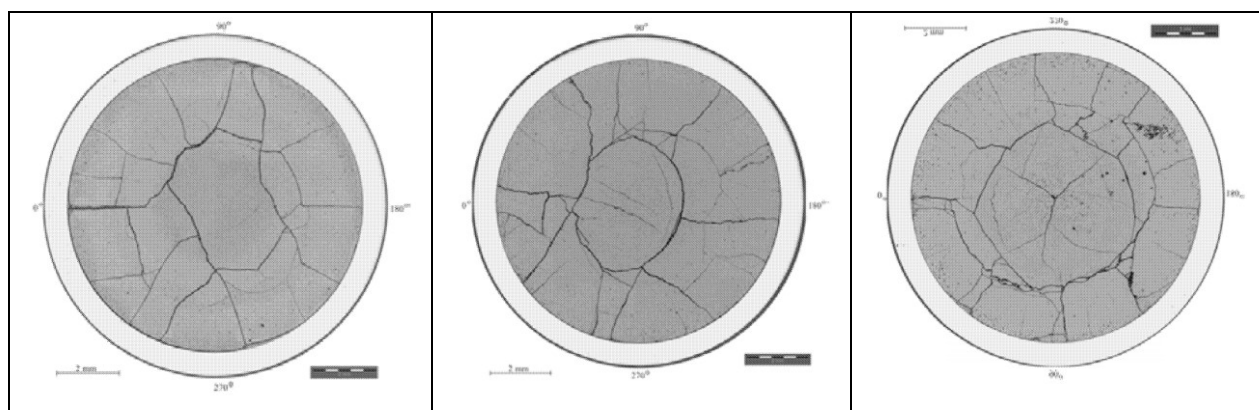


Figure 22: Pellet cracking after irradiation in the IFA-677 experiment for undoped fuel (left), fuel with 500 ppm chromia (middle), and fuel with 900 ppm chromia (right) [2].

4.2.4.2. Power ramps

After base irradiation up to 30 GWd/tU, two segments of Framatome doped PWR fuel and two segments of undoped PWR fuel were ramp tested in 2001 in a loop of the OSIRIS test reactor as part of the CONCERTO irradiation programme (see Section 5.2.1 for more details of this programme). The ramp terminal ratings ranged from 40 to 54 kW/m, and the ramp rate was 10 kW/m/min to simulate a Class 2 transient [24]. From optical microscopy examinations of the irradiated fuel pellets, the cracking pattern was found to be different for the standard UO_2 fuel pellets and the doped pellets (Figure 23) [24]. In the centre of the doped pellets, no radial cracks are observed, consistent with crack healing occurring due to the enhanced fuel creep; this behaviour is not seen for the standard UO_2 [24]. In contrast, there is increased radial cracking in a peripheral zone, and the width of the peripheral zone is narrower due to a larger radial extent of the hot, plastic zone that extends from the pellet centre. In addition, the doped pellets appear to have both intergranular and transgranular crack propagation, as opposed to the standard UO_2 , which tends to only have transgranular [24]. The peripheral cracking of the pellets increases with increasing ramp terminal rating (Figure 24).

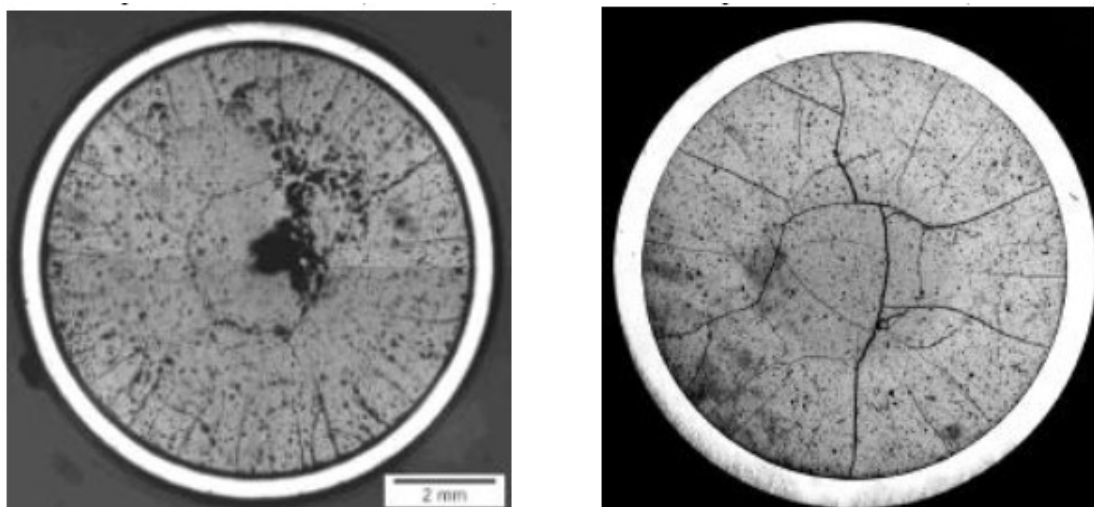


Figure 23: Sections of Framatome chromia doped fuel (left) and standard UO₂ fuel (right) after ramping to 40 kW/m [24].

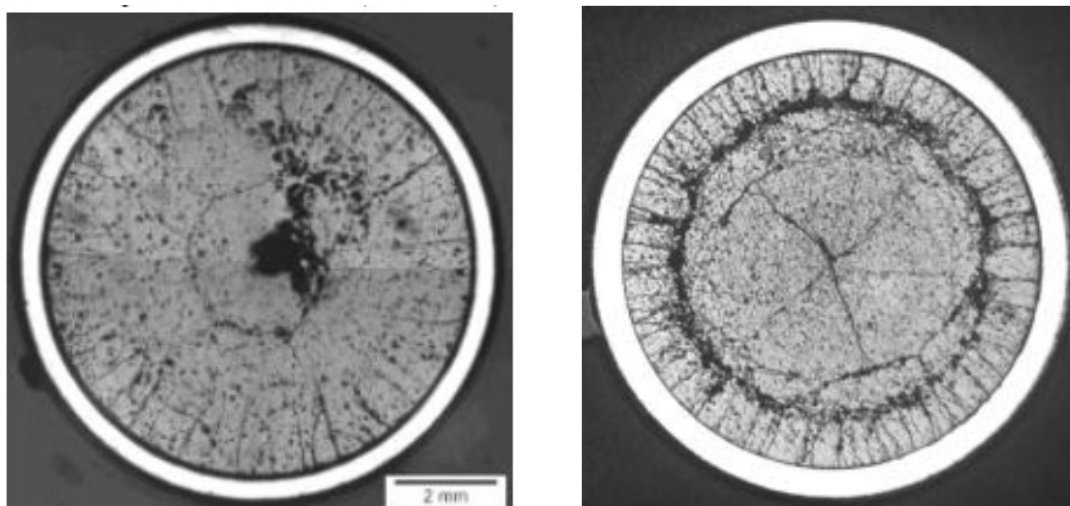


Figure 24: Sections of Framatome chromia doped fuel ramped to 40 kW/m (left) and 47 kW/m (right) [24].

Similar behaviour has been observed for ADOPT fuel [2] [25].

The increased radial cracking in the peripheral zone is consistent with the reduced fracture strength (see Section 3.2.5.3). The wider hot, plastic zone (and hence narrower brittle peripheral zone) may also have an effect via a reduced volume for fracture energy dissipation [24].

4.2.5. Oxidation and washout characteristics

If the fuel pellets come into contact with the coolant as a result of clad failure, they can be oxidised by the chemical reaction with ingressed water, resulting in pellet degradation (due to the associated volume increase) and washout (leaching) of the oxidised material from the rod into the bulk coolant. The oxidation is initially along the grain boundaries, where it proceeds relatively rapidly. Slower oxidation of the resulting separated grains then occurs [43]. Both the fuel pellet microstructure (primarily the grain size) and the fuel matrix composition therefore have an effect on the rate and extent of oxidation.

Delafoy and Zemek describe out-of-pile experiments performed to determine the oxidation (thermogravimetry) and washout (autoclave testing) behaviour of Framatome doped fuels compared to undoped fuels [14]. Pellets with and without gadolinia included as a burnable absorber were tested. All fuel was unirradiated.

The oxidation experiments determined that chromia doping enhances the oxidation resistance of the pellets compared to the UO_2 pellets. The results (Figure 25) show that the oxidation resistance of the chromia doped fuels is mostly due to the larger grain size providing a smaller surface area for the initial oxidation to occur [14]. The increased density of the doped pellets (that is, the reduced porosity volume fraction) is also beneficial to the oxidation resistance, but to a lesser extent.

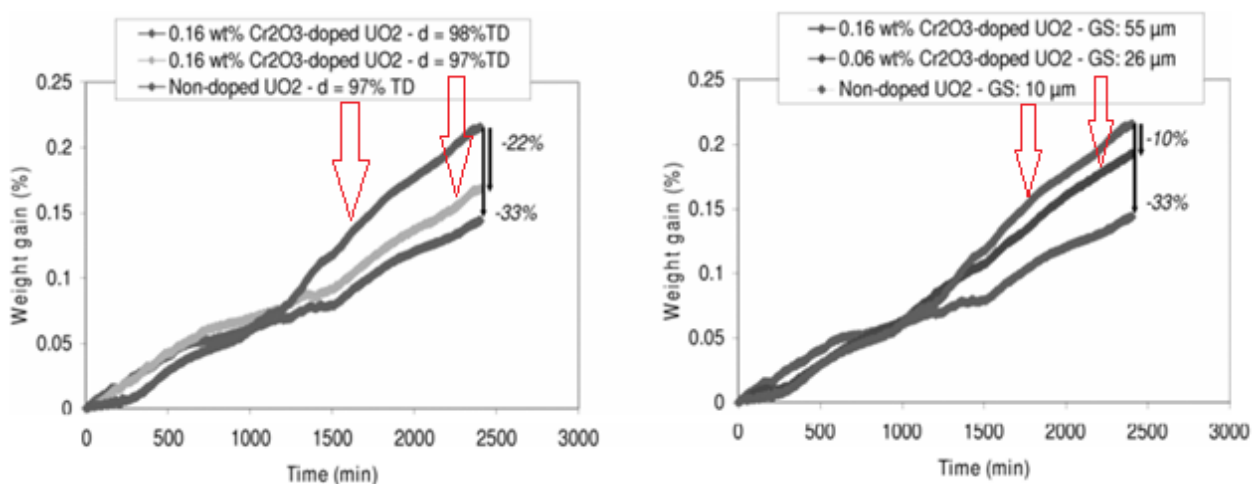
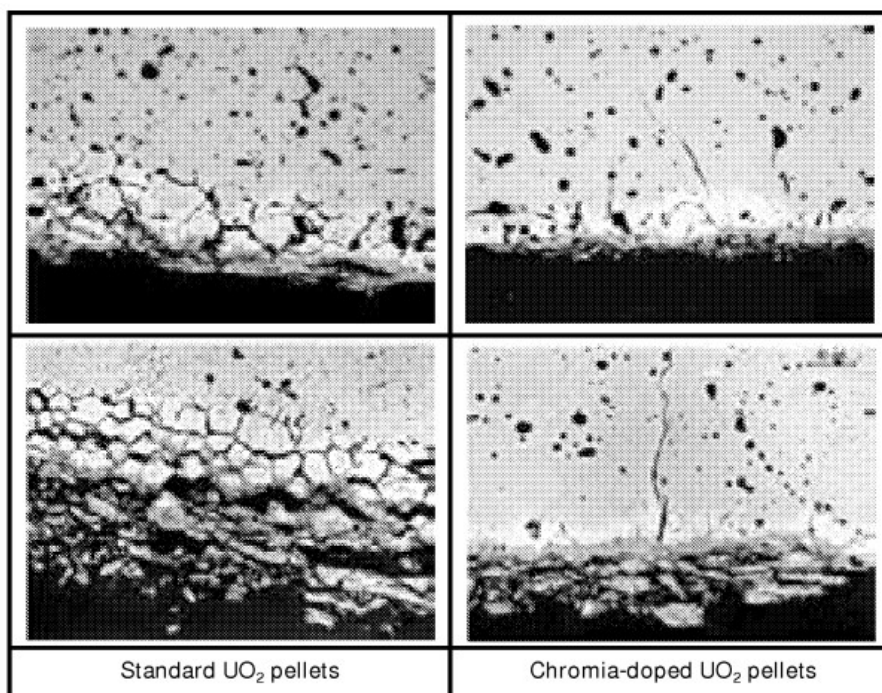


Figure 25: Comparison of the weight gain (measure of oxidation) vs. time for chromia doped and undoped UO_2 fuel pellets with various densities and grain sizes tested at 380°C in an Ar-0.01% O_2 atmosphere [14].

The corresponding pellet degradation is significantly different (Figure 26): in the undoped pellets surface oxidation is followed by significant intergranular oxidation and a resulting cracking and spallation of oxidised grains, whereas in the doped pellets oxidation is primarily limited to the surface and there is spallation only of the surface material.



(top: after 20h bottom: after 40 h)

Figure 26: Pellet degradation associated with the weight gain shown in Figure 25 [14].

The washout experiments, which were performed under both PWR and BWR coolant conditions, found that the washout behaviour depends on the oxygen concentration of the medium. In the low-oxygen PWR conditions, the rate of corrosion was low for all pellets and hence there was no washout of material, despite testing for 30 days in both 360°C water and 400°C steam [14]. In the higher-oxygen BWR conditions, no noticeable washout was seen after 6 days in 290°C water, but after 6 days in 360°C steam there was a significant difference in the level of washout seen for the different pellet types [14]: the chromia-free pellets with and without gadolinia lost ~ 15 wt% and ~ 4.6 wt% of material, respectively, while the chromia doped pellets with and without gadolinia lost ~ 3 wt% and < 1 wt% of material, respectively [14]. In addition, it took over 5 days before washout occurred from the chromia- and gadolinia-doped pellets, but took only 2 days before washout occurred from the chromia-free gadolinia-doped fuel [14].

Overall, the results from the washout experiments show that the Framatome chromia doped fuels had an improved washout resistance of a factor of 5 when compared to the chromia-free pellets; as with the oxidation resistance, this was attributed to the large grain size of the doped pellets [14].

No (in-pile or out-of-pile) testing of the oxidation and washout behaviour of irradiated Framatome CDF has been performed; in US licensing of their CDF product [22], Framatome claim that the "trend observed in unirradiated fuel samples remains valid for irradiated fuel", based on Japanese corrosion testing (in water) of unirradiated and irradiated UO₂ and

(U,Gd)O₂ (that is, chromia-free fuel) with different grain sizes [44] [45], which showed that “irradiation ... had no significant effect on the fuel corrosion” [22].

Both out-of-pile oxidation testing of unirradiated ADOPT pellets and in-pile oxidation and washout testing of irradiated ADOPT fuel have been performed by Westinghouse [1]. In both cases the ADOPT fuel was tested alongside undoped fuel. The out-of-pile oxidation testing involved thermogravimetry of pellets exposed to moist argon at 400°C for 20 hours, while the in-pile oxidation and washout testing involved the irradiation of test rodlets, with an engineered open slot in the cladding, in a loop of the Studsvik R2 test reactor under BWR coolant conditions. The out-of-pile oxidation testing showed that the oxidation rate of the ADOPT pellets was half that of the standard UO₂ pellets, while post-irradiation gamma scanning of the fuel irradiated in the in-pile oxidation and washout test suggested that fuel loss increases with power and decreases with fuel density, and hence that the higher-density ADOPT pellets are more resistant to washout; ceramography of the irradiated fuel was attempted to confirm this, but was inconclusive [1].

4.2.6. Fission gas release (FGR)

In LWRs, around 15% of the generated fission products are xenon and krypton gases. These noble gases have a very low solubility in UO₂, so can diffuse through the fuel matrix to the grain boundaries, free surfaces, pre-existing pores, intra-granular fission gas bubbles, or inter-granular fission gas bubbles [34] [46]. Growth of inter-granular bubbles as fission gas accumulates in them leads to coalescence and interlinkage, whereby gas can be released from the fuel pellets to the rod free volume. Additional gas is released due to (a) the diffusion to free surfaces, (b) ‘ballistic’ release of the as-generated (that is, high kinetic energy) fission gas atoms (so-called recoil release), and (c) intra-granular bubble migration to grain boundaries (only at high temperatures greater than ~ 1800°C) [34]. Due to the mechanisms just described, the volume of fission gases released increases with increasing burnup and increasing fission gas diffusion coefficient (which in turn increases strongly as the fuel temperature increases), and becomes smaller the larger the as-manufactured grain size.

Fission gas release (FGR) causes pressurisation of the fuel rod. Since the thermal conductivity of the gas mixture in the rod free volume (including the pellet-clad gap) is also decreased, the pressurisation can be subject to positive feedback whereby increased fission gas release leads to increased fuel temperatures which in turn leads to a further increase in fission gas release [46]. If the pressure becomes high enough, the cladding can fail due to creep rupture. This failure mechanism is potentially limiting from a fuel performance perspective. Hence, fission gas release is an important phenomenon to understand.

The fission gas release behaviour of ADOPT fuel has been investigated in commercial reactor irradiations, in ramp tests performed in the Studsvik R2 test reactor, and in the IFA-677 and IFA-720.3 Halden Reactor Project experiments. This is described further below.

After irradiation in a commercial reactor, poolside gamma scanning has been used to measure the FGR of two assemblies containing a mixture of ADOPT and standard UO₂ fuel pellets [2]. Measurements were taken at burnups up to 55 MWd/kgU. The results are illustrated in Figure 27. At low burnups, recoil release is dominant and there is a similar FGR measured for the two different fuels. At higher burnups, when diffusional release becomes

dominant, there is an improvement of around a third less FGR for the ADOPT pellets when compared to the standard fuel due to the larger grain size [2].

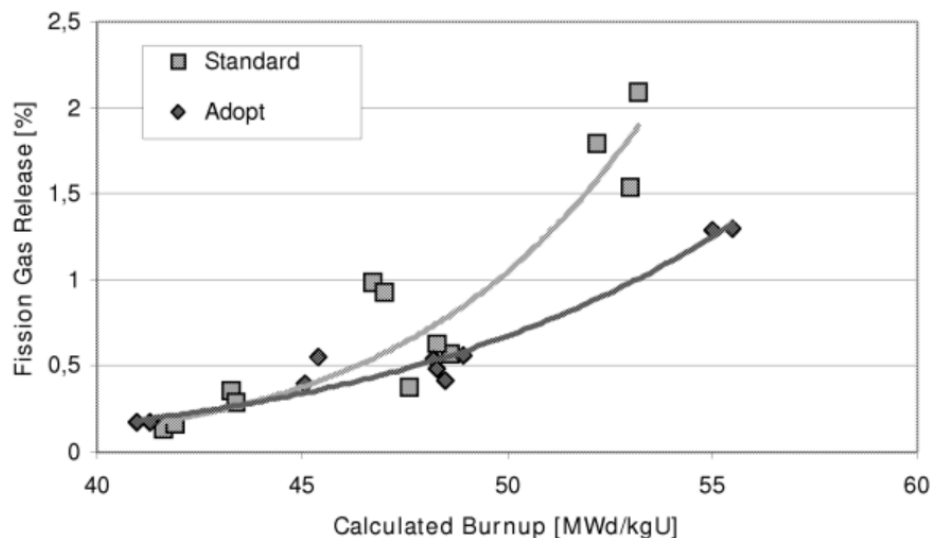


Figure 27: FGR vs. burnup for ADOPT and standard UO₂ pellets after irradiation in a commercial LWR [2].

The ramp tests of ADOPT fuel performed in the Studsvik R2 test reactor are described in Section 5.1.2. Post-test fission gas release was measured via rod puncture. The results were 17% and 30% for the ADOPT and standard UO₂ fuel in the high power ramp test, and 30% and 21% for the ADOPT and standard UO₂ fuel in the medium power ramp test [1]. Thus, FGR was significantly lower in the ADOPT fuel in both cases, with the difference becoming larger at the higher power. Westinghouse infer that this was due to enhanced trapping of gas in intra-granular bubbles [2].

The FGR versus burnup behaviour inferred from the rod internal pressure measurements in IFA-677 is shown in Figure 28; also included in the figure are the peak fuel temperatures estimated from the fuel thermocouple measurements. The FGR values at the end of irradiation – which are in good agreement with rod puncture measurements for the two rods (5 and 6) subjected to rod puncture [47] – are shown in Table 3.

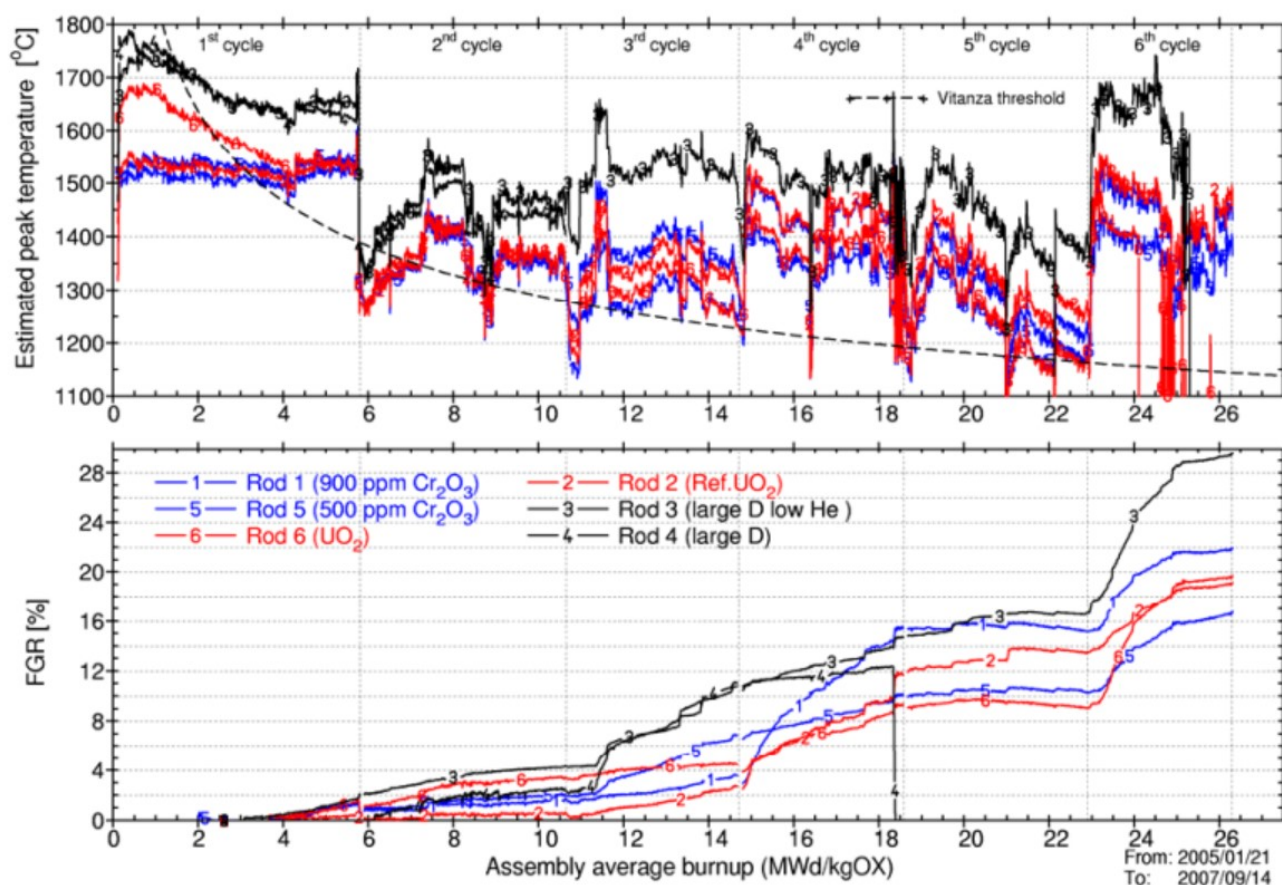


Figure 28: FGR and peak fuel temperature versus burnup behaviour in IFA-677, as inferred from pressure transducer and fuel thermocouple measurements [29].

Table 3: Estimated end-of-life FGR for the IFA-677 rods [29].

Rod	1	2	3	4	5	6
Cr ₂ O ₃ content (ppm)	900	-	-	-	500	-
Grain size (µm)	56	16	15	15	45	12
FGR (%)	22.0	19.7	29.6	Unknown*	16.8	19.1

* Pressure transducer failed at assembly average burnup of ~ 18 MWd/kgOxide

End-of-life FGR is highest for the standard grain size fuel in rod 3, as may be expected, but the large grain size ADOPT fuel in rod 1 also has a relatively high end-of-life FGR, while the

OFFICIAL : COMMERCIAL

NNL 15231

ISSUE 1

large grain size ADOPT fuel in rod 5 has the lowest end-of-life FGR. However, the situation is complicated by the significant differences in peak fuel temperatures, which means that FGR from the different rods cannot be compared on a like-for-like basis. In fact, Westinghouse themselves show that, when the differences in peak fuel temperatures are taken into account, the fission gas release behaviour of the doped fuel is no different to that of the undoped fuel (based on calculations using the STAV fuel performance code) [2]. This is difficult to explain when compared with the FGR results from the commercial irradiations and from the ramp tests, given that the high FGR observed must have occurred via a diffusional (not recoil) mechanism. Westinghouse attempt to dismiss the importance of this finding by noting that the IFA-677 operating conditions were unrepresentative of commercial reactor irradiation [2], but this is not entirely convincing.

The FGR versus burnup behaviour inferred from the rod internal pressure measurements in IFA-720.3 is shown in Figure 29; also included in the figure are the peak fuel temperatures estimated from the fuel thermocouple measurements [33]. The FGR – which excludes the FGR during the base irradiation – is much higher for the ADOPT rod than for the undoped rod. Notwithstanding the somewhat higher peak fuel temperatures, this is difficult to explain given the ADOPT fuel commercial reactor irradiation and ramp test experience described above, and the fact that the base irradiation power histories of the two rods were very similar, with ratings decreasing from ~ 25 kW/m to ~ 5 kW/m over several cycles, such that base irradiation FGR should have been low. It may be that the pressure transducer was faulty in the undoped rod; PIE (including rod puncture) is planned to confirm this, but this has not yet been carried out as far as is known.

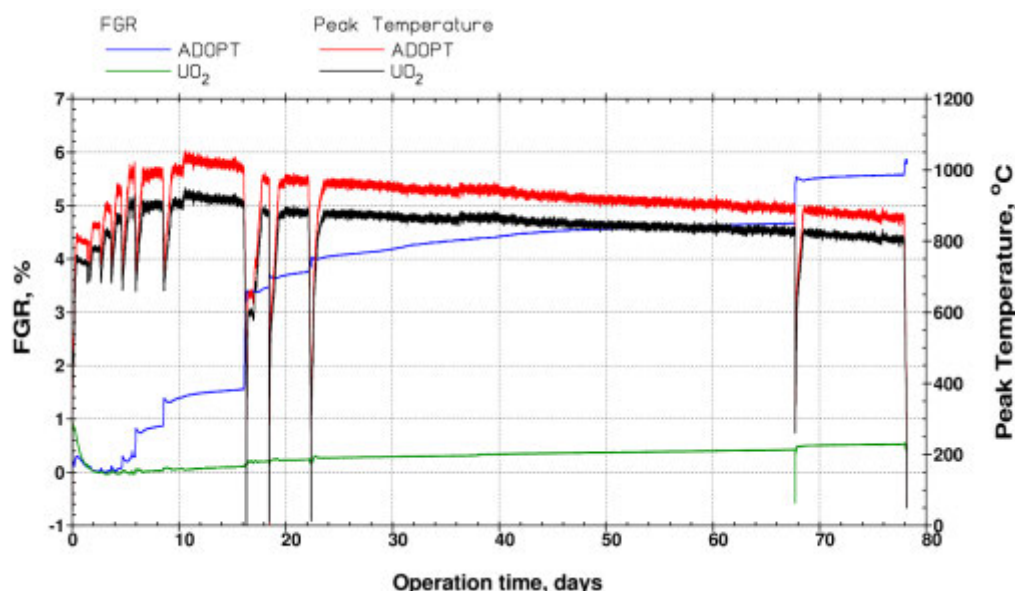


Figure 29: FGR and peak fuel temperature versus burnup behaviour in IFA-720.3, as inferred from pressure transducer and fuel thermocouple measurements [33].

OFFICIAL : COMMERCIAL

OFFICIAL : COMMERCIAL

NNL 15231

ISSUE 1

The fission gas release behaviour of Framatome CDF has been investigated in commercial reactor irradiations, in the TANOX, TANOXOS and REMORA test reactor irradiations, in the IFA-716 Halden Reactor Project experiment, in ramp tests, and in post-irradiation annealing tests. This is described further below. The commercial reactor irradiations include lead rod irradiations in a commercial PWR which were carried out in the framework of the CONCERTO programme (see Section 5.2.1 for further details of this programme).

The fission gas release data available for commercial PWR irradiations of Framatome CDF (presumably via rod puncture) are reproduced in Figure 30; the figure also shows data from undoped fuel (purple diamonds) for comparison purposes. Data are also available for commercial BWR irradiations [11]. Like for ADOPT fuel (see Figure 27), the Framatome CDF FGR up to ~ 50 MWd/kgU is the same as that for undoped fuel, while above this burnup there is a significant reduction in FGR by a factor of a seventh to a quarter; this is ascribed to enhanced trapping of gas in intra-granular bubbles [11].

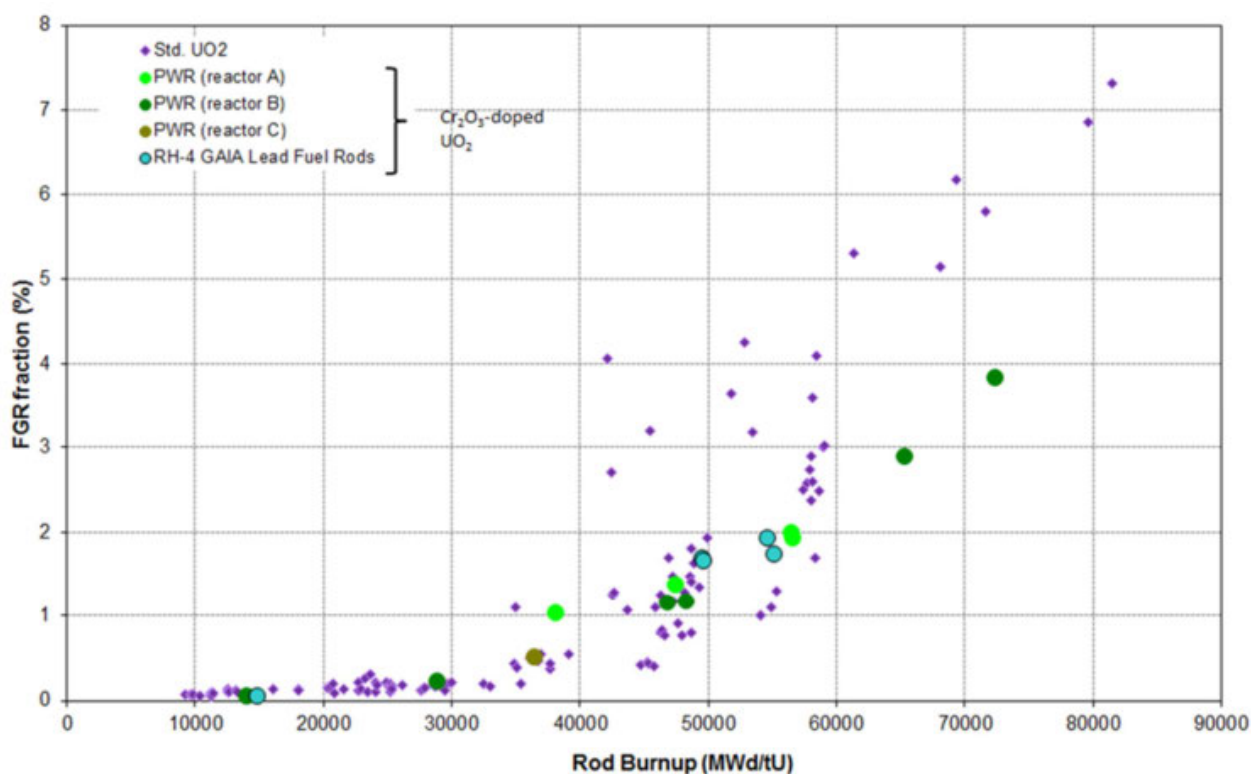


Figure 30: FGR vs. burnup for doped and undoped Framatome fuel after irradiation in commercial PWRs [36].

The fission gas release behaviour observed in commercial PWR irradiations of Framatome CDF is consistent with that observed in the TANOX and TANOXOS irradiations [48] [49]. The TANOX irradiation was performed in the Siloé test reactor at low fuel temperatures to a burnup of ~ 9 MWd/kgU, while the TANOXOS irradiation was performed at higher temperatures in the Osiris test reactor to a burnup of 65-69 MWd/kgU. Both irradiations

OFFICIAL : COMMERCIAL

OFFICIAL : COMMERCIAL

NNL 15231

ISSUE 1

started with fresh doped and undoped fuel; the doped fuel had either 0.07 or 0.2 wt% chromia (that is, lower or higher than the 0.16 wt% used for the commercial fuel product). The fission gas release after the TANOX irradiation was very low at $\sim 0.1\%$, and was comparable for both doped and undoped fuel; this is consistent with fission gas release dominated by recoil release. In contrast, the fission gas release after the TANOXOS irradiation was considerably lower in the doped fuel than in the undoped fuel in most instances ($\sim 2\%$ in the CDF and $\sim 3\%$ in the undoped fuel); this is consistent with fission gas release dominated by diffusional release and the associated enhanced trapping of gas in intra-granular bubbles in CDF.

Unfortunately, the pressure transducer in rod 2 (the only rod with standard grain size undoped fuel) of the IFA-716 experiment was faulty. Thus, the results from IFA-716 cannot be used to compare the FGR of doped fuel and undoped, large grain size fuel with that of standard UO_2 . However, as can be seen in Figure 31, the fission gas release behaviour of the large grain size, undoped fuel is comparable to that of the doped fuel, supporting FGR behaviour in doped fuel dominated by the effect of the large grain size, and not by the presence of the chromia itself. Noting the final burnups of $\sim 36 \text{ MWd/kgU}$ (see Section 4.1.2), the end-of-life FGR values of $\sim 6\text{--}7\%$ are significantly larger than for commercial PWR irradiations; this probably reflects the effects of the December 2013 power uprating at $\sim 20 \text{ MWd/kgU}$.

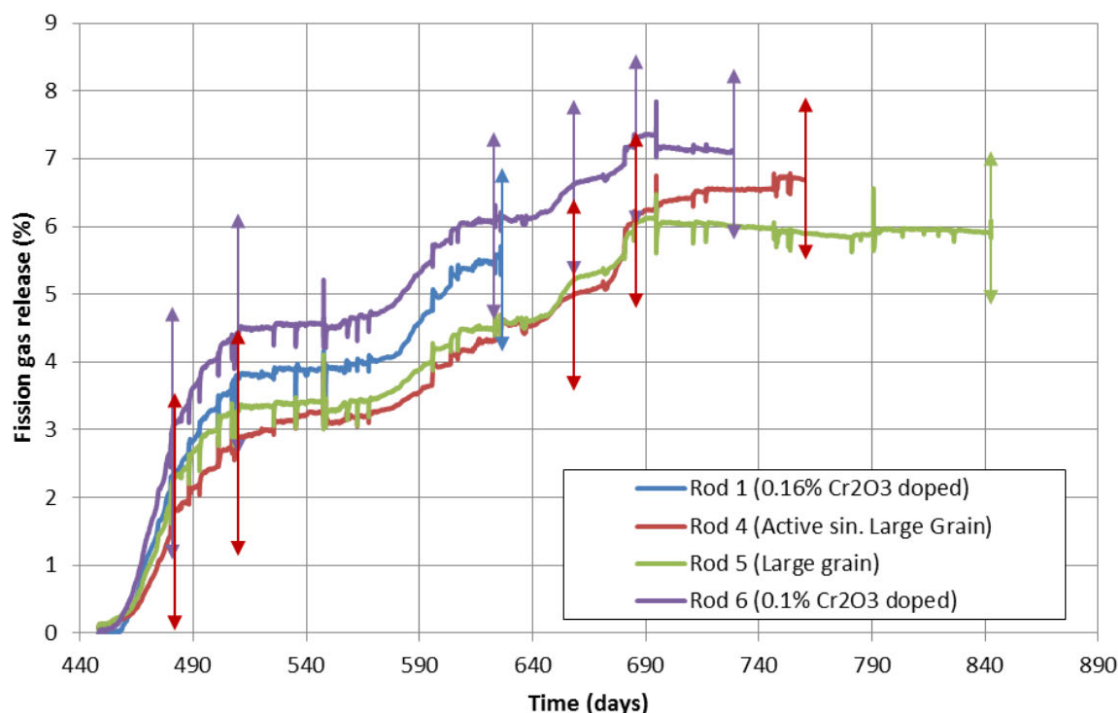


Figure 31: FGR vs. time behaviour in IFA-716 experiment after December 2013 power uprating, as derived from rod internal pressure measurements (the bars represent estimated uncertainties) [31].

OFFICIAL : COMMERCIAL

OFFICIAL : COMMERCIAL

NNL 15231

ISSUE 1

The fission gas release data available from puncture of Framatome CDF rods subjected to ramp tests are shown in Figure 32; also included in the figure is the FGR versus ramp terminal power trend for undoped UO_2 fuel (dashed violet line). Similar results were obtained for both BWR and PWR rods: the FGR has a linear correlation with ramp terminal power. In contrast, FGR in standard UO_2 has an exponential dependence on ramp terminal power. The improved behaviour of the CDF is ascribed to both enhanced trapping of gas in intra-granular bubbles and pinning of these intra-granular bubbles (that is, retardation of bubble migration).

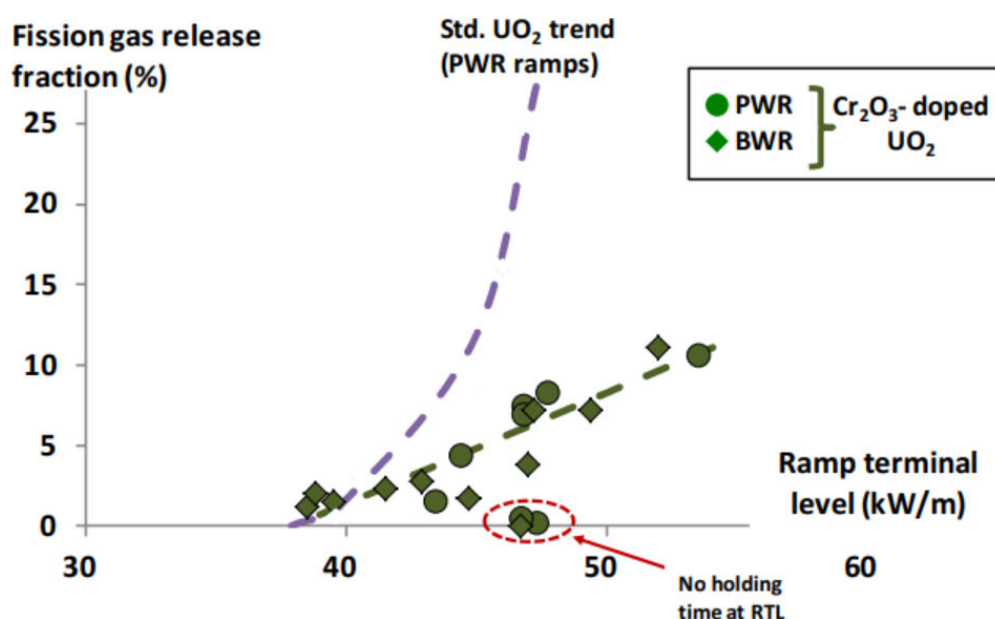


Figure 32: Fission gas release vs. ramp terminal level for Framatome CDF [12].

The fission gas release behaviour observed in ramp testing of Framatome CDF is broadly consistent with that observed in the REMORA irradiation described in Section 3.2.4.4. This irradiation, which included two power ramps, resulted in a FGR of 6.5% for a maximum ramp power of 36 kW/m.

The fission gas release data available from post-irradiation annealing of Framatome CDF are discussed by Valin *et al.* [48] and Caillot *et al.* [49]. Both low and high burnup fuel was investigated, all of which was doped with either 0.07 or 0.2 wt% chromia (that is, lower or higher than the 0.16 wt% used for the commercial fuel product). The low burnup fuel was irradiated at low temperature in the TANOX device in the Siloé test reactor to a burnup of ~ 9 MWd/kgU; it was then annealed at 1700°C for either 30 minutes or 5 hours. The high burnup fuel was irradiated at higher temperatures in the TANOXOS device in the Osiris test reactor to a burnup of 65-69 MWd/kgU; it was then annealed, with temperatures ramped up to either 1200 or 1300°C according to two different annealing sequences (A and B). The ^{85}Kr release results from the annealing tests performed for 5 hours on the low burnup fuel are shown in Figure 33. The ^{85}Kr release in the annealing tests performed on the high burnup

OFFICIAL : COMMERCIAL

CDF ranged from 8-14% for sequence A and 13% for sequence B², compared to 18% for sequence A and 19% for sequence B for undoped fuel. Results are broadly comparable with those from the ramp tests: fission gas release is significantly reduced in the large grain size chromia doped fuel relative to the standard grain size undoped fuel. The behaviour of the low burnup fuel was ascribed to enhanced trapping of gas in intra-granular bubbles and pinning of these bubbles (since the large grain size undoped fuel had relatively high fission gas release of $\sim 30\%$), while the behaviour of the high burnup fuel was ascribed to both these two phenomena and the increased diffusion path associated with the larger grain size.

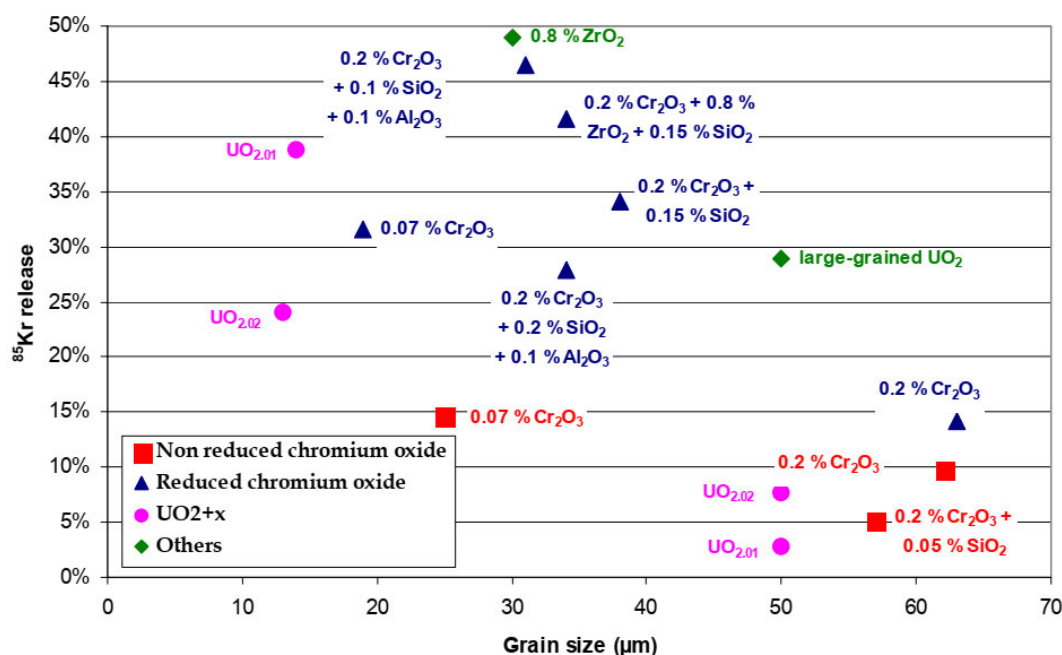


Figure 33: ⁸⁵Kr release vs. grain size for post-irradiation annealing of Framatome low burnup fuel with various dopants at 1700°C for 5 hours [48].

4.2.7. Behaviour during accidents

4.2.7.1. Loss of coolant accidents (LOCAs)

One of the main drivers to developing doped fuels is to enhance their accident tolerance. During a loss of coolant accident (LOCA), there is a sharp increase in the cladding temperature and accelerated cladding oxidation. The former results in creepout of the cladding, which causes clad ballooning and can result in fuel rod burst (via creep rupture) and the dispersal of fuel and volatile fission products into the primary circuit, while the latter results in embrittlement of the cladding, which can cause cladding failure during post-LOCA quenching or fuel handling, and hydrogen generation [50]. The extent of the fuel dispersal

² ignoring results for CDF with hyperstoichiometric UO₂, which are not relevant to Framatome's commercial fuel product

depends on the extent of fragmentation of the fuel pellets and of the relocation of the resulting fuel fragments.

The consequences of a LOCA can be lessened by reducing the extent of clad ballooning, reducing the cladding oxidation, reducing the volatile fission product release, and/or reducing the extent of fuel fragmentation. Hence, the lower normal operation FGR (at higher burnup), lower transient FGR and increased intra-granular fission gas inventory (see Section 4.2.6) of CDF can potentially reduce the consequences of a LOCA by reducing the rod internal pressure driving force for clad creepout, reducing volatile fission product release (which is correlated to fission gas release), and reducing the extent of inter-granular fragmentation due to overpressurisation of inter-granular fission gas bubbles [51]. However, other than the post-irradiation annealing tests on Framatome CDF described in Section 4.2.6, which support reduced transient fission gas release in a LOCA temperature transient, and a heating test on Framatome CDF performed in CEA's MEXIICO facility [16], there are no known experiments that have been performed to support this (although such tests are expected in the US and/or European accident tolerant fuel (ATF) programmes [51] [16], and as part of the Studsvik Cladding Integrity Project (SCIP) and the Halden Reactor Project). The MEXIICO heating test involved an integrated fuel and cladding sample cut from a parent rod irradiated to ~ 64 MWd/kgU in a commercial PWR. Only large pellet fragments were observed after the test, indicating a lack of fine fragmentation [16].

4.2.7.2. Reactivity-initiated accidents (RIAs)

Reactivity-initiated accidents (RIA) can generate a rapid power excursion to very high power for a short duration (that is, a power pulse that occurs over less than one second). This rapid increase in power – which results in high fuel and cladding temperatures, and can lead to fuel fragmentation – can cause cladding failure via four failure modes: (1) brittle failure induced by hard pellet-clad mechanical interaction, which is in turn caused by thermal expansion and gaseous swelling of the fuel pellets; (2) creep rupture due to high-temperature clad ballooning; (3) brittle failure due to post-departure-from-nucleate-boiling re-wetting after embrittlement of the cladding by high-temperature oxidation; and (4) melting of the cladding, or melting of the fuel pellets and interaction of the molten fuel material with the cladding [52].

Hence, the potential benefits of CDF during LOCAs described in Section 4.2.7.1 will also apply to RIAs. On the other hand, the increased intra-granular fission gas bubble swelling of CDF (see Section 4.2.2) may be a detriment to performance during a RIA, although the reduced inter-granular fission gas bubble swelling (again, see Section 4.2.2) should help to counteract this. Once again, however, other than the post-irradiation annealing tests on Framatome CDF described in Section 4.2.6, which support reduced transient fission gas release in a temperature transient, there are no known experiments that have been performed to support this (although such tests are expected in the US and/or European ATF programmes).

5. Operating Experience and Qualification Data

The test reactor experiments used to investigate the behaviour of CDF were described in Sections 3 and 4. Framatome CDF is also under irradiation in the Advanced Test Reactor (ATR) as part of the US EATF programme [16], but this is an un-instrumented, sealed capsule irradiation primarily intended to demonstrate the compatibility of Framatome CDF and Cr-coated M5 cladding, and so is not described further in this report. The operating experience in commercial reactors – via lead rod, lead assembly and reload irradiations – and the resulting fuel qualification data are described in this section. Also covered here is the associated ramp testing and resulting qualification data for PCI performance. Operating experience and qualification data for Westinghouse CDF (ADOPT fuel) are described in Section 5.1, while operating experience and qualification data for Framatome CDF are described in Section 5.2.

5.1. Westinghouse

5.1.1. Commercial reactor irradiations

Westinghouse ADOPT lead fuel rods were first loaded into a commercial LWR in 1999 [2]. Since then there has been at least two full reloads of ADOPT fuel and several lead test rods loaded into different LWRs [2]. Overall, over 2600 assemblies containing ADOPT have been loaded, with irradiation up to a maximum rod average burnup of around 72 MWd/kgU [10]. Irradiation to higher burnups in a European BWR is ongoing as part of a “two-life” (presumably where irradiated rods are moved to a new carrier assembly) high burnup verification programme [10].

For BWRs, the relevant fuel assembly designs utilised by Westinghouse are SVEA-96 Optima2 and SVEA-96 Optima3; use of TRITON11 assemblies is also planned. Both SVEA designs consist of a cruciform water channel separating four sub-bundles of 5x5-1 fuel rods, and have the same arrangement of part-length rods; the only difference is the new spacer grid used in the SVEA-96 Optima3 design [53]. SVEA-96 Optima3 is currently the standard Westinghouse BWR assembly design. TRITON11 is the Westinghouse new advanced fuel product design. Designed to reduce fuel cycle cost and give improved reliability, the 11x11 assembly has 109 fuel rods and three central water rods for improved moderation [53]. The evolution of the Westinghouse BWR fuel assembly designs can be seen in Figure 34.

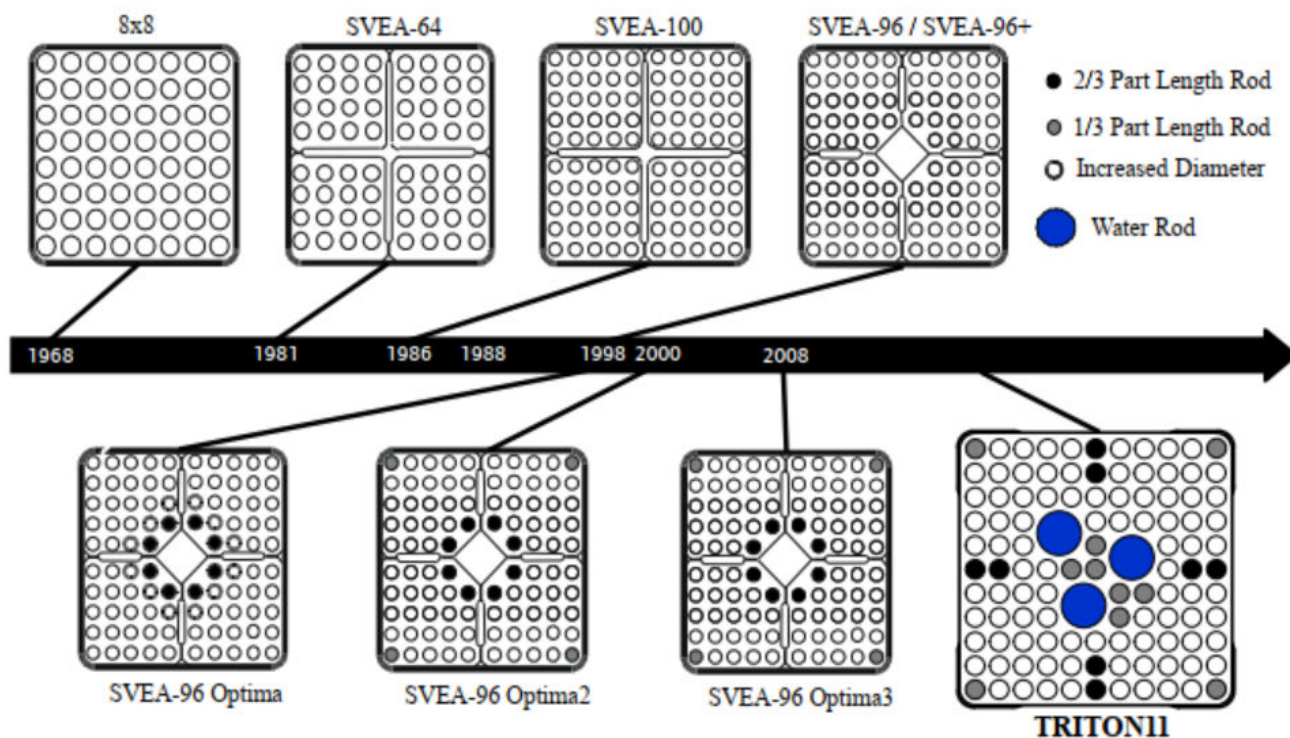


Figure 34: The evolution of Westinghouse BWR assembly designs [53].

For PWRs, the assembly designs used are unclear, but they are likely to include the following 17x17 designs: 2nd generation Robust Fuel Assembly (RFA-2), Next Generation Fuel (NGF) and Optimised Fuel Assembly (OFA) [54] [55]. These assemblies all have a similar design consisting of 264 fuel rods, 24 guide thimbles and a central instrumentation tube held together by top and bottom nozzles and spacer grids [56]. OFA assemblies containing four lead rods with ADOPT fuel and Cr-coated cladding were loaded into the Byron-2 PWR in USA in 2019 as part of the US EATF programme [10].

Qualification data from commercial irradiations include the fission gas release data discussed in Section 4.2.6 and poolside measurements of rod length and diameter [1]. Further qualification data should be obtained from the high burnup verification programme, which includes poolside fission gas release measurements and hot cell PIE. The poolside measurements of rod length and diameter – which include also measurements on rods containing undoped UO₂ – show an increased rod length for the ADOPT fuel and no significant difference in the rod diameters (Figure 35). Westinghouse conclude that this is consistent with reduced densification and unchanged swelling in the ADOPT fuel.

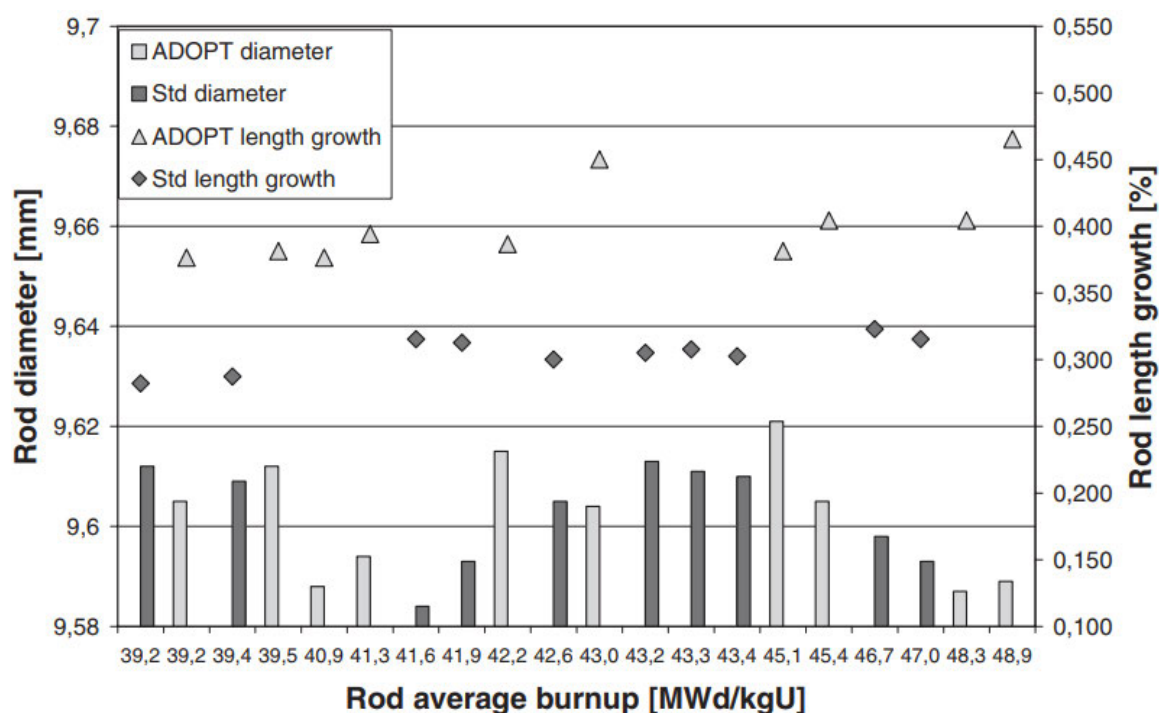


Figure 35: Rod length and diameter vs. rod average burnup for commercially irradiated rods containing ADOPT and undoped UO₂ fuel pellets [1].

5.1.2. Ramp tests

The totality of ramp tests on Westinghouse ADOPT fuel is unclear. What is known is that ramp tests of two ADOPT rods have been performed in the Studsvik R2 test reactor. These tests involved segmented lined fuel rods which were base irradiated in the Barsebäck-2 commercial BWR to a burnup of ~ 30 MWd/kgU [1] [2]. Tests involving both high and medium final powers – both of which employed an undoped fuel rod in addition to the doped fuel rod – were carried out (the latter is referred to as a “bump test” in the cited references). The high power test involved a stepped power ramp to 57 kW/m and a hold time of 8 or 12 hours (doped fuel and undoped fuel, respectively), while the medium power test involved an unstepped power ramp to 45-46 kW/m and a hold time of 18 days. None of the rods tested failed.

Qualification data from the R2 ramp tests include fuel swelling data, pellet cracking data, and fission gas release measurements, as discussed in Sections 4.2.2, 4.2.4.2 and 4.2.6, respectively. There was no real qualification of PCI performance, given only two ADOPT rods were tested, and given there were no rod failures.

5.2. Framatome

5.2.1. Commercial reactor irradiations

Commercial irradiation of Framatome CDF began in 1997 as part of the CONCERTO programme: four assemblies containing lead rods with chromia doped fuel and low-tin Zircaloy-4 cladding were irradiated in an EDF PWR for five annual cycles to a burnup of ~ 57 MWd/kgU [57] [58] [15]. Since then, lead fuel assemblies (LFAs) of different Framatome designs have been irradiated in commercial BWRs and PWRs [11]; as far as is known, no reloads of CDF have yet been irradiated. The current maximum burnup achieved with the Framatome doped fuel is around 75 MWd/kgU [11].

Qualification of CDF in M5 cladding for PWR applications began in 2001 with the irradiation of lead rods in a 1300 MWe reactor [57]. In 2005, four LFAs of this fuel began irradiation, again in a 1300 MWe PWR [57].

The Framatome CDF qualification programme was widened in 2005 to include BWRs as part of the ATRIUM 10XM lead assembly programme. Two out of four of the lead assemblies used in the programme contained 30 rods with chromia doped pellets which were manufactured with both liner and non-liner cladding [13] [57]. In 2007 a similar BWR LTA programme began which was designed to investigate the effects of power history on FGR [13].

In 2009, the Ringhals-4 PWR lead fuel rod irradiation programme started. This involved irradiating 6 different lead test rod designs in two High Thermal Performance (HTP) assemblies over five cycles [36]. One of these test rods was of a GAIA design with chromia doped pellets; rods of this design are now used in the GAIA fuel assembly design (Figure 36), which combines and improves on the best features from the Framatome HTP and AFA 3G designs. In 2012, the first four GAIA lead fuel assemblies began irradiation in the Ringhals-3 PWR [36]. A similar LFA irradiation programme has been completed in the USA. This involved eight GAIA fuel assemblies being irradiated from 2015 to 2019 [36].

It is expected that full reloads of GAIA fuel assemblies will start irradiation in 2020 in Europe and 2021 in the USA [36].

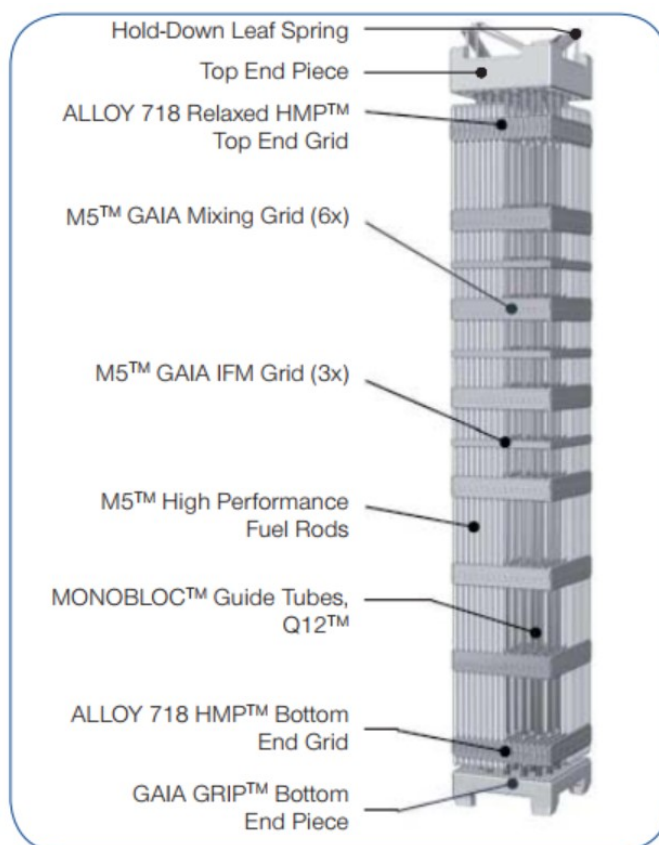


Figure 36: Framatome GAIA fuel assembly design [59].

Qualification data from the commercial reactor irradiations include the fuel density, rod diameter and fission gas release data discussed in Sections 4.2.2 and 4.2.6, rod length data, and clad oxide thickness data (unconnected to the use of CDF). The rod length data are illustrated in Figure 37. Unlike for ADOPT fuel (see Section 5.1.1), there appears to be no difference in rod length between fuel with and without doped pellets; this may be due to differences in as-manufactured pellet diameters, at least for the GAIA rods [9]. The rod diameter data for GAIA fuel (not shown in Section 4.2.2) are illustrated in Figure 38, and demonstrate clad permanent hoop strains within acceptable limits up to 60 MWd/kgU.

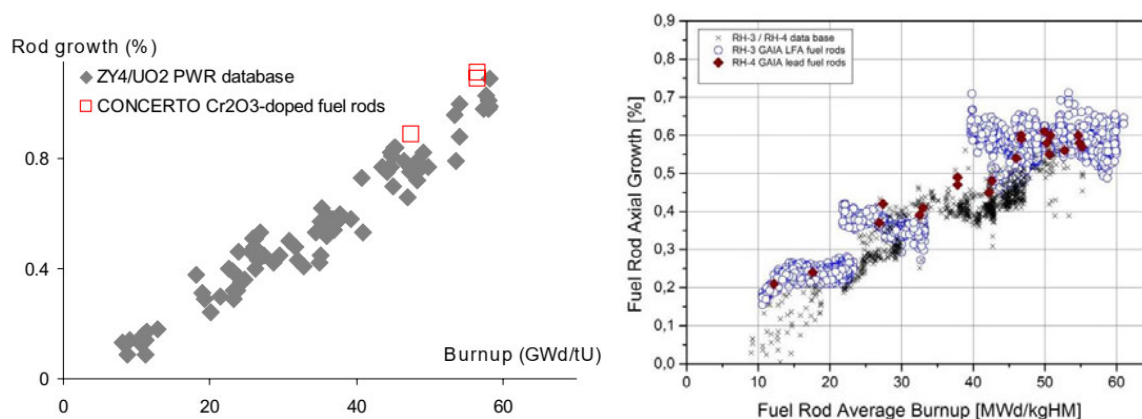


Figure 37: Rod length data from commercial irradiations of Framatome CDF [36] [57].

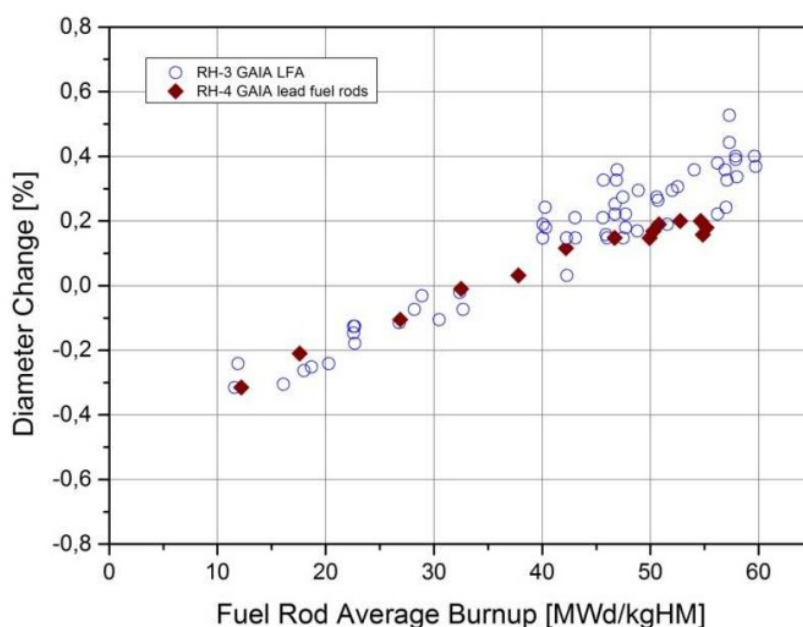


Figure 38: Rod diameter data from commercial irradiations of Framatome GAIA fuel [36].

5.2.2. Ramp tests

As of 2015, 26 ramp tests had been performed for PWR and BWR applications [11]:

- 12 PWR power ramps were performed on Framatome chromia doped fuel pellets in 17x17 fuel design rods (with low-tin Zircaloy-4 and M5 cladding) pre-irradiated in various European commercial reactors to 18-62 MWd/kgU. The tests were performed under typical PWR conditions in the Osiris and Halden test reactors.
- 14 BWR power ramps were performed on Framatome chromia doped fuel pellets in ATRIUM 10XM fuel rods (with LTP2 non-liner cladding) pre-irradiated in various

OFFICIAL : COMMERCIAL

NNL 15231

ISSUE 1

European commercial reactors to 20-45 MWd/kgU. The tests were performed under typical BWR conditions in three successive ramp tests in the Halden test reactor.

The ramp tests in both the PWR and BWR conditions showed a notable improvement in the PCI failure threshold when compared to the standard UO₂ rods. The power increment to failure is higher by ~ 4 kW/m for the PWR rods, and by ~ 7-10 kW/m for the BWR rods [11], as illustrated in Figure 39 and Figure 40.

The qualification data from the PCI ramp tests primarily consist of the fail/no fail data illustrated in Figure 39 and Figure 40. Other qualification data obtained were discussed in Section 4.2.3.

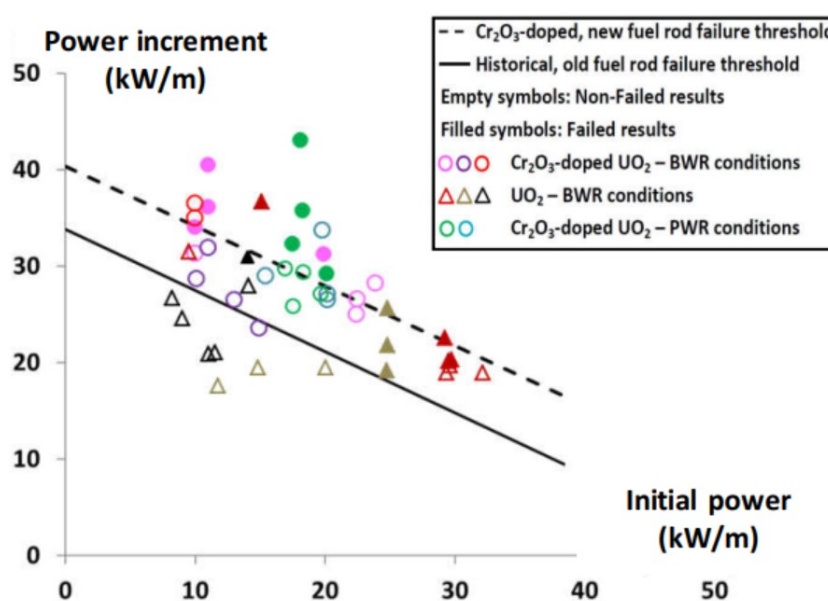


Figure 39: Ramp test results for Framatome chromia doped fuel and standard UO₂ fuel: BWR data (the lines represent BWR failure thresholds, and PWR data are included for comparison purposes) [12].

OFFICIAL : COMMERCIAL

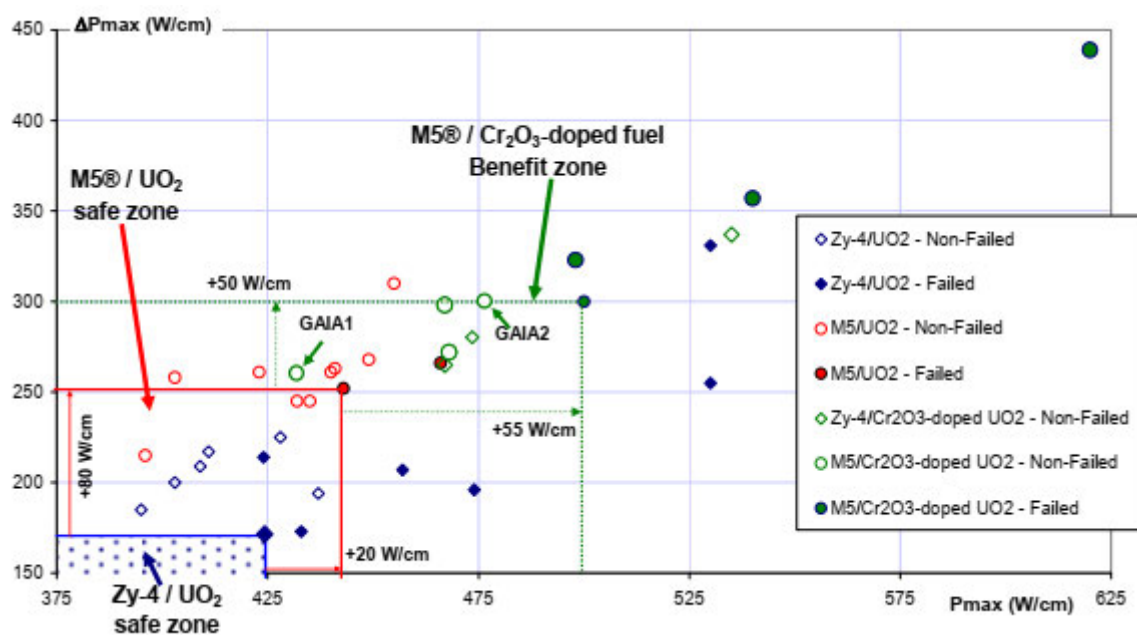
OFFICIAL : COMMERCIALNNL 15231
ISSUE 1

Figure 40: Ramp test results for Framatome chromia doped fuel and standard UO₂ fuel: PWR data [9].

OFFICIAL : COMMERCIAL

6. Prediction of Behaviour and Validation

Accurate and validated fuel performance codes are essential for the concept development and licensing stages of any fuel type. There are already several fuel performance codes which are able to predict the behaviour of standard UO_2 fuels in both normal operating conditions and accident scenarios. The thermal properties of doped and standard UO_2 fuels are very similar (see Section 3.2.4), so the same model correlations can generally be used for both types [21]. However, due to the differences in their mechanical properties and phenomenology, existing codes generally need to be modified to model chromia doped fuels.

Information on the modelling of chromia doped fuel is only available for the BISON [60] [61], COPERNIC [11] [62], RODEX [22] [63], STAV [2] and ALCYONE [42] [64] fuel performance codes. Based on this information, only RODEX has been validated for modelling of chromia doped fuel or used for licensing of such fuel (for BWR applications) [22]. However, in reality, it is likely that COPERNIC (the main code used by the French division of Framatome) and STAV (the main code used by Westinghouse Sweden) have also been validated and used for licensing, given the irradiation of lead rods and lead assemblies of Framatome CDF in French PWRs, and the irradiation of reloads of ADOPT fuel in commercial BWRs. Details of the modelling are provided below.

BISON used material properties and models as for undoped UO_2 fuel with the exception of an increased fission gas diffusion coefficient, and a modification to the fuel densification model to ensure 0.1-0.2 vol% densification as per experiments. The modelling was applied to the IFA-677 and IFA-716 Halden Reactor Project experiments, Framatome ramp tests (with some details estimated), and a LOCA simulation.

COPERNIC used material properties and models as for undoped UO_2 fuel with the exception of a modified fuel creep model and "slight adjustments ... to correctly predict strains and FGR in transient conditions". The modelling was applied to the simulation of an AGORA fuel rod irradiation in a commercial PWR.

RODEX used material properties and models as for undoped UO_2 fuel with the exception of an adjusted fuel thermal conductivity model and a modified intra-granular fission gas bubble swelling model. The modelling was validated against Framatome's commercial reactor irradiation and ramp test databases and was applied to analysis of the IFA-677 and IFA-716 experiments.

STAV used material properties and models as for undoped UO_2 fuel and was applied to analysis of the IFA-677 experiment.

ALCYONE used material properties and models as for undoped UO_2 fuel with the exception of an adjusted gaseous swelling model ("slight" increase of the irradiation-induced re-solution and "slight" increase of the intra-granular fission gas bubble diffusion coefficient) and an adjusted fuel thermal creep model and was applied to analysis of the IFA-716 experiment. More recently, a fuel thermochemistry assessment of two of the Framatome CDF ramp tests was performed in which some enhancements were made to the fuel thermochemistry modelling.

Other than for the COPERNIC fuel creep model and the ALCYONE fuel thermochemistry model, further details of the modelling changes are unavailable for all five codes. Details of the validation of RODEX are similarly unavailable. In terms of the application of the codes, the focus was on FGR behaviour. This explains why only COPERNIC has had the fuel creep model updated for CDF (the AGORA fuel rod irradiation simulation included a calculation of clad strain energy density in PCI-limiting Class 2 transients). Sample FGR results are illustrated in Figure 41 to Figure 47.

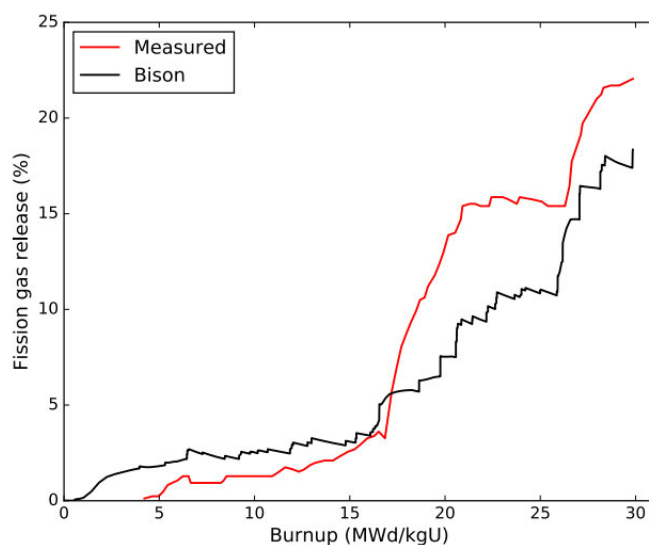


Figure 41: BISON prediction and measurement of FGR in IFA-677 rod 1 (ADOPT with 900 ppm chromia) [61].

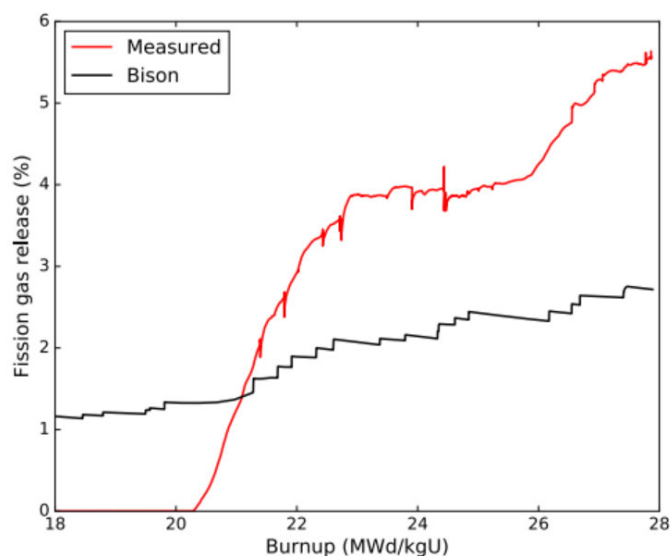


Figure 42: BISON prediction and measurement of FGR in IFA-716 rod 1 (Framatome CDF with 1600 ppm chromia) [61].

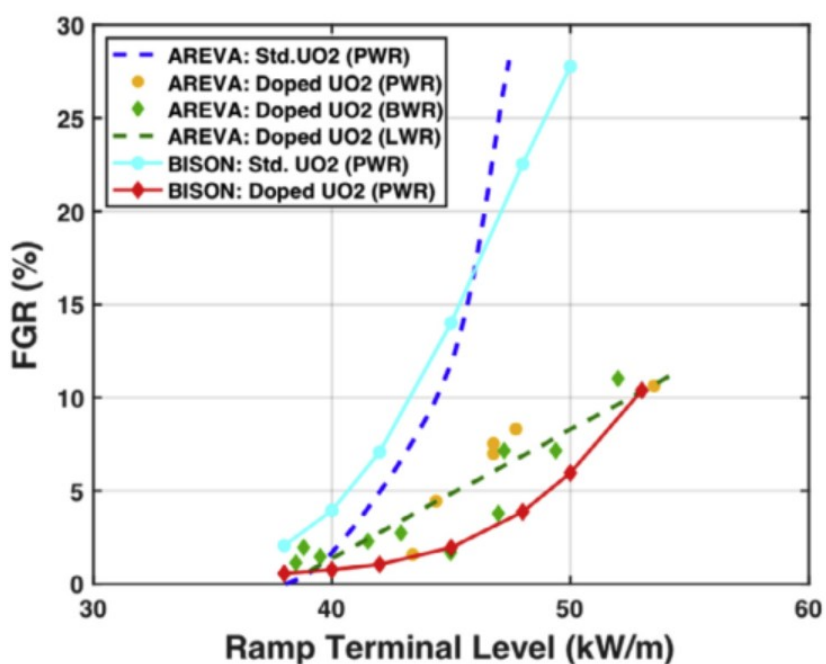


Figure 43: BISON prediction and measurement of FGR vs ramp terminal level for Framatome ramp tests [60].

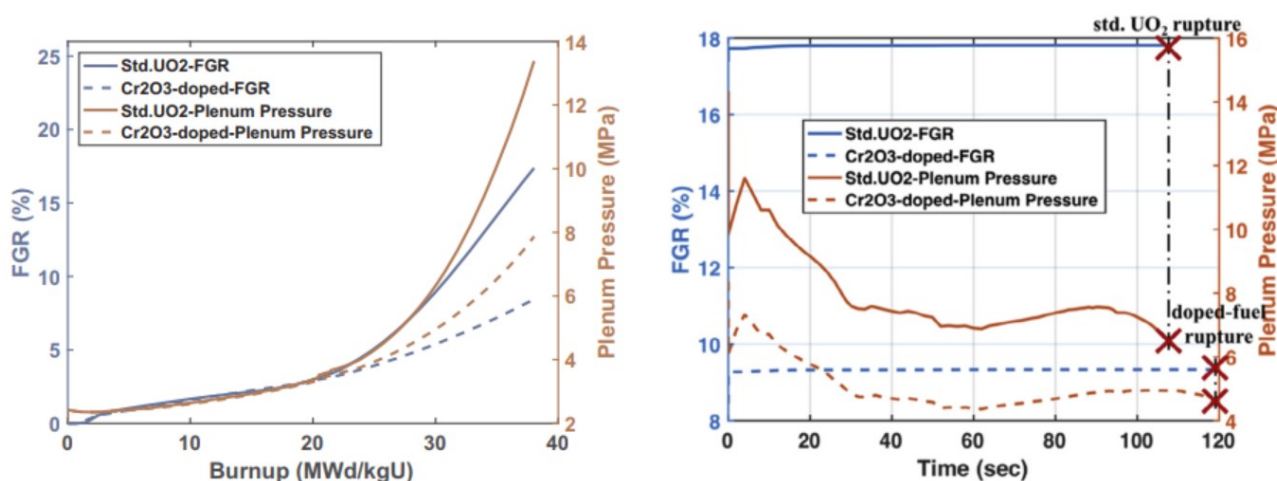


Figure 44: BISON predictions of the FGR and plenum pressure for chromia doped and standard UO₂ rods during a LOCA simulation (pre-fault predictions are on the left, and LOCA predictions are on the right) [60].

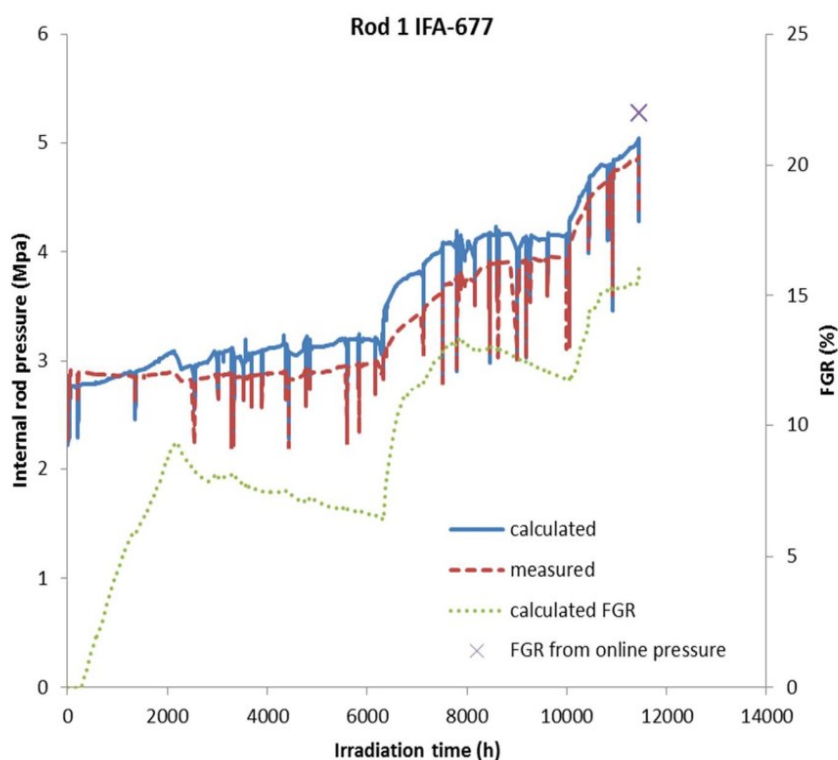


Figure 45: RODEX prediction and measurement of FGR in IFA-677 rod 1 (ADOPT with 900 ppm chromia) [63].

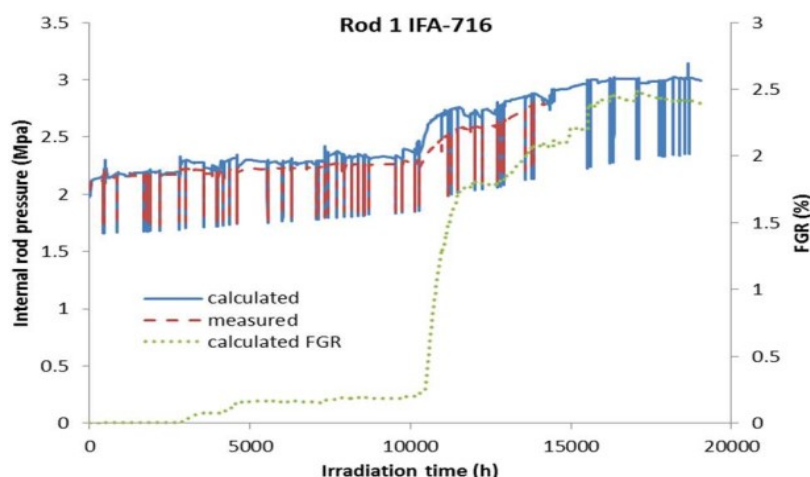


Figure 46: RODEX prediction and measurement of FGR in IFA-716 rod 1 (Framatome CDF with 1600 ppm chromia) [63].

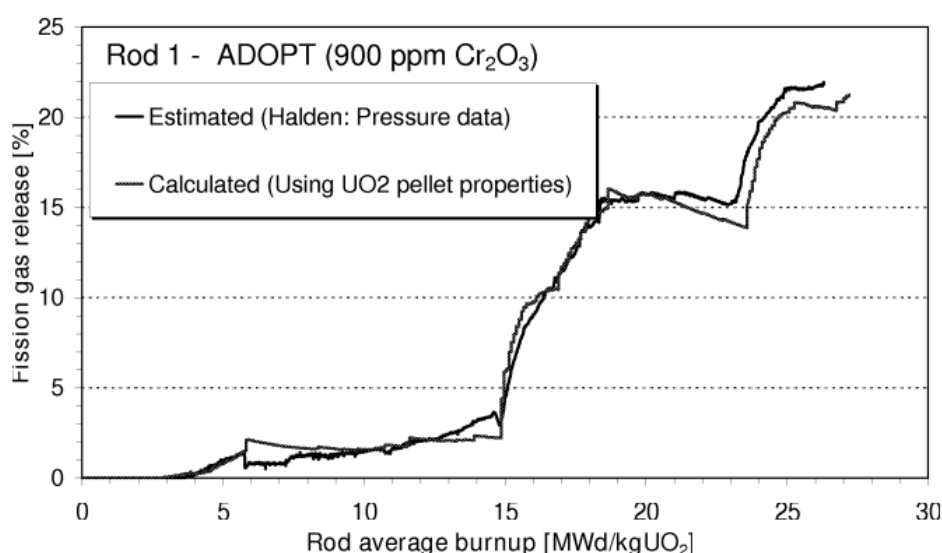


Figure 47: STAV prediction and measurement of FGR in IFA-677 rod 1 (ADOPT with 900 ppm chromia) [2].

It can be seen that FGR can be predicted reasonably accurately with no changes, or only minor changes, to the material property or phenomenological models; only the large grain size (a user input) needs to be modelled to capture the fission gas release behaviour.

With respect to LOCA simulation results in Figure 44, BISON predicts significantly reduced FGR compared to the standard UO₂ fuel, both before and during the fault. However, both doped and undoped fuel rods are still predicted to fail, and the impact on the predicted time to failure is only a modest improvement of an ~ 10 s increase for the doped fuel [60].

ALCYONE's predictions of the pellet Cr concentration radial distribution at both the start and end of the PR1 ramp test hold period (HP) are compared to measurements in Figure 48 (thick lines are predictions and thin lines are measurements; start of hold period predictions and measurements are in orange, and end of hold period predictions and measurements are in blue³). The PR1 test was described in Section 4.2.3.

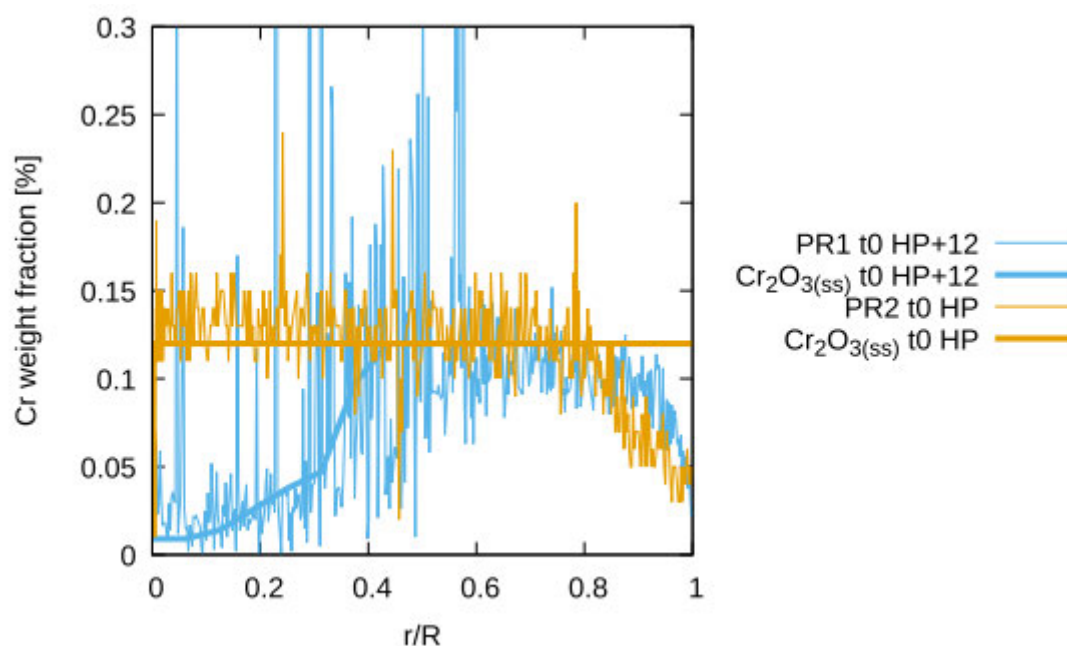


Figure 48: ALCYONE prediction and measurement of Cr concentration radial distribution before and after the hold period of the Framatome PR1 ramp test [42].

Figure 48 demonstrates that chromia dissociation (as described in Section 4.2.3) can be accurately predicted using equilibrium thermodynamics. However, the oxygen transport modelling was calibrated using the oxygen potentials inferred from (a) the measured Cr concentration radial distributions after the PR1 test and other ramp tests, (b) the known solubility of Cr as a function of temperature and oxygen potential, and (c) the fuel temperatures predicted by ALCYONE. Thus, the good agreement between measured and predicted Cr concentration radial distributions is, to some extent, engineered.

³ the start of hold period measurement is actually the post-ramp measurement from a second ramp test, PR2, where there was a zero hold period and so no chromia dissociation

7. Spent Fuel Storage and Disposal

The storage of spent CDF is discussed in Section 7.1, while the disposal of spent CDF (in a geological repository) is discussed in Section 7.2.

7.1. Spent fuel storage

No information was available on the storage of spent CDF. This is probably because storage is/will be as per existing storage routes (wet storage in ponds, potentially followed by dry storage in casks, vaults or silos) with no impact foreseen for CDF. It is also consistent with the main mechanisms for fuel degradation in wet storage – cladding corrosion and hydriding [65] – being independent of the fuel pellet type. Corrosion of the fuel pellets in failed fuel can also be a problem during wet storage [65], but the better oxidation resistance of CDF (see Section 4.2.5) should make this less of an issue than for undoped fuel (although there are no known corrosion experiments in pondwater conditions to support or refute this).

The main mechanisms for degradation in dry storage are oxidation in air of failed fuel (in the event of a containment breach, or high levels of residual air or moisture after pre-storage drying), thermal creep of the cladding, stress-corrosion cracking (SCC) of the cladding, delayed hydride cracking (DHC) of the cladding, and cladding hydride re-orientation or re-distribution (via hydrogen migration) [65]. The better oxidation resistance of CDF (see Section 4.2.5) should make oxidation in air of failed fuel less of an issue than for undoped fuel (although there are no known corrosion experiments in dry storage conditions to support or refute this). With respect to SCC, DHC and hydride re-orientation or re-distribution in the cladding, the presence of CDF should not directly affect these degradation mechanisms. However, the reduced fission gas release (see Section 4.2.6) should give lower rod internal pressures during dry storage, thereby reducing clad hoop stresses and reducing the risk of these degradation mechanisms occurring. The corresponding reduced volatile fission product release should also further reduce the (already arguably negligible) risk of SCC at the clad inner surface.

7.2. Spent fuel disposal

The important mechanisms for fuel degradation after spent fuel disposal are: (a) leaching and matrix dissolution after disposal canister penetration by groundwater; (b) fuel matrix damage due to alpha decay; and (c) fuel swelling or fragmentation due to the accumulation of helium [65] (since, post-penetration, the cladding is not taken credit for in the geological repository safety case). No information is available on (b) or (c) for CDF. With respect to (a), the only information available is the reporting from two Euratom projects: the 7th Framework Programme Fast / Instant Release of Safety Relevant Radionuclides from Spent Nuclear Fuel (FIRST-Nuclides) project (2012-2014) and the Horizon 2020 Modern Spent Fuel Dissolution and Chemistry in Failed Container Conditions (DisCo) project (2017-2021). See <http://firstnuclides.eu> and <https://www.disco-h2020.eu> for more information.

The FIRST-Nuclides project researched the release of fission products from fuel after disposal canister penetration by groundwater, with the focus on the leaching (short-term) release mechanism. The DisCo project is continuing this research theme, with the focus on the matrix dissolution (long-term) release mechanism. Since the results from the FIRST-Nuclides project [66] [67] (which include leach testing results for BWR ADOPT fuel irradiated to 59 MWd/kgU) have to some extent been superseded by those of the DisCo project, only the latter are described further here.

The DisCo project involves work packages covering experiments on spent fuel simulants, experiments on spent fuel samples, and modelling. CDF is being considered in all three of these work packages. The spent fuel simulants include UO₂ doped with Cr and Cr/Al, while the spent fuel samples include BWR ADOPT fuel irradiated to 59 MWd/kgU and PWR CDF (presumably Framatome fuel) irradiated to 58 MWd/kgU [68] [69]. Of primary interest are the results from the leaching/dissolution experiments on spent CDF samples, where each sample is immersed in simulated groundwater in an autoclave and the concentrations of fission product, dopant and actinide isotopes in the groundwater and the composition of the gas phase are routinely measured. Results from the experiment on spent PWR CDF are not yet available [69]. Preliminary groundwater concentration results from the first six months of the experiment on spent BWR ADOPT fuel are reproduced in Figure 49; the corresponding gas phase composition results show a Xe release fraction of 5.0% for the undoped fuel and 3.8% for the ADOPT fuel after six months.

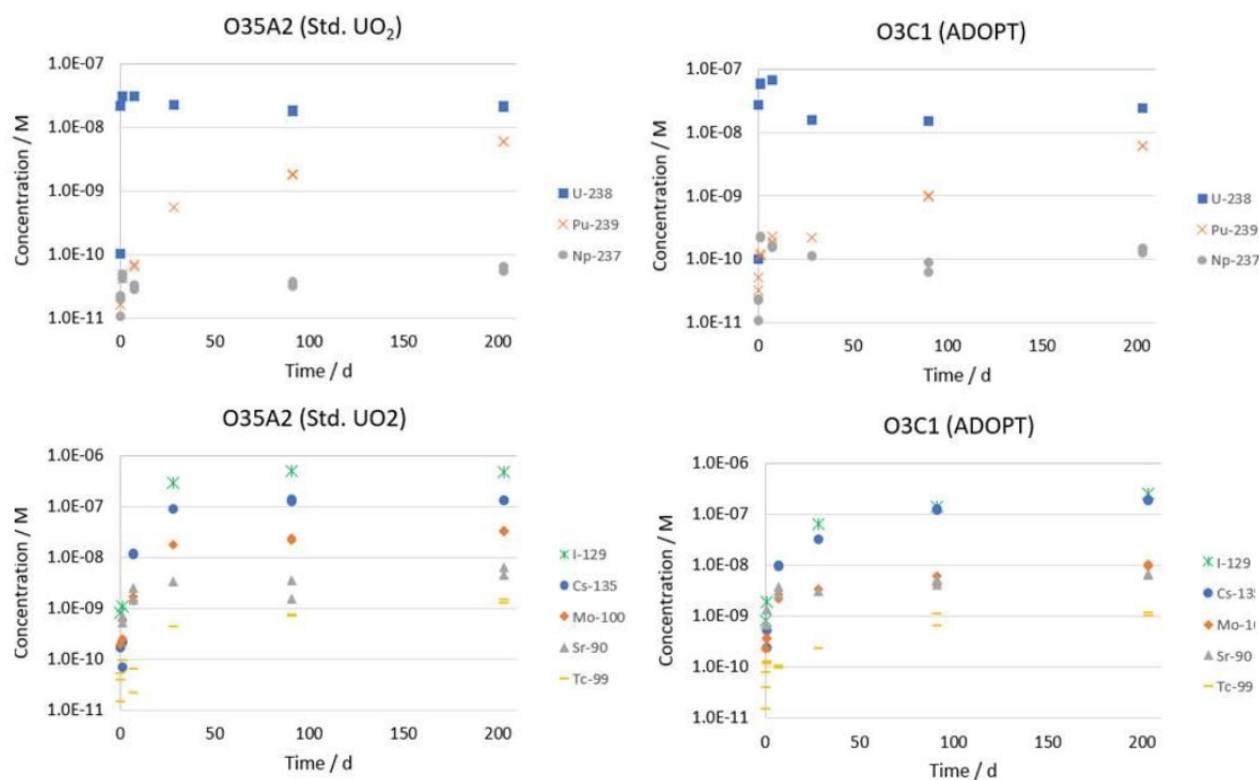


Figure 49: Measured concentrations of fission product and actinide isotopes in simulated groundwater obtained as part of DisCo leaching/dissolution experiments on 59 MWd/kgU BWR ADOPT fuel and 57 MWd/kgU BWR undoped fuel [69].

The groundwater concentration results shown in Figure 49 suggest comparable leaching behaviour of all isotopes from both the doped and undoped UO₂. However, a more nuanced picture emerges when the concentrations are converted to release fractions: the release fractions for the volatile ¹²⁹I isotope after six months are 6.7% for the undoped fuel and 3.2% for the ADOPT fuel. The combined Xe and ¹²⁹I release fraction results are consistent with reduced grain boundary concentrations of Xe and ¹²⁹I in the ADOPT fuel at the start of the experiment, which is in turn consistent with the larger grain size and reduced in-pile fission gas and volatile fission product release of this fuel. Thus, as per expectations, there is preliminary evidence (albeit only for ADOPT fuel) that the larger grain size of CDF reduces the instant release fractions (IRFs) of volatile fission products after disposal canister penetration by groundwater. Further evidence, together with data on fuel matrix dissolution rates, should be acquired in the remainder of the DisCo project. It should be noted that the working hypothesis in the project is that the dissolution rate of the spent doped fuel will be no different to that of the spent undoped fuel.

In addition to the sparsity of information on CDF degradation in post-disposal conditions, no information was found on current or planned disposal routes for CDF; this is consistent with such routes being as per existing routes for undoped UO₂ fuel.

8. Future Qualification, Research, Development and Testing Needed

The principal claims for CDF performance benefits made by Framatome and Westinghouse (relative to undoped UO₂) are summarised in Table 4. Also included in this table are suitable metrics (or measures) for determining whether or not the claimed fuel performance benefits are achieved.

Table 4: Claims for CDF performance benefits made by Framatome and Westinghouse, together with suitable metrics for determining whether or not claimed benefits are achieved.

Benefit	Description	Suitable metric
1	Improved fission gas retention [2] [9] **	Reduced fission gas release
2	Increased thermal creep [2] [9] *	Increased deformation rate during out-of-pile compressive creep tests
3	Increased cracking at periphery during power ramp [2] [11] *	Increased cracking in ceramographs of ramped fuel rod cross-sections
4	Increased oxidation resistance [2] [9] ***	Reduced oxidation rate in dissolution tests
5	Increased chipping resistance (Framatome only) [9] *	Reduced chipping during pellet impact tests
6	Reduced porosity (increased fissile density) and associated thermal stability (reduced densification) [2] [9]	Increased density of as-manufactured pellets
7	Improved PCI failure resistance (combined effects of benefits 2, 3 and 5 and any unclaimed chemical benefits)	Increased local rating and/or local rating increase thresholds for PCI-induced failures in ramp tests

* Contributors to increased PCI failure resistance

** Helps reduce rod internal pressure

*** Helps reduce fuel washout after a cladding failure

The measured data needed to assess performance against these metrics are generally proprietary, with only a subset of data published. In addition, there is generally no fuel-vendor-independent source of such measured data. Thus, determining whether or not the claimed fuel performance benefits are achieved basically comes down to evaluating the measured data published by the fuel vendors, together with that available from the OECD Halden Reactor Project experiments described in Section 4.1. This is done in Table 5 and Table 6, where data which demonstrate that suitable metrics have been met are identified.

Table 5: Available data for Framatome CDF demonstrating that suitable metrics from Table 4 have been met.

Suitable metric	Available data?
Reduced fission gas release	Yes (but only (1) at high burnup during normal operation and (2) during power ramps) [9] [36]
Increased deformation rate during out-of-pile compressive creep tests	Yes [15]
Increased cracking in ceramographs of ramped fuel rod cross-sections	Yes [11]
Reduced oxidation rate in dissolution tests	Yes [14]
Reduced chipping during pellet impact tests	Yes [9]
Increased density of as-manufactured pellets	Yes [9]
Increased local rating and/or local rating increase thresholds for PCI-induced failures in ramp tests	Yes [9]

Table 6: Available data for Westinghouse CDF demonstrating that suitable metrics from Table 4 have been met.

Suitable metric	Available data?
Reduced fission gas release	Yes (but only for commercial irradiations, and only (1) at high burnup during normal operation and (2) during power ramps; data from IFA-677 and IFA-720.3 experimental irradiations do not support reduced fission gas release) [2]
Increased deformation rate during out-of-pile compressive creep tests	Yes [2]
Increased cracking in ceramographs of ramped fuel rod cross-sections	Yes [2]
Reduced oxidation rate in dissolution tests	Yes [2]
Increased density of as-manufactured pellets	Yes [1]

Increased local rating and/or local rating increase thresholds for PCI-induced failures in ramp tests	No (ramp test data for rodlets with ADOPT pellets available only for one BWR rodlet which did not fail [2], so failure threshold cannot be evaluated)
---	---

Table 5 shows that all seven claimed performance benefits for Framatome CDF are supported by available data. In contrast, Table 6 shows that one of six claimed performance benefits for Westinghouse CDF is unsupported by available data: the claim for improved PCI resistance of Westinghouse ADOPT fuel – in particular in a PWR context – requires more evidence. Thus, further qualification and testing in the form of in-pile ramp tests on Westinghouse CDF may be required.

In addition, further PIE on ramp-tested fuel may be required if the potential chemical benefits of CDF with respect to PCI resistance – that is, improved corrosive fission product retention, and chromia dissociation and associated generation of free oxygen [12] [38] [39] [40] [41] [42] – are to be properly understood and/or taken credit for (over and above what is already implicitly taken credit for on the basis of ramp test results).

Future plans for testing of Framatome CDF include surveillance programmes associated with irradiation of lead fuel rods and lead fuel assemblies in the USDOE EATF programme [70] and more generally. GAIA lead fuel assembly and reload programmes will be the main focus for PWR applications [36].

Future testing of Westinghouse ADOPT fuel will take place as part of the Westinghouse-Exelon EnCore® lead fuel rod programme and the ADOPT high burnup verification programme [10] (see Section 5.1.1 for more details).

9. Impact on Limits and Conditions of Operation

The main impact of CDF on Limits and Conditions of Operation (LCO) is likely to be on PCI thresholds (limits on final power and/or power increase during an operational transient or frequent fault) built into reactors' primary protection systems (see Section 5.2.2 for details of potential changes in PCI thresholds for Framatome fuel). There is also the possibility that reactor power ramp-up rate limits could be relaxed to take credit for the increased PCI resistance and/or increased chipping resistance of CDF, although there is no evidence that fuel vendors or utilities are pursuing this; indeed, the essentially empirical nature of ramp-up rate limits means that it is unlikely that these would be changed.

Reduced fission gas release at high burnup during normal operation (see Section 4.2.6) may also allow increased burnup limits (assuming it can be demonstrated that rod internal pressure and clad hoop strain during normal operation remain below existing limits). However, there is no evidence that fuel vendors are currently pursuing such increased burnup limits (Framatome note that the GAIA lead fuel rod and lead fuel assembly programmes "validate the GAIA high performance fuel rod design until burnup of 62 GWd/tHM [the current standard rod average burnup limit applied in the USA and elsewhere]" [36]).

10. Licensing and Regulatory Issues

The likely impact of chromium doped fuels on Limits and Conditions of Operation (LCO) is covered in Section 9. The main remaining in-reactor fuel licensing issues are likely to be as follows:

- The reduced densification and increased intra-granular gas bubble swelling of CDF may (notwithstanding the increased fuel creep)
 - reduce margin to clad hoop strain and rod growth limits during normal operation
 - reduce margin to clad hoop strain increment limits during frequent faults
 - increase the number of rod failures during a RIA
- A lack of sufficient data (in particular for Westinghouse CDF) on ramp test behaviour to justify proposed PCI thresholds in a statistically meaningful manner.
- The lack of data on performance of the fuel during a RIA, and the limited data on performance of the fuel during a LOCA.
- The use of data on fuel from the early phases of product development which is not prototypic of the commercial fuel product (for example, fuel with dopant concentrations, grain sizes, porosity volume fractions, or porosity size distributions outside the ranges of the commercial fuel product, or with alternative or additional secondary dopants included); in particular, this would apply to the use of material property data and irradiation data for calibration and/or validation of the fuel performance code used in the licensing.
- Where applicable, the lack of data on the material properties and/or performance of CDF including the chosen burnable absorber material (which may mean that it is difficult to prove that the fuel incorporating the burnable absorber is non-limiting from a fuel performance perspective).

Further impacts on in-reactor fuel licensing and on reactor licensing are likely to be positive rather than negative. For example, the following benefits are anticipated for reactor licensing (assuming sufficient data are available to support them):

- Due to the reduced FGR in CDF (during both normal operation and transient conditions), there will be reduced clad ballooning, and hence a reduced number of rod failures, in a LOCA.
- Due to the reduced inter-granular fission gas bubble porosity, there will be reduced fuel fragmentation, relocation and dispersal during events with high fuel temperatures (principally LOCAs and RIAs).
- There will be a reduction in the source term associated with each failed rod in an infrequent fault due to the reduced fuel fragmentation, the reduced inter-granular volatile fission product inventories, and the reduced fuel oxidation and washout. (Whether there would be a reduction in the overall source term would depend upon whether there is an increase or decrease in the number of failed rods.)

The licensing and regulatory issues associated with storage of spent fuel will depend on the storage method. There is likely to be no impact on wet storage of irradiated fuel, since the

primary concern here is corrosion of the cladding outer surface, which is unaffected by CDF; there may even be a benefit in the sense that reduced corrosion of fuel pellets in any failed fuel rods is expected due to the large grain size. The impact on dry storage of irradiated fuel is likely to be beneficial: other than hydride re-orientation, which is dependent only on the cladding behaviour (and will therefore be unaffected by the presence of CDF), the limiting phenomenon is thermal creep of the cladding, which should be reduced in CDF due to the reduced in-reactor fission gas release and hence reduced rod internal pressures. As a result, there may be increased margin to clad creep strain limits; this in turn could potentially be used to reduce minimum cooling time limits for assemblies to be dry stored.

With respect to geological disposal, the larger grain size and reduced fission gas release behaviour of CDF suggests reduced instant release fractions (IRFs) of volatile fission products after disposal canister penetration by groundwater. This is supported by preliminary results from the DisCo project (see Section 7.2). There may also be an impact on (a) long-term source terms due to differences in groundwater dissolution of the spent fuel matrix relative to undoped material, and (b) contamination of groundwater due to release of chromium from leached/dissolved pellets. However, there are currently no known experimental data to support or refute these hypotheses; such data are being generated as part of the DisCo project.

Successful irradiation in commercial reactors of reload quantities of Westinghouse ADOPT fuel, and lead fuel rods and lead fuel assemblies of Framatome CDF demonstrates that fuel licensing for irradiation of CDF has been successfully carried out in France, USA, Sweden and elsewhere. Based on the information in Sections 5.1.1 and 5.2.1, this licensing pedigree should be bolstered in the coming years with further penetration of CDF into the international fuel market, primarily via Framatome's GAIA assemblies and Westinghouse's RFA-2, 17x17 NGF and OFA assemblies for PWRs, and via Framatome's ATRIUM assemblies and Westinghouse's SVEA and TRITON11 assemblies for BWRs. In particular, irradiations of reload quantities of GAIA assemblies are planned to start in 2020 in Europe and 2021 in the USA [36].

11. Conclusions

Chromium doped fuels (CDF) – that is, fuel doped with chromium and any other complementary additives – has been developed to make the fuel cycle more economical, to increase fuel reliability and to increase flexibility to meet energy demand. With a current focus on reducing the consequences of severe accidents in LWRs, a further demand has been placed on the development of accident tolerant (or advanced technology) fuel (ATF), a classification in which CDF is one option.

The addition of a small amount of chromia has been proven to significantly enhance grain growth during the sintering process employed in fuel manufacture. This leads to larger grain sizes than standard UO_2 fuel pellets for shorter sintering times. There is also greater densification of the pellets during sintering than for standard UO_2 , leading to a greater mass of uranium in the pellets and a reduced porosity volume fraction. These factors make the manufacturing process more economical, although careful control of the dopant concentrations and sintering conditions is needed to avoid volatilisation of the chromium and to ensure solubility of the chromia in the fuel matrix.

In reactor, the reduced porosity volume fraction leads to reduced in-pile densification, and hence greater dimensional stability of the fuel pellets. The larger grain size increases the fission product diffusion path to grain boundaries and so reduces the fission gas release from the pellets; this in turn reduces the rod internal pressures and inter-granular fission gas bubble swelling. However, there is a significant increase in intra-granular fission gas bubble swelling. The chromia also enhances the fuel thermal creep rate (despite the larger grain size), without significantly affecting any of the other thermal or mechanical properties, so there is an improvement in the pellet-clad interaction (PCI) behaviour during power transients, making the cladding less susceptible to failure by stress-corrosion cracking. The PCI behaviour is further improved through increased radial cracking of the thinner brittle outer zone of the fuel pellets (noting that the fracture strength is reduced due to the large grain size), and, arguably, by chemical effects (improved corrosive fission product retention, and chromia dissociation and associated generation of free oxygen which can oxidise the cladding inner surface, thereby protecting it from SCC). Finally, post-failure oxidation and washout of CDF is reduced due to the large grain size, thereby reducing the consequences of leaking rods during normal operation and of failed rods after an infrequent fault.

The consequences of limiting infrequent faults – that is, loss of coolant accidents (LOCAs) and reactivity-initiated accidents (RIAs) – can be lessened by reducing the extent of clad ballooning, reducing the cladding oxidation, reducing the volatile fission product release, and/or reducing the extent of fuel fragmentation. Hence, the lower FGR and increased intra-granular fission gas inventory of CDF can potentially reduce the consequences of these faults by reducing the rod internal pressure driving force for clad creepout, reducing volatile fission product release (which is correlated to fission gas release), and reducing the extent of inter-granular fragmentation due to overpressurisation of inter-granular fission gas bubbles. However, there are currently limited experimental data – and no data from integral rod testing – to support this.

OFFICIAL : COMMERCIAL

NNL 15231

ISSUE 1

There are two main vendors of CDF: Westinghouse and Framatome. The Westinghouse product uses a combination of chromia and alumina as dopants (ADOPT fuel), while the Framatome product uses only chromia. Both Westinghouse and Framatome have significant operating experience associated with lead fuel rods and lead fuel assemblies of their CDF products in commercial LWRs; in addition, reload quantities of Westinghouse ADOPT fuel have been irradiated. Ramp tests have also been performed to determine the PCI behaviour (although these appear to be limited in the case of Westinghouse ADOPT fuel), and various experimental irradiations have been carried out to investigate the phenomenology. Further irradiations are planned in the near future.

Modelling of CDF using fuel performance codes has been relatively limited, both in terms of codes used and their application. The necessary modifications to the material properties and models for undoped UO₂ have also been relatively minor. Of the five codes for which information is available – BISON, COPERNIC, RODEX, STAV and ALCYONE – only RODEX is known to have been validated for modelling of chromia doped fuel or to have been used for licensing of such fuel (for BWR applications).

No information was available on the storage or disposal of spent CDF. This is probably because storage and disposal are/will be as per existing routes (wet storage in ponds, potentially followed by dry storage in casks, vaults or silos, followed by disposal in a geological repository) with no impact foreseen for CDF. It is also consistent with the main mechanisms for fuel degradation in wet storage – cladding corrosion and hydriding – being independent of the fuel pellet type. In addition, there is a sparsity of information on the behaviour of CDF when exposed to water in post-irradiation storage and disposal conditions. The only information available is on fuel pellet leaching and dissolution in groundwater in the context of disposal of spent CDF, and is only from two sources: the Euratom FIRST-Nuclides and DisCo projects. Preliminary results from the DisCo project suggest that the larger grain size of CDF reduces the instant release fractions (IRFs) of volatile fission products after disposal canister penetration by groundwater.

Further qualification and testing in the form of in-pile ramp tests on Westinghouse CDF may be required. In addition, additional PIE on ramp-tested fuel may be required if the potential chemical benefits of CDF with respect to PCI resistance are to be properly understood and/or taken credit for (over and above what is already implicitly taken credit for on the basis of ramp test results).

The main impact of CDF on Limits and Conditions of Operation (LCO) is likely to be on PCI thresholds. Reduced fission gas release during normal operation may also allow increased burnup limits (assuming it can be demonstrated that rod internal pressure and clad hoop strain during normal operation remain below existing limits). The main remaining in-reactor fuel licensing issues are likely to be as follows:

- The reduced densification and increased intra-granular gas bubble swelling of CDF may (notwithstanding the increased fuel creep)
 - reduce margin to clad hoop strain and rod growth limits during normal operation
 - reduce margin to clad hoop strain increment limits during frequent faults
 - increase the number of rod failures during a RIA

OFFICIAL : COMMERCIAL

OFFICIAL : COMMERCIAL

NNL 15231

ISSUE 1

- A lack of sufficient data (in particular for Westinghouse CDF) on ramp test behaviour to justify proposed PCI thresholds in a statistically meaningful manner.
- The lack of data on performance of the fuel during a RIA, and the limited data on performance of the fuel during a LOCA.
- The use of data on fuel from the early phases of product development which is not prototypic of the commercial fuel product; in particular, this would apply to the use of material property data and irradiation data for calibration and/or validation of the fuel performance code used in the licensing.
- Where applicable, the lack of data on the material properties and/or performance of CDF including the chosen burnable absorber material.

Further impacts on in-reactor fuel licensing and on reactor licensing are likely to be positive rather than negative.

OFFICIAL : COMMERCIAL

12. References

- [1] J. Arborelius, K. Backman, L. Hallstadius, M. Limback, J. Nilsson, B. Rebensdorff, G. Zhou, K. Kitano, R. Lofstrom and G. Ronnberg, "Advanced doped UO₂ pellets in LWR applications," *Journal of Nuclear Science and Technology*, vol. 43, no. 9, pp. 967-976, 2006.
- [2] K. Backman, L. Hallstadius and G. Ronnberg, "Westinghouse advanced doped pellet - characteristics and irradiation behaviour," in *IAEA Technical Committee Meeting on Advanced Fuel Pellet Materials and Fuel Rod Designs for Water-Cooled Reactors*, Villigen, 2009.
- [3] P. Van Uffelen, J. Hales, G. Rossiter and R. Williamson, "A review of fuel performance modelling," *Journal of Nuclear Materials*, vol. 516, pp. 373-412, 2019.
- [4] C. Delafoy, J. Jonnet, Y. Rugama and V. Garat, "Plutonium recycling through LWR MOX fuel: today and tomorrow," in *International conference on the management of spent fuel from nuclear power reactors: learning from the past, enabling the future*, Vienna, 2019.
- [5] D. J. Shepherd, G. D. Rossiter, I. D. Palmer, G. Marsh and M. Fountain, "Technology readiness level (TRL) assessment of advanced nuclear fuels," in *TopFuel*, Zurich, 2015.
- [6] J. E. Lindbäck, "Westinghouse doped pellet technology," in *IAEA technical committee meeting on advanced fuel pellet materials and designs for water cooled reactors*, Brussels, 2003.
- [7] L. Hallstadius, K. Backman, S. Borell, I. Hallman, D. Mitchell and H. Widegren, "Westinghouse fuel pellet evolution," in *TopFuel*, Seoul, 2008.
- [8] J. Wright, J. Arborelius, K. Backman, L. Hallstadius, M. Limback, J. Nilsson, B. Rebensdorff and G. Zhou, "Development of Westinghouse Advanced Doped Pellet Technology," in *IAEA technical committee meeting on water reactor fuel performance modelling*, Kendal, 2005.
- [9] S. E. Cole, C. Delafoy, R. F. Graebert, P.-H. Louf and N. Teboul, "AREVA optimized fuel rods for LWRs," in *TopFuel*, Manchester, 2012.
- [10] H. Shah, J. Romero, P. Xu, R. Oelrich, J. Walters, J. Wright and W. Gassmann, "Westinghouse-Exelon EnCore fuel lead test rod (LTR) program including coated cladding development and advanced pellets," in *TopFuel*, Prague, 2018.
- [11] C. Delafoy, V. I. Arimescu, R. M. Hengstler-Eger, H. Landskron, A. Moeckel and P. Bellanger, "AREVA Cr₂O₃-doped fuel: increase in operational flexibility and licensing margins," in *TopFuel*, Zurich, 2015.

- [12] C. Delafoy and I. Arimescu, "Developments in fuel design and manufacturing in order to enhance the PCI performance of AREVA NP's fuel," in *Pellet-Clad Interaction (PCI) in Water-Cooled Reactors*, Lucca, 2016.
- [13] C. Delafoy, P. Dewes and T. Miles, "AREVA NP Cr₂O₃-doped fuel development for BWRs," in *International LWR Fuel Performance Meeting*, San Francisco, 2007.
- [14] C. Delafoy and M. Zemek, "Washout behaviour of chromia-doped UO₂ and gadolinia fuels in LWR environments," in *IAEA Technical Committee Meeting on Advanced Fuel Pellet Materials and Fuel Rod Designs for Water-Cooled Reactors*, Villigen, 2009.
- [15] C. Delafoy, P. Blanpain, C. Maury, P. Dehaut, C. Nonon and S. Valin, "Advanced UO₂ fuel with improved PCI resistance and fission gas retention capability," in *TopFuel*, Wurzburg, 2003.
- [16] Framatome, "Development of LWR fuels with enhanced accident tolerance: EATF phase 2 final scientific technical report," FS1-0041211, 2018.
- [17] V. Peres, L. Favergeon, M. Andrieu, J. C. Palussiere, J. Balland, C. Delafoy and M. Pijolat, "High temperature chromium volatilization from Cr₂O₃ powder and Cr₂O₃-doped UO₂ pellets in reducing atmospheres," *Journal of Nuclear Materials*, vol. 423, pp. 93-101, 2012.
- [18] T. Cardinaels, K. Govers, B. Vos, S. Van den Berghe, M. Verwerft, L. de Tollenaere, G. Maier and C. Delafoy, "Characterisation of Cr₂O₃ doped fuel," in *Enlarged Halden Programme Group (EHPG) meeting*, Storefjell, 2010.
- [19] A. Leenaers, L. de Tollenaere, C. Delafoy and S. Van den Berghe, "On the solubility of chromium sesquioxide in uranium dioxide fuel," *Journal of Nuclear Materials*, vol. 317, pp. 62-68, 2003.
- [20] C. Riglet-Martial, P. Martin, D. Testemale, C. Sabathier-Devals, G. Carlot, P. Matheron, X. Iltis, U. Pasquet, C. Valot, C. Delafoy and R. Largenton, "Thermodynamics of chromium in UO₂ fuel: A solubility model," *Journal of Nuclear Materials*, vol. 447, pp. 63-72, 2014.
- [21] A. Massih, "Effects of additives on uranium dioxide fuel behaviour," Swedish Radiation Safety Authority report 2014:21, 2014.
- [22] AREVA Inc., "Incorporation of chromia-doped fuel properties in AREVA approved methods," ANP-10340NP, 2016.
- [23] E. Muller, T. Lambert, N. L'Hullier, K. Silberstein, C. Delafoy and B. Therache, "Thermal behavior of advanced UO₂ fuel at high burnup," in *International LWR Fuel Performance Meeting*, San Francisco, 2007.

- [24] C. Nonon, J. C. Menard, S. Lansart, J. Noriot, S. Martin, G. M. Decroix, O. Rabouille, O. Delafoy and D. Petitprez, "PCI behaviour of chromium oxide doped fuel," in *NEA/CEA Seminar on Pellet-Clad Interaction in Water Reactor Fuels*, Cadarache, 2004.
- [25] J. Wright, C. Anghel, S. Middleburgh and M. Limback, "Fuel hardware considerations for BWR PCI mitigation," in *TopFuel*, Boise, 2016.
- [26] K. Sakai, "The fuel creep test IFA-701: results after four irradiation cycles," OECD Halden Reactor Project report HWR-1039, 2013.
- [27] K. I. Björk, J. F. Kelly, C. Vitanza, S. S. Drera, S. Holcombe, T. Tverberg, H. Tuumisto, J. Wright, M. Sarsfield, T. Blench, J. Ho Yang, D. Kim, H. Kim and C. W. Lau, "Irradiation testing of enhanced uranium oxide fuels," *Annals of Nuclear Energy*, vol. 125, pp. 99-106, 2019.
- [28] J. A. Turnbull, "The high initial rating experiment: IFA-677; A review of important phenomena and predictions of its behaviour," OECD Halden Reactor Project report HWR-765, 2004.
- [29] R. Josek, "The high initial rating test IFA-677.1: Final report on in-pile results," OECD Halden Reactor Project report HWR-872, 2008.
- [30] O. Bremond, "IFA-716.1 fission gas release mechanisms," OECD Halden Reactor Project report HWR-1008, 2011.
- [31] K. Fuglesang, "In-pile results from the fission gas release mechanisms study in IFA-716 after final unloading," OECD Halden Reactor Project report HWR-1161, 2016.
- [32] T. Tverberg, "Continued irradiation of four rods from IFA 716," in *Enlarged Halden Programme Group (EHPG) meeting*, Lillehammer, 2017.
- [33] K. Okamoto, "Fission gas release from Cr-doped fuel in IFA-720.3," OECD Halden Reactor Project report HWR-1270, 2019.
- [34] G. Rossiter, "Understanding and modelling fuel behaviour under irradiation," in *Nuclear Fuel Cycle Science and Engineering*, Woodhead Publishing, 2012, pp. 396-424.
- [35] B. Therache, "The high initial rating test, IFA-677.1: Results after first cycle of irradiation," OECD Halden Reactor Project report HWR-819, 2005.
- [36] G. Gentet, J. Peucker and C. Gebhardt, "Post irradiation examinations of GAIA lead fuel assemblies," in *TopFuel*, Prague, 2018.
- [37] N. Marchal, C. Campos and C. Garnier, "Finite element simulation of Pellet-Cladding Interaction (PCI) in nuclear fuel rods," *Computational Materials Science*, vol. 45, pp. 821-826, 2009.

- [38] D. Jadernas, F. Corleoni, A. Puranen, P. Tejland and M. Granfors, "Chemical and structural characterization of ramp tested fuel with different additives," in *Pellet-Clad Interaction (PCI) in Water-Cooled Reactors*, Lucca, 2016.
- [39] J. Wright, C. Anghel, S. Middleburgh and M. Limback, "Towards an increased understanding of fuel pellet and cladding features enhancing the PCI resistance of LWR fuel," in *Pellet-Clad Interaction (PCI) in Water-Cooled Reactors*, Lucca, 2016.
- [40] V. I. Arimescu and J. K.-H. Karlsson, "Slow power ramps: Are the mitigating factors mechanical or chemical in nature?," in *Pellet-Clad Interaction (PCI) in Water-Cooled Reactors*, Lucca, 2016.
- [41] C. Riglet-Martial, J. Sercombe, J. Lamontagne, J. Noirot, I. Roure, T. Blay and L. Desgranges, "Experimental evidence of oxygen thermo-migration in PWR UO₂ fuels during power ramps using in-situ oxido-reduction indicators," *Journal of Nuclear Materials*, vol. 480, pp. 32-39, 2016.
- [42] P. Konarski, J. Sercombe, C. Riglet-Martial, L. Noirot, I. Zacharie-Auburn, K. Hanifi, M. Fregonese and P. Chantrenne, "3D simulation of a power ramp including fuel thermochemistry and oxygen thermodiffusion," *Journal of Nuclear Materials*, vol. 519, pp. 104-120, 2019.
- [43] B. J. Lewis, "Fundamental aspects of defective nuclear fuel behaviour and fission product release," *Journal of Nuclear Materials*, vol. 160, pp. 201-217, 1988.
- [44] K. Une, S. Kashibe and K. Nogita, "Corrosion behavior of unirradiated oxide fuel pellets in high temperature water," *Journal of Nuclear Materials*, vol. 227, no. 1-2, pp. 32-39, 1995.
- [45] K. Une and S. Kashibe, "Corrosion behavior of irradiated oxide fuel pellets in high temperature water," *Journal of Nuclear Materials*, vol. 232, no. 2-3, pp. 240-247, 1996.
- [46] J. Rest, M. W. D. Cooper, J. Spino, J. A. Turnbull, P. Van Uffelen and C. T. Walker, "Fission gas release from UO₂ nuclear fuel: A review," *Journal of Nuclear Materials*, vol. 513, pp. 310-345, 2019.
- [47] H. K. Jenssen, "PIE report on six UO₂ fuel rods irradiated in IFA-677 high initial rating test," OECD Halden Reactor Project report HWR-968, 2010.
- [48] S. Valin, L. Caillot, P. Dehaut, Y. Guerin, A. Mocellin, C. Delafoy and A. Chotard, "Synthesis of the results obtained on the advanced UO₂ microstructures irradiated in the TANOX device," in *IAEA technical committee meeting on advanced fuel pellet materials and designs for water cooled reactors*, Brussels, 2003.
- [49] L. Caillot, J. Noirot, Y. Pontillon and S. Valin, "TANOXOS: an analytical irradiation program aiming at understanding the behaviour of various doped UO₂ fuels," in *TopFuel*, Salamanca, 2006.

- [50] Nuclear Energy Agency, "Nuclear fuel behaviour in loss-of-coolant accident (LOCA) conditions," NEA No. 6846, ISBN 978-92-64-99091-3, 2009.
- [51] C. Delafoy, J. Bischoff, J. Larocque, P. Attal, L. Gerken and K. Nimishakavi, "Benefits of Framatome's E-ATF evolutionary solution: Cr-coated cladding with Cr₂O₃-doped fuel," in *TopFuel*, Prague, 2018.
- [52] Nuclear Energy Agency, "Nuclear fuel behaviour under reactivity-initiated accident (RIA) conditions: state-of-the-art report," NEA No. 6847, ISBN 978-92-64-99113-2, NEA/CSNI/R(2010)1, 2010.
- [53] U. C. Bergmann and J. King, "TRITON11 TM - Westinghouse 11x11 BWR fuel design," in *TopFuel*, Boise, 2016.
- [54] J. L. Bradfute, D. L. Chapin, A. Reparaz, M. Quecedo Gutierrez and C. Munoz-Reja Ruiz, "Westinghouse fuel designs and performance overview," in *TopFuel*, Manchester, 2012.
- [55] D. L. Chapin, R. W. Brashier, D. E. Staub, M. B. O'Cain, J. S. Hogle, A. Jasiulevicius, B. Josefsson, T. Andersson, A.-L. Ohman and M. Aullo, "Design and operation of EFG fuel in Ringhals PWRs," in *TopFuel*, Charlotte, 2013.
- [56] Nuclear Engineering International, "Fuel design data," 2004.
- [57] C. Delafoy and P. Dewes, "AREVA NP new UO₂ fuel development and qualification for LWRs applications," in *TopFuel*, Salamanca, 2006.
- [58] C. Delafoy, P. Blanpain, S. Lansart, P. Dehaut, G. Chiarelli and R. Castelli, "Advanced PWR fuels for high burnup extension and PCI constraint elimination," in *IAEA technical committee meeting on advanced fuel pellet materials and designs for water cooled reactors*, Brussels, 2003.
- [59] AREVA GmbH, "GAIA: the new generation fuel for 17x17 PWR fuel assemblies," G-338-V1-15-ENGPB, 2015.
- [60] Y. Che, G. Pastore, J. Hales and K. Shirvan, "Modelling of Cr₂O₃-doped UO₂ as a near-term accident tolerant fuel for LWRs using the BISON code," *Nuclear Engineering and Design*, vol. 337, pp. 271-278, 2018.
- [61] G. Pastore, J. D. Hales, Y. Che and K. Shirvan, "Simulation of Cr₂O₃-doped Fuel Tests in IFA-677 and IFA-716 using BISON," in *Enlarged Halden Programme Group (EHPG) meeting*, Sandefjord, 2019.
- [62] C. Garnier, P. Mailhe, P. Vesco, L. C. Bernard, C. Delafoy and P. Garcia, "The COPERNIC mechanical model and its application to doped fuel," in *NEA/CEA Seminar on Pellet-Clad Interaction in Water Reactor Fuels*, Aix-en-Provence, 2004.
- [63] I. Arimescu and T. Davis, "Analysis of IFA-677 and IFA-716 tests results by using RODEX4 fuel code," in *Enlarged Halden Programme Group (EHPG) meeting*, Lillehammer, 2017.

- [64] J. Julien, C. Bassi, A. Bouloire, C. Struzik, B. Baurens and C. Delafoy, "Analysis of IFA-716-6 tests results using the ALCYONE fuel code," in *Enlarged Halden Programme Group (EHPG) meeting*, Sandefjord, 2019.
- [65] P. N. Standing, "Behaviour of spent fuel during storage," in *15th International High-Level Radioactive Waste Management Conference (IHLRWM 2015)*, Charleston, 2015.
- [66] K. Lemmens, E. Gonzalez-Robles, B. Kienzler, E. Curti, D. Serrano-Purroy, R. Sureda, A. Martinez-Torrents, O. Roth, E. Slonszki, T. Mennecart, I. Gunther-Leopold and Z. Hozer, "Instant release of fission products in leaching experiments with high burn-up nuclear fuels in the framework of the Euratom project FIRST-Nuclides," *Journal of Nuclear Materials*, vol. 484, pp. 307-323, 2017.
- [67] K. Nilsson, O. Roth and M. Jonsson, "Oxidative dissolution of ADOPT compared to standard UO₂ fuel," *Journal of Nuclear Materials*, vol. 488, pp. 123-128, 2017.
- [68] I. Farnan, D. Bosbach, D. Wegen, E. Gonzales-Robles Corrales, C. Jegou, C. Corkhill, D. I. Hambley and J. Cobos Sabate, "Initial state report: sample characterisation and experimental set-up," DisCo deliverable D2.1, 2018.
- [69] M. Herm, E. Gonzalez-Robles, L. Iglesias, P. Carbol, D. Serrano-Purroy, A. Barreiro, O. Roth and I. Casas, "Spent fuel experiments: first dissolution results," DisCo deliverable D3.1, 2019.
- [70] N. A. P. Kiran Kumar, J. N. Stevens, M. Savela, B. Mays and J. Strumpell, "AREVA enhanced accident tolerant fuel program - Current results and future plans," in *TopFuel*, Idaho, 2016.

OFFICIAL : COMMERCIAL

NNL 15231

ISSUE 1

Distribution

Name	Email Address	Location
[REDACTED]	[REDACTED]	University of Manchester
[REDACTED]	[REDACTED]	NNL, Chadwick House
[REDACTED]	[REDACTED]	ONR
[REDACTED]	[REDACTED]	NNL, Central Laboratory
[REDACTED]	[REDACTED]	NNL, Preston Laboratory
[REDACTED]	[REDACTED]	NNL, Central Laboratory
NNL Document Controller		

OFFICIAL : COMMERCIAL